Parallele Synthese, Charakterisierung und zelluläre Pharmakokinetik von fluoreszenten zell-penetrierenden Peptiden

Parallel Synthesis, Characterization and Cellular Pharmacokinetics of Fluorescent Cell-Penetrating Peptides

DISSERTATION

der Fakultät für Chemie und Pharmazie
der Eberhard-Karls-Universität Tübingen
zur Erlangung des Grades eines Doktors
der Naturwissenschaften

2005

vorgelegt von

Rainer Fischer

Tag der mündlichen Prüfung 11.02.2005

Dekan:	Prof. Dr. S. Laufer
1. Berichterstatter:	Prof. Dr. G. Jung
2. Berichterstatter:	Prof. Dr. S. Stevanović
3. Berichterstatter:	Prof. Dr. M. Bienert

Die vorliegende Arbeit wurde unter der Anleitung von

Herrn Prof. Dr. Günther Jung

und unter Co-Betreuung von **Herrn Dr. Roland Brock**

in der Zeit von März 2001 bis September 2004 am Institut für Organische Chemie und am Institut für Zellbiologie der Eberhard-Karls-Universität Tübingen durchgeführt.

Herrn Prof. Dr. Günther Jung und Herrn Dr. Roland Brock danke ich sehr herzlich für ihre intensive Förderung, das fortwährende Interesse an meiner Arbeit, die Freiheit in der Bearbeitung des gestellten Themas, die exzellenten Arbeitsbedingungen und ihr mir entgegengebrachtes Vertrauen.

Danksagungen

Herzlich bedanken möchte ich mich bei allen Kollegen aus den Gruppen von Dr. R. Brock, Prof. Dr. G. Jung, Prof. Dr. J. Rademann, Prof. Dr. R. Süssmuth, Prof. Dr. H.-G. Rammensee und Prof. Dr. S. Stevanović für das sehr angenehme Arbeitsklima. Die freundliche und konstruktive Atmosphäre hat mich immer motiviert and vorangetrieben.

Frau Ursula Becker-Sanzenbacher danke ich für ihre unendliche Geduld und Hilfsbereitschaft alle bürokratischen Hürden betreffend.

Besonders herzlich bedanken möchte ich mich bei Söhnke Voss für die Freundschaft, seine Anregungen und die vielen heiteren Momente innerhalb der letzten drei Jahre.

Dr. Oliver Mader und Oda Stoevesandt danke ich für ihre Mühen und die Bereitschaft bei der Durchführung von Fluoreszenzmessungen immer ihr Bestes zu geben.

Für die Unterstützung bei allen Computerfragen danke ich ganz herzlich Thomas André und Dr. Gerhard Sorg.

Herzlich bedanken möchte ich mich bei den Laborkollegen Dr. Oliver Mader, Dr. Mariola Fotin-Mleczek, Dr. Martin Elbs, Aleksandra Velkova, Oda Stoevesandt, Günter Roth, Karsten Köhler, Antje Hoff, Thomas Waizenegger, Michael Hulko, Thomas André, Hans-Jörg Hufnagel, Dr. Udo Marquardt und Falk Duchardt für das angenehme Arbeitsklima und zahlreiche Diskussionen innerhalb der Gruppe von Dr. Roland Brock.

Dr. Mariola Fotin-Mlcezek, Thomas Waizenegger, Karsten Köhler, Hans-Jörg Hufnagel und Falk Duchardt danke ich ganz speziell für die erfolgreiche Zusammenarbeit bei den verschiedenen CPP-Projekten.

Dr. Jörg Rademann und Dr. Michael Barth danke ich für die angenehme und erfolgreiche Zusammenarbeit bei dem PEI-Projekt.

Prof. Dr. Karl-Heinz Wiesmüller, Thomas André, Antje Hoff, Oda Stoevesandt und Dr. Martin Elbs danke ich für die Kooperation bei den Microarray-Projekten.

Bei Prof. Dr. S. Stevanović möchte ich mich ganz herzlich für seine Hilfsbereitschaft, seine Geduld und die Möglichkeit, in seinem Labor die notwendigen Routine MALDI-TOF-Messungen durchführen zu können, bedanken.

Daniel Bächle und Dr. Hubert Kalbacher danke ich für die erfolgreiche Zusammenarbeit beim Cathepsin D-Substrat-Projekt und den HPLC-Fluoreszenz-Messungen.

Dr. Jörn Dengjel danke ich für die Zusammenarbeit beim Autophagie-Projekt.

PD Dr. Olaf Heidereich und PD Dr. Michaela Scherr danke ich für die Kooperation beim siRNA-Projekt.

Meinen wissenschaftlichen Hilfskräften Susanne Vollmer, Hans-Jörg Hufnagel, Ivo Rüttelkolk und Julia Krissler danke ich für ihre Unterstützung.

Dr. Bernd Thern und Dr. Tobias Seyberth danke ich für die Routine ES-MS-Messungen.

Nicole Sessler danke ich für Peptidsynthesen und immer wieder erfrischende Unterhaltungen während des Laboralltags.

Franziska Löwenstein danke ich für die zuverlässige Erledigung der Spüldienste.

Allen Kolleginnen und Kollegen, die nicht namentlich erwähnt worden sind, danke ich für das gute Klima im Arbeitskreis.

TABLE OF CONTENTS

Abbreviations

For amino acids the suggestions of the IUPAC-IUB-commission for biological nomenclature [*Eur. J. Biochem.* **1984**, *138*, 9-37] were applied.

Ac	Acetyl
ACN	acetonitrile
AcOH	acetic acid
Ac_2O	acetic acid anhydride
Ado	8-amino-3,6-dioxaoctanoic acid
Ahx	6-aminohexanoic acid
Antp	Antennapedia (here referring to the 16 amino acid Penetratin peptide)
AntpHD	Antennapedia homeodomain
bFGF	basic fibroplast growth factor
Boc	*tert*.-butyloxycarbonyl
CPP	cell-penetrating peptide
DCM	dichloromethane
Dde	1-(4,4-dimethyl-2,6-dioxocyclohexylidene)ethyl
DHAP	2,5 dihydroxyacetophenone
DIC	N,N'-diisopropyl carbodiimide
DIPEA	N,N'-diisopropylethylamine
DMF	N,N'-dimethylformamide
DMSO	dimethylsulfoxide
DMEM	Dulbecco´s Modified Eagle's Medium
EDT	ethanedithiole
EDTA	ethylenediaminetetraacetic acid
eq	equivalent
ER	Endoplasmic reticulum
ES	Electrospray
EtOH	ethanol
FCM	fluorescence correlation microscopy
FCS	fluorescence correlation spectroscopy

FITC	fluorescein isothiocyanate
Fluo	5(6)-carboxyfluorescein
Fmoc	N-(9-fluorenyl)methoxycarbonyl
FRET	fluorescence resonance energy transfer
FT-ATR-IR	fourier transform attenuated total reflection-infra red
HBS	HEPES buffered saline
HBSS	Hank's buffered salt solution
HEPES	N-(2-hydroxyethyl) piperazine-N´-(2-ethanesulfonic acid)
HFIP	hexafluoro-2-isopropanol
HIV	human immunodeficiency virus
HOBt	1-hydroxybenzotriazol
HPLC	high-performance liquid chromatography
λ	wave length
M	molar
MALDI	matrix-assisted laser desorption ionisation
MeOH	methanol
MHC	major histocompatibility complex
MS	mass spectrometry
Mtt	4-methyltrityl
MTS	membrane translocating sequence
m/z	mass/charge ration
NDGA	nordihydroguaiaretic acid
NMR	nuclear magnetic resonance
Pamb	4-aminomethyl benzoic acid
Pam_3Cys	tripalmitoyl-S-glycerylcysteinyl
Pbf	2,2,5,7,8-pentamethyl-dihydrobenzofuran-5-sulfonyl
PBS	phosphate-buffered saline
POPC	1-palmitoyl-2-2-oleoyl-phosphocholine
POPG	1-palmitoyl-2-2-oleoyl-phosphoglycerol
RP	reversed phase
RT	room temperature
S0387	2-(4-acetanilino-1,3-butadienyl)-3,3-dimethyl-1-(4-sulfobutyl)-indolium inner salt

SPPS	solid-phase peptide synthesis
t	time
Tamra	5(6)-carboxytetramethylrhodamine
t_R	retention time
tBu	*tert*.-butyl
tBuOH	*tert*.-butyl alcohol
TBTU	2-(1*H*-benzotriazol-1-yl)-1,1,3,3-tetramethyluronium tetrafluoroborate
TGN	*trans*-Golgi Network
TIS	triisopropylsilane
TFA	trifluoroacetic acid
TOF	time-of-flight
Tris	tris(hydroxymethyl)aminomethane
Trt	trityl
UV	ultraviolet
V	volume

Preface

Contents of this PhD thesis

The content of this PhD thesis has been adapted from a total of four manuscripts. Three out of these four manuscripts deal with cell-penetrating peptides (CPPs) and one manuscript describes the preparation of fluorescently labeled peptides in solid-phase synthesis (Fischer et al., 2003). Three of the four manuscripts have already been published, whereas the one in preparation will be submitted in 2005. In addition, the methods and reagents presented have contributed to other manuscripts, which are summarized in Chapter 2.

This PhD thesis can be considered as witness of the dramatic change of view within the CPP research field. When the first manuscripts were prepared (Waizenegger et al., 2002;Fischer et al., 2002) most cationic CPPs were still supposed to enter cells via a non-endocytic mechanism. Nevertheless some of the findings obtained in our laboratory which were partially shown in these initial contributions, disagreed with some of the findings obtained by others. Afterwards these discrepancies could be attributed to the fact that our investigations were all performed with living, non-fixed cells. In 2003 fixation was identified as the major source of artefacts in the analysis of the cellular trafficking of CPPs.

Chapter 3 deals with the application of carboxyfluorescein in solid-phase synthesis and the establishment of the synthesis of doubly-labeled peptides (Fischer et al., 2003). These protocols were the prerequisites for chapters 4 to 6. Chapter 4 investigates the fluorophore and cargo-dependence of cell-penetrating peptides (Fischer et al., 2002). The manuscript “A stepwise dissection of the intracellular fate of cationic cell-penetrating peptides” elucidated the endosomal fate of cationic CPPs (Fischer et al., 2004). The fourth manuscript represents the merger of the two converging fields of this PhD thesis, i.e. the synthesis and cell-biological testing of doubly-labeled CPPs (Fischer et al., 2005b). The introduction was partially adapted from a review (Fischer et al., 2005a).

1. Fischer,R., Fotin-Mleczek,M., and Brock,R. (2005a). Break on through to the other side - Biophysics and cell biology shed light on cell-penetrating peptides. *ChemBioChem, in print 2005.*

2. Fischer,R., Hufnagel,H.-J., Baechle,D., Stoevesandt,O., Jung,G., and Brock,R. (2005b). *In vitro* and *in vivo* applications of doubly-labelled fluorescent cell-penetrating peptides. *To be submitted 2005*.

3. Fischer,R., Köhler,K., Fotin-Mleczek,M., and Brock,R. (2004). A stepwise dissection of the intracellular fate of cationic cell-penetrating peptides. *J. Biol. Chem.,* **279,** 12625-12635.

4. Fischer,R., Mader,O., Jung,G., and Brock,R. (2003). Extending the applicability of carboxyfluorescein in solid-phase synthesis. *Bioconjug. Chem,* **14,** 653-660.

5. Fischer,R., Waizenegger,T., Köhler,K., and Brock,R. (2002). A quantitative validation of fluorophore-labelled cell-permeable peptide conjugates: fluorophore and cargo dependence. *Biochim. Biophys. Acta,* **1564,** 365-374.

1. Introduction

Viruses provide expressive examples for the potential of perturbing molecular mechanisms inside the cell via introduction of foreign molecules, especially DNA (Smith and Helenius, 2004). For this reason, it is no surprise that today's molecular and cellular biology exploit very similar strategies. Introduction of DNA into cells for the expression of proteins that either modulate or interfere with cellular function is a commonplace for the analysis of intracellular molecular processes. In addition, the function of gene products has been analyzed by the introduction of oligonucleotides, either antisense DNA or siRNA, that inhibit the translation of messenger RNA into a protein (Scherer and Rossi, 2003). A further class of molecules that has proven useful in the analysis of molecular events inside cells are peptides that specifically disrupt molecular interactions, e. g. in cellular signal transduction (Prochiantz, 1996).

For viruses and molecular biologists alike, crossing of the plasma membrane is a common challenge. The lipid bilayer of the plasma protects the cellular content from entry of pathogens and molecules that interfere with cellular function and replication. Import and export of non-permeable molecules into and out of the cytoplasm is a tightly regulated process. Only molecules within a narrow range of molecular size, net charge and polarity are able to directly cross the plasma membrane by passive diffusion along a concentration gradient (Lipinski et al., 2001). In mammalian cells a large number of transporters are expressed that maintain the balance of entry and exit. In contrast, for large hydrophilic macromolecules it is generally assumed that endocytosis is the mode of internalization (Rejman et al., 2004). Endocytosis, however, guides external molecules through compartments with high hydrolytic activity, thereby exerting an important protective role (Pillay et al., 2002).

Pathogens have therefore evolved sophisticated means for bypassing or stunning the hydrolytic guards for obtaining access to the cytoplasm. For viruses the docking of molecules to cell surface receptors followed by internalization and release of genetic information into the cytoplasm provides a highly specific mode of entry into only those cells that express the respective receptor. For biologists working with a homogeneous population of cells in tissue culture experiments, such specificity is usually not required. For this reason, most strategies to cross

the plasma membrane for laboratory purposes are poised to efficiency and robustness rather than specificity and lack the sophistication of viral entry.

1.1 Crossing the plasma membrane – a crucial prerequisite for cell-biological investigations

Give the demand for introducing macromolecules into living cells, cell-biologists have developed a variety of techniques in order to get molecules in. Many cell-biological experiments aim at the understanding of intracellular biochemical events, such as chemical modifications of proteins or intermolecular interactions. Many of these experiments require the introduction of molecules into the cytoplasm of living cells.

The strategies developed can roughly be subdivided into those based either on a transient disruption of the integrity of the plasma membrane or based on carrier-mediated approaches (Stephens and Pepperkok, 2001). Examples for the former are the generation of pores by application of short high-power electric pulses in electroporation or the incubation with pore forming molecules such as streptolysine O. Techniques that are based on the transient permeabilization suffer from harsh experimental conditions, which clearly limit the survival rate of the cells.

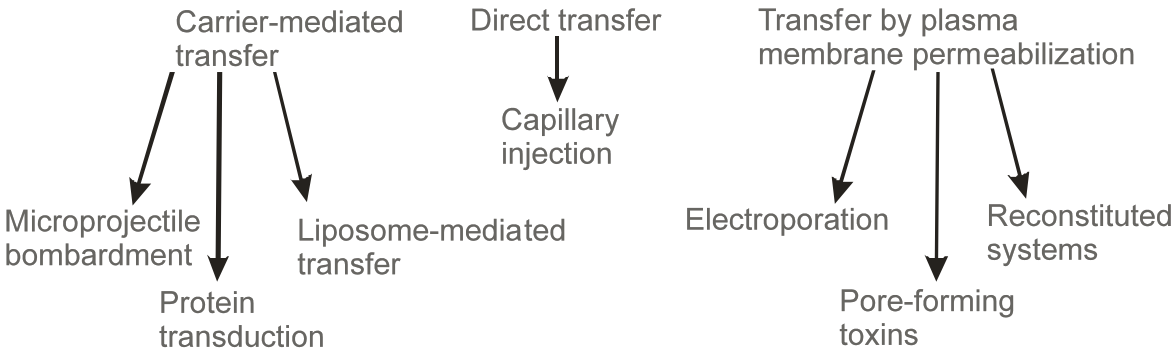

Figure 1.1 Different techniques for the introduction of macromolecules into cells (adapted from Stephens and Pepperkok, 2001).

Capillary injection on the other hand is another widely used method. Thin glass micropipettes are used to inject the sample of interest directly into the cytoplasm.

The so-called “carrier-mediated transfer” methods require the linkage of the cargo molecule to a moiety that possesses the ability to mediate the transfer of other molecules into cells.

Transfection reagents

Especially for the introduction of foreign DNA into mammalian cells, carrier-mediated approaches are well established. Transfection reagents (Surovoy et al., 1998;Flechsler et al., 1998) improve the import efficiency of cargo molecules by (i) neutralization of negative charge and (ii) conferring hydrophobicity, characteristics that facilitate the interaction of the resulting complexes with the plasma membrane. However despite the fact that these so-called lipoplexes are rather hydrophobic, a mechanism that involves internalization via endocytosis has received considerable support (Zuhorn et al., 2002). Similarly, loading of molecules into liposomes incorporates the cargo into a high molecular weight complex with physicochemical characteristics that more closely match those of the plasma membrane. Evidently, these carriers exert their activity to a major part by disguising the physicochemical characteristics of the cargo.

Lipopeptides

Another very compelling strategy for the carrier-mediated uptake, especially in the case of biologically active peptides, is the covalent conjugation of a lipid moiety to the cargo. This approach has attracted considerable attention for the import of peptides (Gras-Masse, 2003). A straight-forward synthetic access to lipopeptides based on standard solid-phase synthesis protocols makes these lipoconjugates very attractive agents for various biological applications.

The first works on synthetic lipopeptides were based on the immunologically active N-terminal moiety of the principal lipoprotein of *Escherichia coli*, also known as Braun’s lipoprotein (Braun, 1975). The tripalmitoyl-S-glycerylcysteinyl- (Pam_3Cys) scaffold mediates attachment to the cell membrane, internalization into the cytoplasm, and activates macrophages to secrete cytokines (Hoffmann et al., 1988;Wolf et al., 1989;Metzger et al., 1993). Synthetic viral peptides covalently linked to Pam_3Cys were demonstrated to efficiently prime influenza virus-specific CTLs *in vivo* (Deres et al., 1989), making these conjugates attractive agents for the generation of fully synthetic vaccines. Due to its immune system modulating activity and the identification of the Toll like receptor 2 as its physiological receptor

(Lien et al., 1999;Aliprantis et al., 1999), Pam_3Cys-conjugates have seen a tremendous growth in interest within the last 5 years.

Peptides conjugated to one single lipid chain have also been applied for a large variety of purposes. Myristoylated pseudosubstrate domains of protein kinase C were demonstrated to be delivered into the cytoplasm of mammalian cells and exert an inhibitory activity (Verhoeven et al., 1993;Eichholtz et al., 1993). Monolipidated peptides were also shown to be applicable for targeting of MHC I (Loing et al., 2000) and MHC II molecules (Papini et al., 2001). The internalization of lipopeptides is suggested to be endocytosis-dependent (Schörner, 1999;Andrieu et al., 2000).

1.2 Cell-penetrating peptides as a carrier-mediated delivery strategy

CPPs are small molecules of mostly 9 to 30 amino acids in length. Efficient cellular import has been achieved for cargos as diverse as peptides (Prochiantz, 1996;Hawiger, 1999), proteins as large as 120 kDa (Rojas et al., 1998;Schwarze et al., 1999), oligonucleotides (Astriab-Fisher et al., 2002), plasmids (Singh et al., 1999), peptide nucleic acids (Pooga et al., 1998b), siRNA (Muratovska and Eccles, 2004;Chiu et al., 2004) and even nanoparticles (Lewin et al., 2000).

In most of these applications conjugation of only one carrier peptide to a cargo renders the molecule import competent. However, a nine amino acid peptide will have little impact on the physicochemical characteristics of a 120 kDa protein (Schwarze et al., 1999) or a duplex 21 nt siRNA (Chiu *et al.*, 2004). As a consequence, in contrast to the transfection reagents described above, rather than disguising the physicochemical characteristics, CPPs are well defined pharmacokinetic modifiers that add a new functionality to a specific site of an otherwise unperturbed molecule. Rapid cellular uptake (Richard et al., 2003) in combination with a highly defined molecular structure and ease of handling renders the CPPs highly attractive mediators of import. Moreover, the advantages of CPPs as peptide-based transport vehicles are the accessibility of large collections of different peptides by well-established automated procedures (Jung and Beck-Sickinger, 1992) allowing detailed structure-activity relationships and a

rational and straight-forward approach to the generation of new and optimized CPPs.

Applications of CPPs exceed well beyond mere tissue culture experiments. CPP/peptide conjugates and CPP-fusion proteins that interfere with protein-protein interactions have been successfully applied as therapeutic agents in animal models (Fujihara et al., 2000;Myou et al., 2003). In contrast to liposomes, CPP-peptide conjugates possess many beneficial drug-like characteristics. In the case of peptide cargos, covalent CPP-conjugates are analytically well defined, storable, and no leakage of the active moiety occurs.

1.3 The origin of cell-penetrating peptides

In 1965, Ryser and Hancock demonstrated that the addition of homopolymers of cationic amino acids (~ 100 kDa) to tissue culture media containing radio labeled albumin enhanced the uptake of the radiolabel into the cell (Ryser and Hancock, 1965). In the 1970ies again Ryser et al. demonstrated that covalent coupling of poly (L-lysine) to proteins or small molecules enhances their cellular uptake and, in the case of methotrexate, the biological activity of this drug (Ryser and Shen, 1978;Shen and Ryser, 1978).

About 10 years later Frankel et al. observed that the HIV-1 Tat protein is taken up by tissue culture cells. The internalized Tat protein is then capable of transactivating the viral promoter in the nucleus of the targeted eukaryotic cell (Frankel and Pabo, 1988). Only some years later, the 60-amino acid polypeptide corresponding to the sequence of the homeodomain of the *Drosophila* Antennapedia transcription factor was shown to penetrate neurons and augment their morphological differentiation (Joliot et al., 1991). These findings suggested that the efficient internalization of proteins into cells, first observed for a synthetic oligopeptide by Ryser and Hancock, has a correspondence in nature.

In the case of the HIV-1 Tat protein the internalization was attributed to a basic domain comprising amino acids 48 to 60 (Vives et al., 1997). The peptide corresponding to this region of the protein is termed “Tat peptide”. In the case of the Antennapedia protein a peptide of 16 amino acids in length corresponding to the third helix of the homeodomain was still capable of “translocating through the plasma membrane” (Derossi et al., 1994). As a CPP, this domain is also referred to as Penetratin. During the following years, the compelling properties of these

peptides promoted the identification of further CPPs. These peptides were either based on small domains of naturally existing proteins (Lin et al., 1995;Pooga et al., 1998a;Oess and Hildt, 2000) or designed *de novo* (Sheldon et al., 1995;Morris et al., 2001). An overview of the current diversity of cell-penetrating peptides is given in Figure 1.2.

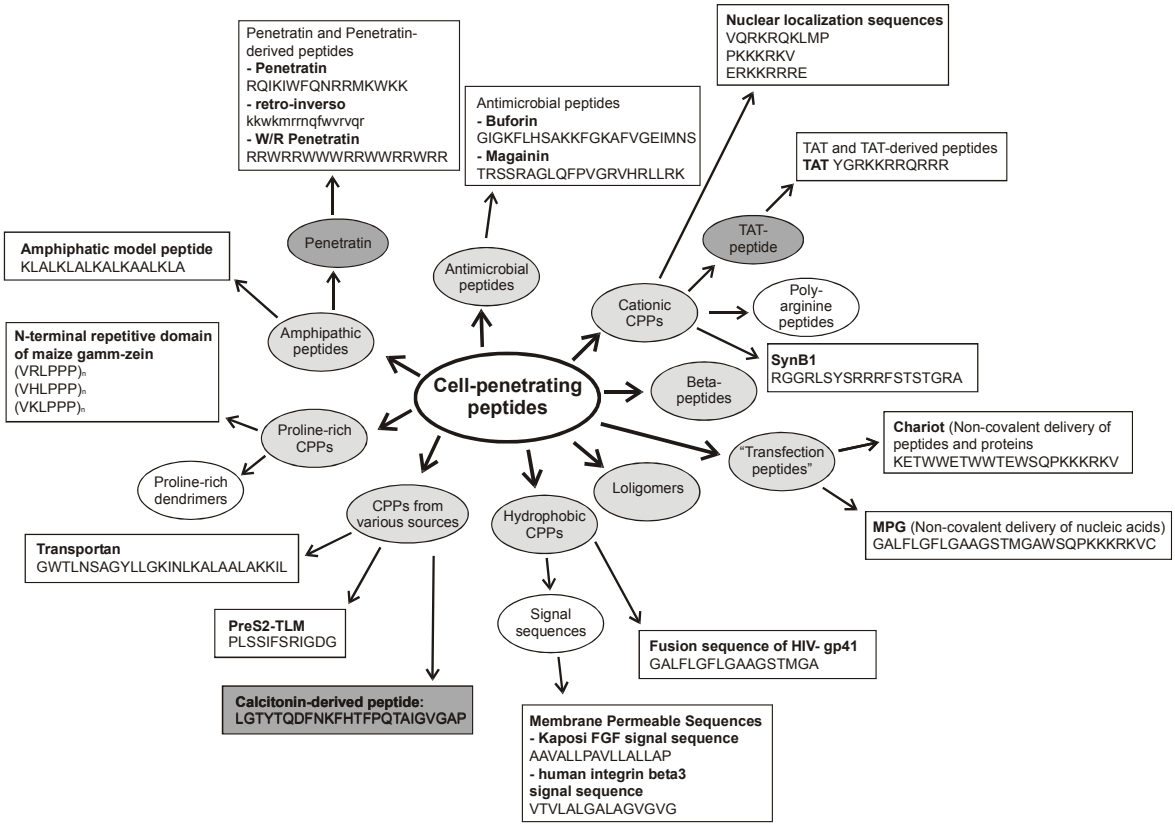

Figure 1.2 An overview of the current peptide motifs considered to be cell-penetrating.

1.4 Cell-penetrating peptides versus antimicrobial and membrane-active peptides

Membrane-active peptides

Many membrane-active peptides, including antimicrobials and toxins, are known to induce transmembrane pores. The first peptide discovered to do so is alamethicin (Mueller and Rudin, 1968). Alamethicin was first supposed to induce pores only in the presence of a transmembrane potential. However, it was shown that alamethicin could insert into bilayers also in the absence of an external field (Fringeli and Fringeli, 1979). At micromolar concentrations alamethicin has also been shown to cause hemolysis in human erythrocytes. In black lipid membranes at nanomolar concentrations the peptide induces the formation of voltage-dependent pores with multi-state properties (Irmscher and Jung, 1977).

Two other extensively studied peptides, the bee venom toxin melittin (Habermann, 1972) and the frog peptide magainin (Zasloff, 1987) exhibit similar behaviours. Both melittin (Hanke et al., 1983;Matsuzaki et al., 1997) and magainin cause the leakage of fluorescent dyes from lipid vesicles indicating formation of pores. In the last 15 years, a great variety of antimicrobial peptides have been shown to similarly induce transmembrane pores in bacterial cells as well as in lipid vesicles (Jack and Jung, 1998;Zasloff, 2002).

Cell-penetrating peptides versus antimicrobial peptides

The Penetratin peptide was initially demonstrated to traverse a pure lipid bilayer (Thoren et al., 2000) without forming pores (Thoren *et al.*, 2000;Persson et al., 2003), a finding that clearly distinguishes this CPP from antimicrobial peptides. Moreover CPPs such as Tat and Penetratin are considerably less toxic and haemolytic than most antimicrobial peptides (Vives *et al.*, 1997;Trehin et al., 2004).

Antimicrobial peptides as CPPs

Recent findings indicate that CPPs and antimicrobial peptides share common functional characteristics. Both groups of peptides bind to lipid membranes. Magainin was demonstrated to be internalized rapidly into mammalian cells exhibiting a cooperative concentration dependence of uptake. This finding suggests that the peptide forms a pore as an intermediate similar to the

observations in membranes. Furthermore, translocation was accompanied by cytotoxicity (Takeshima et al., 2003). In contrast, buforin another cationic antimicrobial peptide, translocated by a less concentration-dependent, passive mechanism, without showing any significant toxicity (Takeshima *et al.*, 2003).

CPPs as antimicrobial peptides

Given that CPPs are cationic and often amphipathic, similar to membrane active antimicrobial peptides, a recent work investigated whether CPPs may also act as antimicrobial peptides (Nekhotiaeva et al., 2004). TP10, a 21-amino acid deletion analogue of the chimeric CPP transportan (Pooga et al., 2001), inhibited *Candida albicans* and *Staphylococcus aureus* growth. pVEC, another cationic CPP (Elmquist et al., 2001), inhibited *Mycobacterium smegmatis* growth at low micromolar doses, below the levels that harmed human HeLa cells. Therefore, TP10 and pVEC can enter both mammalian and microbial cells and preferentially permeabilize and kill microbes (Nekhotiaeva et al., 2004).

1.5 Mode of action

Up until recently, flow cytometric and microscopic experiments addressing the uptake of CPPs were conducted by incubation of cells with fluorescently labeled peptides and subsequent fixation. Alternatively, biotinylated CPPs were visualized post fixation and permeabilization via staining with fluorescently labeled streptavidin. The results of these experiments suggested that the uptake of Penetratin, the HIV-1 Tat peptide and oligo-arginine was insensitive to low temperature (Derossi *et al.*, 1994;Vives *et al.*, 1997;Futaki et al., 2001) and to inhibitors of endocytosis (Vives *et al.*, 1997;Suzuki et al., 2002). For this reason, a mechanism of import by direct crossing of the plasma membrane was postulated (Derossi *et al.*, 1994;Vives *et al.*, 1997). The data was fully supported by biophysical experiments according to which Penetratin was able to traverse a pure lipid bilayer without forming pores (Thoren *et al.*, 2000;Persson *et al.*, 2003).

Although having difficulties to explain how hydrophilic macromolecules cross a lipid bilayer and given the reports on the endocytic uptake of the Tat protein (Mann and Frankel, 1991) this model remained more or less unchallenged until 2003. At the beginning of 2003 Olsnes et al. stated that “experiments to exclude that the entry of endocytosed (Tat) peptide into the nucleus occurred after fixation and permeabilization are highly desirable” (Olsnes et al., 2003). The same group had reported earlier that neither the Tat basic domain nor the viral protein VP22 had been able to mediate membrane translocation of Diphteria toxin A-fragment (Falnes et al., 2001). Import of the Diphteria A toxin into the cytoplasm provided a highly sensitive functional assay for detecting the cytoplasmic delivery of a cargo. The authors therefore concluded that the CPP-mediated import was inefficient.

State-of-the-art findings: Post-fixation era

In 2003 it was shown by Richard et al. (Richard et al., 2003) that the earlier cell-biological experiments had suffered from an artifactual uptake of CPPs caused by fixation of cells. These researchers used live cell fluorescence microscopy to monitor the uptake of fluorescein-labeled peptides. Moreover, it was demonstrated that cationic CPPs associated with the outer leaflet of the plasma membrane. Removal of these peptides was achieved by incubation of cells with trypsin. Very likely, this population of peptides accounted for the intracellular fluorescence observed previously for fixed cells which had been incubated at 4°C. The data

presented in this work demonstrated the involvement of endocytosis in the cellular internalization of the Tat peptide and the $(Arg)_9$ peptide. In a second, rather unnoticed work, cationic CPPs were demonstrated to bind to plastic and glass, materials which are commonly used in cellular assays applied in the CPP field (Chico et al., 2003). It was stated that “under certain conditions, such non-specific to plastic or glass surfaces binding could be mistaken for cellular penetration”(Chico *et al.*, 2003).

Within the past two years the role of endocytosis for the uptake of CPP-protein conjugates was substantiated by several publications. Inhibitors of metabolism or endocytosis, such as cytochalasin D were demonstrated to impair the uptake of Penetratin (Drin et al., 2003). Moreover Penetratin and the Tat peptide were shown to promote endocytosis of high molecular weight cargo upon binding to cell surface glycosaminoglycans (Console et al., 2003). Another comparison of CPPs revealed that endocytosis depends only on the number of positives charges within the peptide whereas oligopeptide transduction requires the guanidine structure of arginine (Zaro and Shen, 2003).

The contribution of the individual endocytic pathways is still under dispute. For Tat fusion proteins caveolar endocytosis (Fittipaldi et al., 2003) as well as macropinocytosis (Wadia et al., 2004) were proposed. It should be emphasized that both contributions included reliable functional cellular assays for detecting the delivery of functional proteins into the cytoplasm. These assays were based either on the transactivating activity of the Tat-protein (Fittipaldi et al., 2003) or on the enzymatic activity of the Cre-recombinase (Wadia *et al.*, 2004). For short CPPs alone, to our knowledge no functional assay has been established so far, to reliably compare the arrival of intact and biologically active CPPs in the cytosolic compartment under different experimental conditions. This deficit may still lead to wrong conclusions on the cellular uptake and intracellular fate of CPPs. Even though, our understanding of the cellular trafficking of CPPs has benefited enormously from the use of fluorescently tagged CPPs in live cell microscopy, we should be aware that the subcellular distribution of the fluorescent dye may not represent the one of the CPP but rather the one of a proteolytic product.

In spite of the accumulating evidence for endocytosis, the refined experimental approaches, as well, provide new evidence for at least a contribution of membrane permeation to the cellular uptake of these peptides (Thoren et al., 2003). In two different cells lines an endocytic uptake was observed for Penetratin. However, a hepta-arginine peptide, with a tryptophane residue added to the C-terminus, was found to be internalized via an energy-independent, non-endocytic pathway. For the Antennapedia protein and the HIV Tat protein, minute amounts that directly enter the cytoplasm and transfer into the nucleus may already be sufficient for these proteins to exert their physiological functions.

1.6 Applications of CPPs

Despite the fact that the mode of action of CPPs is still not understood in detail and currently a matter of great debate, the applications of CPPs are undoubtedly a story of great success. The applications range from mere cell-culture experiments to animal studies and show promise for potential therapeutics.

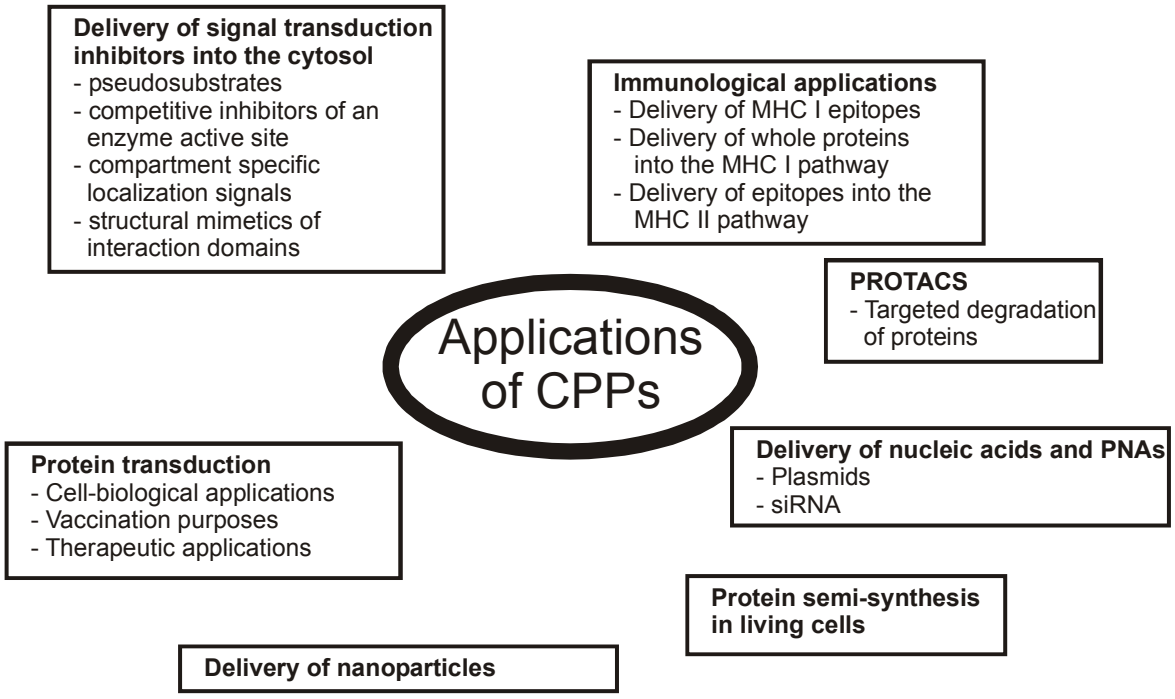

Figure 1.3 An overview of the applications of cell-penetrating peptides.

Delivery of peptides into the cytoplasm for the interference with cellular signal transduction

Most applications of CPPs include the introduction of peptides into the cytoplasm in order to interfere with signal transduction (Prochiantz, 1996;Hawiger, 1999). Peptide cargos delivered by conjugation to CPPs included pseudo-substrates (Theodore et al., 1995), competitive inhibitors of an enzyme active site (Nishikawa et al., 2000), compartment-specific localization sequences (Lin *et al.*, 1995), and structural mimetics of interaction domains (Horng et al., 2001). The advantages of peptide-based functional analyses in cell biology are the accessibility of large

collections of different compounds by well-established automated procedures (Jung *et al.*, 1992) as well as a rational approach to the generation of biologically active compounds based on available structural information of interaction domains.

Within the last two years several successful animal studies using CPP-peptide conjugates have been published. One of the most astonishing studies showed that a cell-penetrating inhibitor of NFAT (nuclear factor of activated T-cells) based on the polyarginine delivery system was able to provide immunosuppression for fully mismatched islet allografts in mice. In addition, this compound did not affect insulin secretion, whereas FK506, as established calcineurin inhibitor, caused a dose-dependent decrease in insulin secretion (Noguchi et al., 2004). This surprising study implies that CPP-based drugs may represent more than just a laboratory approach but an alternative to traditional low molecular weight drugs. Nevertheless the antigenicity of those peptides may limit their broad applicability.

CPPs for immunological applications

The delivery of exogenous antigens into the MHC class I processing pathway using CPPs has been presented *in vitro* and in whole animals (Schutze-Redelmeier et al., 1996;Pietersz et al., 2001). On dendritic cells CPP-epitope conjugates were shown to enable prolonged antigen presentation on MHC I molecules (Wang and Wang, 2002). CPPs therefore have the promise to represent a widely applicable means to enhance immune responses against cancer and infectious diseases. A more recent work showed that the detailed knowledge of the intracellular fate of CPPs allows a rational design of CPP-epitope constructs for the optimization of peptide-based vaccines (Lu et al., 2004). In this work it was also demonstrated that CPPs bearing a CTL and a T helper cell epitope can generate both the corresponding MHC class I – and II-binding peptides and elicit a strong CTL and T helper cell response.

Proteins as cargos

The application of CPPs for the delivery of proteins renders them an attractive alternative to genetic intervention (Ford et al., 2001). Cargo proteins have been as large as 120 kDa (Rojas *et al.*, 1998;Schwarze *et al.*, 1999). Their principal applicability to animal studies has been demonstrated using the 120 kDa-β-galactosidase protein (Schwarze *et al.*, 1999). The therapeutic potential of protein transduction has been proven in a recent work reporting on the blockade of

inflammation and airway hyper responsiveness in immune–sensitized mice using a cell-penetrating dominant-negative phosphoinositide 3-kinase (Myou *et al.*, 2003). Protein transduction has also been applied to the introduction of proteins into the MHC class I processing pathway (Kim et al., 1997).

Nucleic acids

CPPs have moreover been used for the transfer of plasmid DNA (Rudolph et al., 2003) and siRNA (Simeoni et al., 2003;Muratovska *et al.*, 2004;Chiu *et al.*, 2004) into mammalian cells and for the successful application of peptide nucleic acids in an animal model (Pooga *et al.*, 1998b).

Nanoparticles

CPP-derivatized super magnetic nanoparticles have been demonstrated to be suitable for cell labeling (Lewin *et al.*, 2000).

Generation of chemical knockouts

A compelling strategy for the generation of a transient protein knock-out has been described by Crews et al. (Schneekloth, Jr. et al., 2004). A ligand for an intracellular target protein was chemically linked to a peptide sequence that binds to the E3 ubiquitin ligase. This chimeric molecule was introduced into mammalian cells using a CPP leading to the recruitment of the target protein to the proteasome and subsequently to its degradation.

Protein semi-synthesis in living cells

Muir et al. have developed an approach to obtain semi-synthetic proteins in living cells (Giriat and Muir, 2003). The protein of interest was expressed in living cells with the first half of the naturally occurring Ssp Dna split intein fused to its C-terminus. Then, a semi-synthetic polypeptide, consisting of the second half of the intein covalently linked to a synthetic probe (which may be a fluorescent dye) and a CPP, was added to the culture media. The CPP delivered the probe into the cell, whereupon the probe associated with its complementary half triggering protein splicing. This splicing event resulted in the removal of the intein and ligation of the probe to the selected protein through a normal peptide bond.

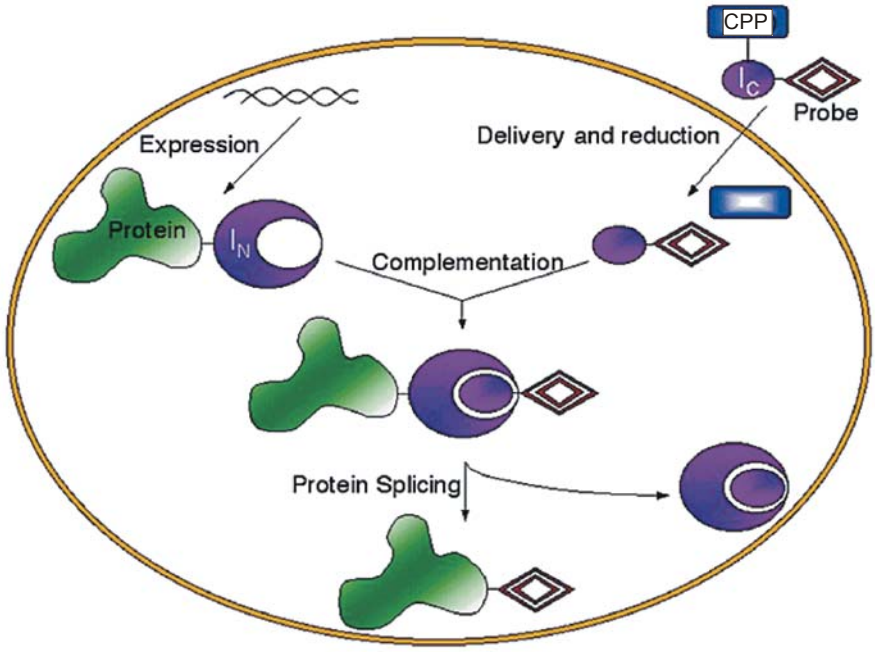

Figure 1.4 Principle of semi-synthetic protein trans-splicing in living cells. I_N is the first half of the naturally occurring *Ssp* DnaE intein, I_C is its second half (adapted from (Giriat *et al.*, 2003).

2. Contributions to other projects

Listed below are the contributions to other projects that led to already published scientific articles and manuscripts which have either been submitted or which are preparation.

2.1 Intracellular concentration measurements in adherent cells: A comparison of import efficiencies of cell-permeable peptides (Waizenegger et al., 2002)

The author of this thesis synthesized all peptides used in this study. Moreover he established the analysis of cell-penetrating peptides using Fluorescence Correlation Microscopy (FCM) during his diploma thesis.

2.2 Structure property analysis of pentamethine indocyanine dyes: Identification of a new dye for life science applications (Mader et al., 2004)

The author of this thesis tested several pentamethine indocyanine dyes with respect to their applicability in solid-phase synthesis. Moreover several peptides labeled with S0387 were prepared, e.g. an MHC I binding peptide, that was used in this study.

2.3 Chemolabile cellular microarrays for screening of small compounds and peptides (Hoff et al., 2004)

The author of this thesis synthesized several peptides used in the experiments. He performed experiments to validate the proof of principle for the non-covalent attachment of peptides on glass substrates for their use in cellular microarrays. Moreover he assisted the diploma student M. Hulko in the design and synthesis of the chemolabile compounds presented in the manuscript.

2.4 Reversible cross-linking of hyperbranched polymers: A strategy for the combinatorial decoration of multivalent scaffolds (Barth et al., 2005)

The author of this thesis tested peptide-decorated hyperbranched polymers, synthesized by Dr. M. Barth, with respect to their biological applicability, i.e. evaluation of toxicity and investigation of internalization using confocal fluorescence microscopy and flow cytometry.

2.5 Peptide microarrays for the detection of molecular interactions in cellular signal transduction (Stoevesandt et al., 2005)

The author of this thesis synthesized the bis-phosphorylated ZAP-70 binding peptide used in this study.

2.6 Autophagy promotes presentation of MHC-II peptides from intracellular source proteins (Dengjel et al., 2005)

The author of this thesis performed fluorescence microscopy und fluorescence spectroscopy measurements in order to identify conditions under which autophagy was induced in the investigated cell line.

2.7 A ratiometric fluorescence-based LPS-sensor (Voss et al., 2005)

The author of this thesis conceived the concept of a doubly-labeled peptide as biosensor for LPS based on an LPS-binding peptide and intramolecular Fluorescence Resonance Energy Transfer (FRET). He moreover synthesized a doubly-labeled LPS-binding peptide and performed initial experiments to establish the proof of principle. S. Voss successfully continued these initial experiments and substantially extended the scope of this application.

1. Barth,M., **Fischer,R.**, Brock,R., and Rademann,J. (2005). Reversible cross-linking of hyperbranched polymers: A strategy for the combinatorial decoration of multivalent scaffolds. *Angew. Chem. Int. Ed.,* **44,** 1560-1563.

2. Dengjel,J., Schoor,O., **Fischer,R.**, Reich,M., Kraus,M., Kreymborg,K., Altenberend,F., Kalbacher,H., Brock,R., Driesen,C., Rammensee,H.-G., and Stevanovic,S. (2005). Autophagy promotes MHC-II presentation of peptides from intracellular source proteins. *Proc. Natl. Acad. Sci. U. S. A.,* **in print 2005**.

3. Hoff,A., André,T., **Fischer,R.**, Voss,S., Hulko,M., Marquardt,U., Wiesmüller,K.-H., and Brock,R. (2004). Chemolabile cellular microarrays for the screening of small compounds and peptides. *Mol. Divers.,* **8,** 311-320.

4. Mader,O., Reiner,K., Egelhaaf,H.-J., **Fischer,R.**, and Brock,R. (2004). Structure property analysis of pentamethine indocyanine dyes: Identification of a new dye for life science applications. *Bioconjug. Chem.,* **15,** 70-78.

5. Stoevesandt,O., Elbs,M., Köhler,K., Lellouch,A.C., **Fischer,R.**, André,T., and Brock,R. (2005). Peptide Microarrays for the Detection of Molecular Interactions in Cellular Signal Transduction. *Proteomics,* **in print 2005**.

6. Voss,S., **Fischer,R**., Ulmer,A.J., Jung,G., Wiesmuller,K.H., and Brock,R. (2005). A ratiometric fluorescence-based LPS-sensor*.,* **to be submitted 2005**.

7. Waizenegger,T., **Fischer,R.**, and Brock,R. (2002). Intracellular concentration measurements in adherent cells: A comparison of import efficiencies of cell-permeable peptides. *Biol. Chem.,* **383,** 291-299.

3 Extending the applicability of carboxyfluorescein in solid-phase synthesis

This chapter was published in Bioconjugate Chemistry in 2003. The author of this thesis contributed Figures 1, 2, 3, 4, and 6. Figure 5 was contributed by Dr. O. Mader.

3.1 Summary

Optimized coupling protocols are presented for the efficient and automated generation of carboxyfluorescein-labeled peptides. Side products, generated when applying earlier protocols for the *in situ* activation of carboxyfluorescein, were eliminated by a simple procedure, yielding highly pure fluorescent peptides and minimizing post-synthesis work-up. For the cost-efficient labeling of large compound collections, coupling protocols were developed reducing the amount of coupling reagent and fluorophore. In order to enable further chemical derivatization of carboxyfluorescein-labeled peptides in solid-phase synthesis, the on-resin introduction of the trityl group was devised as a protecting group strategy for carboxyfluorescein. This protecting group strategy was exploited for the synthesis of peptides labeled with two different fluorescent dyes; essential tools for bioanalytical applications based on fluorescence resonance energy transfer (FRET). Tritylation and optimized labeling conditions led to the development of a fluorescein-preloaded resin for the automated synthesis of fluorescein-labeled compound collections with uniform labeling yields.

3.2 Introduction

A growing number of applications in bioanalytical chemistry depend on fluorescently labeled molecules with biological activity (Brand and Johnson, 1997). Carboxyfluorescein has remained a reagent of choice for the preparation of hydrolytically stable fluorescent peptides and protein conjugates (Brinkley, 1992;Weber et al., 1998). Fluorescein owes this popularity to its biocompatibility, low price and availability of instrumentation for the detection of its fluorescence. Fluorescein-labeled peptide derivatives have been employed as fluorescent markers in bioanalytical applications, such as confocal laser scanning microscopy (Schmidt et al., 1998), flow cytometry (Owens and Loken, 1995), and more recently fluorescence polarization measurements (Dedier et al., 2001) and intracellular fluorescence correlation spectroscopy (Waizenegger et al., 2002). Moreover, carboxyfluorescein has been shown to be a useful educt for the synthesis of further fluorescent reagents (Mattingly, 1992;Theisen et al., 1992;Adamczyk et al., 1997).

Labeling of peptides with fluorescein can either be performed in solution or using side chain-protected polymer bound peptides in solid-phase peptide synthesis (SPPS). In most cases reported so far, labeling has been accomplished using activated reagents, namely fluorescein isothiocyanate (Dettin et al., 1998) or carboxyfluorescein-N-succinimidylester (Hoogerhout et al., 1999). However, these activated fluorescein derivatives are rather expensive in comparison to 5(6)-carboxyfluorescein (Weber *et al.*, 1998).

In solid-phase synthesis, coupling of carboxyfluorescein has been accomplished using *in situ* activation with different coupling reagents (Weber *et al.*, 1998;Fulop et al., 2001). However, when applying the published protocols, we detected the formation of various side products. Here we present the elucidation of these side products and their removal by a very simple procedure yielding highly pure carboxyfluorescein-labeled peptides.

When dealing with the synthesis of large peptide collections (Jung *et al.*, 1992) and combinatorial compound libraries (Jung, 1996;Jung, 1999) the use of a large excess of fluorophore is not economical. This is especially the case when isomerically pure carboxyfluorescein is desired (Rossi and Kao, 1997). Thus we

have established a protocol employing far less equivalents of carboxyfluorescein, which still results in complete turnover of the solid-phase bound peptides.

Peptides bearing two different fluorescent dyes extend the use of fluorescently labeled reporter molecules to fluorescence resonance energy transfer (FRET) experiments (Clegg, 1995). These peptides can be used for various *in vitro* applications, e.g. the detection of metal ions (Pearce et al., 1998), the investigation of protein-ligand interactions (Wei et al., 1994) and monitoring of transpeptidation reactions (Kruger et al., 2002) or proteolytic activity (Cummings et al., 2002). In combination with large genetically encoded libraries of protein variants, such compounds have been used as substrates in order to identify proteolytic enzymes with novel substrate specificities (Olsen et al., 2000). For *in vivo* studies, such peptides have been employed for the analysis of cellular uptake and proteolytic processing of peptides (Hoogerhout *et al.*, 1999;Bark and Hahn, 2000).

During solid-phase synthesis of such doubly-labeled peptides, two complications are encountered. (i) The first fluorophore introduced must be chemically inert to the reaction conditions required for the selective deprotection of the second attachment site. (ii) Moreover, the first fluorophore may itself possess functional groups that may react with the activated second fluorophore.

Here a generally applicable strategy is presented in which carboxyfluorescein is introduced as the first fluorophore. By introducing an O-trityl-protecting group to polymer bound carboxyfluorescein, the reaction of an activated second fluorophore with the phenolic hydroxy groups of the fluorescein moiety could be prevented. In addition, carboxyfluorescein was rendered chemically inert to the removal of the Dde-protecting group by hydrazine treatment enabling the orthogonal exposure of a second functional group. Trityl deprotection is achieved during the final TFA-cleavage of the peptide from the resin.

The ability to render carboxyfluorescein chemically inert to a broad range of conditions in SPPS led to the development of a carboxyfluorescein-preloaded resin. This resin is ideally suited for the automated synthesis of large collections of fluorescein-labeled peptides with uniform labeling efficiency, and for the generation of large numbers of doubly-labeled peptides, bearing a fluorescein moiety at the C-terminus and a second dye of choice at the N-terminus.

3.3 Results

3.3.1 Optimization of reaction conditions for fluorescein labeling

The *in situ* generation of active esters in solid-phase peptide synthesis circumvents the need for the synthesis, work-up and storage of water-labile amino acid active esters. Nevertheless the introduction of amine-reactive fluorescent reporter groups has mostly relied on the use of cost-intensive preformed active ester derivatives (Hoogerhout *et al.*, 1999). We applied a protocol describing the introduction of 5(6)-carboxyfluorescein by *in situ* activation using 10 equivalents of dye, DIC and HOBt (1:1:1) and a reaction time of 1 h for the labeling of several peptides (Weber *et al.*, 1998). Using this protocol, we detected several additional products by analytical HPLC and MALDI-MS. The molecular weights of the additional products differed from the masses of the carboxyfluorescein-labeled peptides by additional masses of n times 358.3 Da. These mass differences correspond to the masses of one, and several additional 5(6)-carboxyfluorescein groups.

In order to analyze the identity of the side-products in more detail, Wang resin bound L-phenylalanine was chosen as a model compound. The phenyl moiety enables the detection of unlabeled material by UV-spectroscopy. HPLC-MS analysis of the product (1a) formed by reacting Phe-Wang resin with excess 5(6)-carboxyfluorescein, as described (Weber *et al.*, 1998), confirmed the formation of side products (29% according to HPLC-analysis [214 nm], Fig. 3.1 B). The two positional isomers of Fluo-Phe-OH showed retention times of 21.5 and 22 min ($[M+H]^+$ = 524.2 Da]. Three further products eluted at about 25.5 min ($[M+H]^+$ = 882.3 Da] followed by further additional products eluting at about 27.7 min ($[M+H]^+$ = 1241.1 Da]. The masses of these side products corresponded to carboxyfluorescein-labeled phenylalanine, carrying two and three additional carboxyfluorescein molecules. These side products could also be detected by MALDI-MS (Fig. 3.1 A). Treatment of resin 1 with piperidine/DMF (1:4, v/v) prior to TFA cleavage removed these side products, yielding highly pure Fluo-Phe-OH (Fig. 3.1 B, 1a).

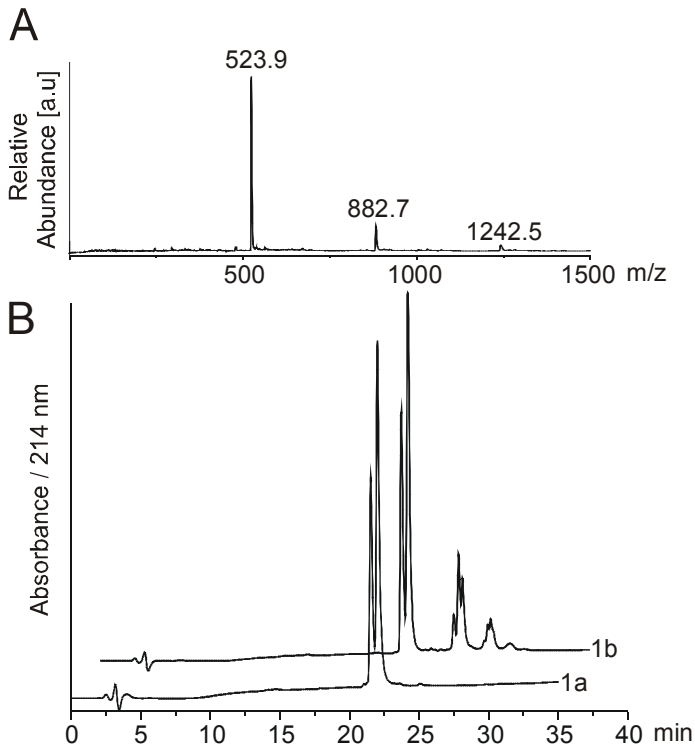

Figure 3.1 (A) MALDI mass spectrum of Fluo-Phe-OH (compound 1b, theor. $[M+H]^+$ = 524.5 Da) without piperidine treatment. The side products ($[M+H]^+$ = 882.7 Da, $[M+H]^+$ = 1242.5 Da) differ by mass differences corresponding to one and two additional carboxyfluorescein moieties. (B) HPLC elution profiles of Fluo-Phe-OH synthesized with (compound 1a) and without (compound 1b) subsequent piperidine treatment. LC-MS analysis revealed the following masses: products eluting at 21.5 and 22 min, $[M+H]^+$ = 524.2 Da; three products at 25.5 min, $[M+H]^+$ = 882.3 Da; several additional products at 27.7 min $[M+H]^+$ = 1241.1 Da. The larger number of peaks for side products with higher molecular masses and eluting at later times may be explained by side products carrying different combinations of 5- and 6-carboxyfluorescein.

Even though complete turnover of the starting material was achieved in only 1 h, the use of 10 equivalents of dye and coupling reagent is uneconomical. For this reason, fewer equivalents but longer reaction times were tested as an alternative coupling condition. Labeling of Phe-Wang resin with only 2.5 equivalents of 5(6)-carboxyfluorescein, DIC and HOBt (1:1:1) for 16 h resulted in complete acylation as monitored by Kaiser-Test. However, side products bearing additional carboxyfluorescein moieties were still formed. Again, the removal of these side products was achieved by piperidine treatment (data not shown).

Next, we validated this labeling procedure for the octapeptide DYGIPADH, which has been shown to exhibit selective protein kinase C ε isozyme agonist activity (Chen et al., 2001). Acylation with 2.5 eq of 5(6)-

carboxyfluorescein/DIC/HOBt (1:1:1) for 16 h again resulted in complete formation of the desired product Fluo-DYGIPADH (Fig. 3.2). Without piperidine/DMF treatment of the resin bound carboxyfluorescein-labeled peptide, more than 40% (HPLC, [214 nm]) of the peptide was labeled with more than one molecule of 5(6)-carboxyfluorescein. These analytical data for an N-terminally labeled octapeptide again outline the importance of the piperidine treatment for the generation of carboxyfluorescein-labeled pure products.

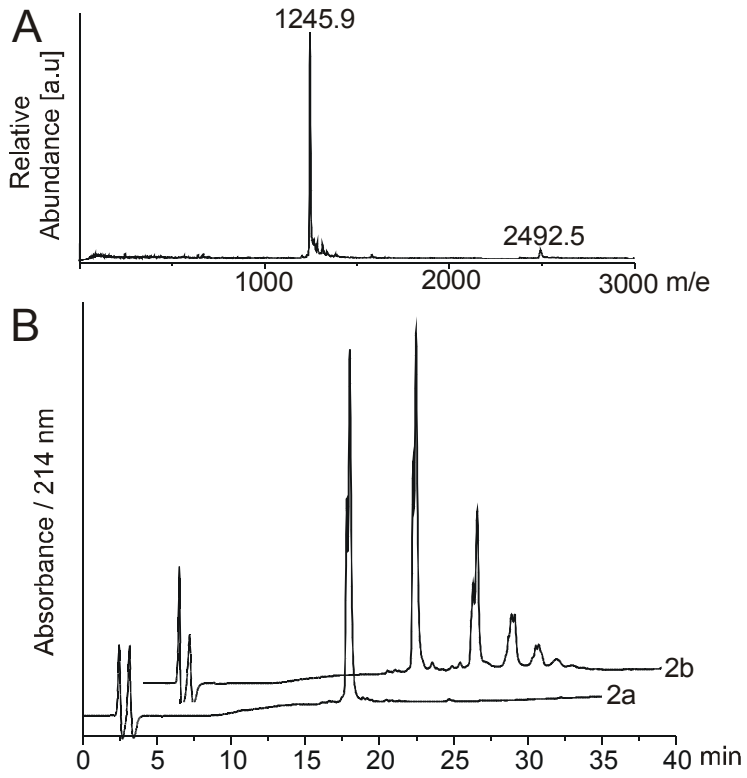

Figure 3.2 (A) MALDI mass spectrum of Fluo-DYGIPADH-OH synthesized with piperidine treatment following the coupling of carboxyfluorescein (compound 2a) (theor. $[M+H]^+$ = 1246.2 Da). (B) HPLC elution profiles of Fluo-DYGIPADH-OH with (compound 2a) and without (compound 2b) piperidine treatment. The unlabeled peptide H-DYGIPADH-OH eluted at 13.5 min, the positional isomers of Fluo-DYGIPADH-OH at 17.8 and 18.0 min. In 2b the side products eluting at 22.5 min, 24.7 min and 26.6 min correspond to peptides carrying several molecules of carboxyfluorescein ($[M+H]^+$ = 1604.4 Da, $[M+H]^+$ = 1963.0 Da, $[M+H]^+$ = 2322.3 Da, respectively).

The MHC class I-binding peptide ligand SIINFEK(Fluo)L (Wiesmüller et al., 1955;Rötzschke et al., 1991) was synthesized in order to confirm that our strategy is also applicable to the labeling of peptides via a lysine side chain. Fmoc-

Lys(Dde)-OH was incorporated by automated SPPS, yielding resin bound SIINFEK(Dde)L. After introducing the Boc protecting group at the N-terminus, the Dde protecting group was removed and the free ε-amino group was labeled with 5(6)-carboxyfluorescein according to our protocol, yielding highly pure peptide.

3.3.2 On-resin O-tritylation of carboxyfluorescein

Peptides labeled with two different fluorescent dyes can either be generated in solution or using side chain-protected polymer bound peptides in SPPS in combination with orthogonal protecting group strategies. The scope of solution phase labeling is severely limited to sequences with special side-chain characteristics (Wei *et al.*, 1994;Geoghegan et al., 2000). Moreover, several laborious purification steps are often required for this approach. In order to explore and optimize the generation of doubly-labeled peptides by an SPPS-based approach, Fmoc-Lys(Dde)-OH (Bycroft et al., 1993;Augustyns et al., 1998) was selected as a building block for the introduction of a second fluorescent dye via a selectively deprotectable lysine side chain (Hoogerhout *et al.*, 1999). The Dde-protecting group can be removed by treatment of the resin bound peptide with 2% hydrazine hydrate/DMF. We chose this strategy instead of the incorporation of Fmoc-Lys(Mtt)-OH (Aletras et al., 1995). When working with Fmoc-Lys(Mtt)-OH in the presence of other trityl-based protecting groups, selective Mtt removal had been difficult to achieve (Bourel et al., 2000). Our strategy, described here, is based on the introduction of carboxyfluorescein at the N-terminus of a solid-phase bound peptide and of a second fluorophore via the selectively deprotectable lysine side chain.

However, exposure of carboxyfluorescein-labeled peptides to 2% hydrazine hydrate/DMF twice for 3 min resulted in the formation of side products eluting several minutes earlier in analytical HPLC and possessing a mass 14 Da higher than that of the desired product.

In order to assess whether this side product was due to the fluorescein moiety, the Fluo-Phe-Wang resin was also treated with 2% hydrazine hydrate/DMF. Again the formation of a side product with a mass surplus of 14 Da decreased the purity of the Fluo-Phe-OH compound by 24% (Fig. 3.3 B). This mass difference is indicative of the formation of a hydrazone or a hydrazide with peptide bound carboxyfluorescein.

At this point we realized that the phenolic hydroxy groups of carboxyfluorescein could be protected by treatment with anhydrides, such as acetic anhydride or

trimethylacetic anhydride. These reactions lead to the conversion of carboxyfluorescein into the corresponding phenolic diesters of the lactone form (Mattingly, 1992;Theisen *et al.*, 1992;Rossi *et al.*, 1997). The conversion of the fluorescein moiety into its lactonic form can be monitored visually by the color change from orange to yellow and the loss of fluorescence. However, due to the lability of these phenolic esters to basic conditions, this protecting group strategy is incompatible with the conditions of hydrazine treatment. Instead, phenols can also be efficiently protected by base-stabile trityl-based protecting groups (Barlos et al., 1991) using trityl chloride for the introduction (Jung, 1996). Removal can be accomplished during TFA cleavage of the peptide from the resin.

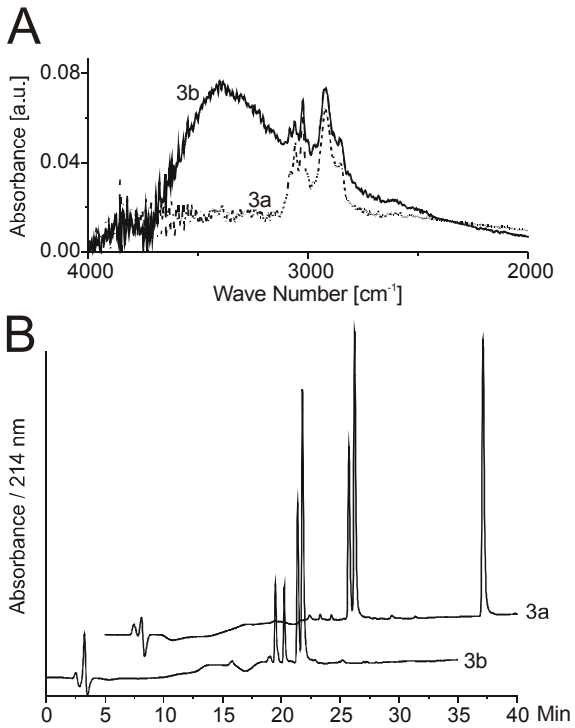

Figure 3.3 (A) Relevant regions of the on-bead FT-ATR-IR spectra of the Fluo(Trt)-Phe-Wang resin (3a) and of the Fluo-Phe-Wang resin (3b). The broad peak at 3300 cm^{-1} indicates the presence of unprotected hydroxy groups of resin bound carboxyfluorescein (3b). For the Fluo(Trt)-Phe-Wang resin no such peak is detectable. The intensities of the two spectra were adjusted according to the intensity of the amide band at 1670 cm^{-1}. (B) Analytical HPLC profile of Fluo-Phe-OH after treatment with 2% hydrazine/DMF, with (compound 3a) and without (compound 3b) prior tritylation. Apart from the two positional isomers of Fluo-Phe-OH ($[M+H]^+$ = 524.1 Da) two side products of compound 3b eluted at 19.5 min and 20.2 min ($[M+H]^+$ = 538.1 Da). In the upper HPLC trace (3a) triphenylmethane, originating from the trityl-protecting group, eluted at 32.1 min.

Fluo-Phe-Wang resin was treated with trityl chloride/DIPEA in DCM. Completeness of the tritylation was confirmed by the disappearance of the infrared band due to free

hydroxy groups (3600-3200 cm^{-1}) by on-bead FT-ATR-IR spectroscopy (Fig. 3.3 A). Moreover, consistent with a conversion of carboxyfluorescein from its acid into its lactone form, the color of the resin changed from orange to yellow. Subsequently, the Fluo(Trt)-Phe-Wang resin was treated with 2% hydrazine hydrate/DMF twice for 3 min. In this case, almost no side product with a mass difference of 14 Da was formed (Fig. 3.3 B). This result clearly demonstrates that the trityl-protecting group renders resin bound carboxyfluorescein stable to the modification by hydrazine.

3.3.3 Synthesis of a doubly-labeled peptide

In order to evaluate the trityl-protecting group strategy for the generation of doubly-labeled peptides, the peptide amide Fluo-APPPEPPP-Pamb-Lys(Tamra) was synthesized using SPPS on Rink amide resin (Fig. 3.4).

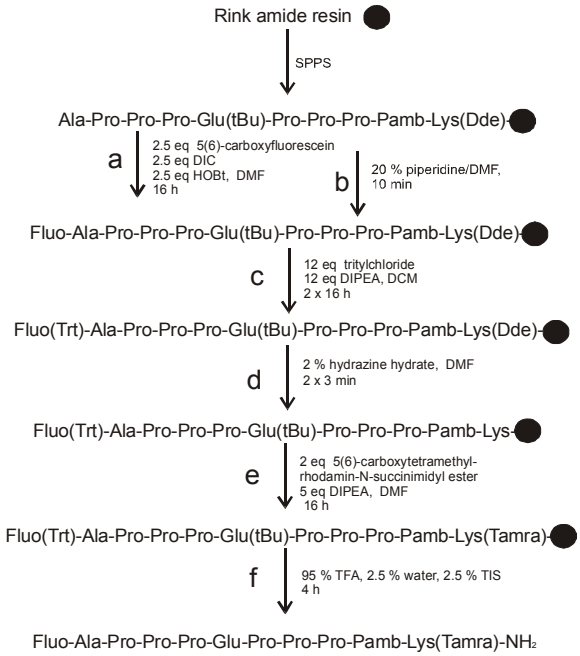

Figure 3.4 Synthesis of the doubly-labeled peptide amide Fluo-APPPEPPP-Pamb-Lys(Tamra)-NH_2 (compound 4). Optimized procedures include the introduction of 5(6)-carboxyfluorescein as the first fluorophore (a), cleavage of the phenolic ester (b), protection of the phenol (c), cleavage of the Dde-group (d), introduction of the second fluorophore (e), cleavage of the peptide (f).

Such L-proline oligomers had been presented as peptide-bridged fluorescence resonance energy transfer cassettes (Li and Glazer, 1999) in order to study FRET characteristics of different dye-pairs. After introducing carboxyfluorescein at the N-

terminus of the resin bound peptide amide APPPEPPP-Pamb-Lys(Dde), piperidine treatment and subsequent tritylation, the Dde-protecting group was removed by hydrazinolysis. The ε-amino group of the C-terminal lysine was dye labeled using activated 5(6)-carboxytetramethylrhodamine-N-succinimidylester. According to analytical HPLC, the purity of the crude Fluo-APPPEPPP-Pamb-Lys(Tamra) peptide amide after cleavage was 85%, (calc. $[M+H]^+$ = 1833.0 Da, exp. $[M+H]^+$ = 1833.2 Da, determined by MALDI-MS). Figure 3.5 shows the fluorescence emission spectra of the doubly-labeled peptide, of 5(6)-carboxytetramethylrhodamine and of 5(6)-carboxyfluorescein. When compared with the free fluorophores the fluorescence of both labels in this peptide was quenched significantly as reported previously for other peptides carrying this combination of fluorophores (Wei *et al.*, 1994;Hoogerhout *et al.*, 1999;Geoghegan *et al.*, 2000).

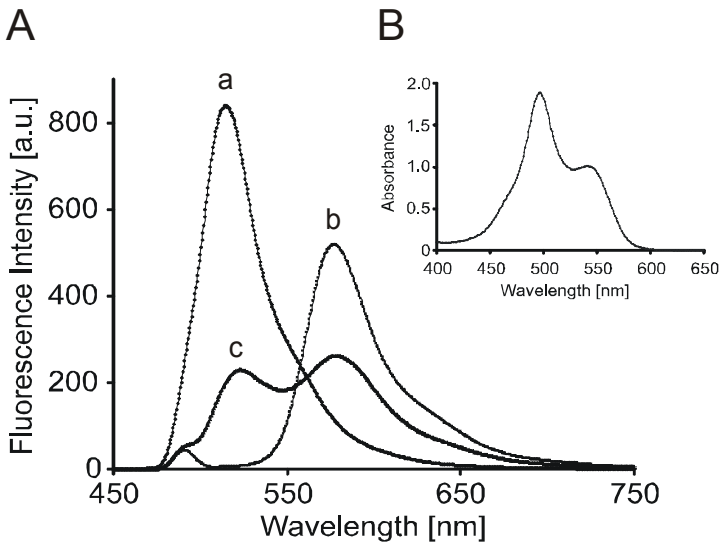

Figure 3.5 (A) Fluorescence emission spectra of 5(6)-carboxyfluorescein (500 nM, curve a), 5(6)-carboxytetramethylrhodamine (1 µM, curve b) and the peptide amide Fluo-APPPEPPP-Pamb-Lys(Tamra)-NH_2 (1 µM, curve c). Fluorescence was excited at 492 nm. (B) Absorption spectrum of the peptide Fluo-APPPEPPP-Pamb-Lys(Tamra)-NH_2.

3.3.4 Generation of a fluorescein-preloaded resin for the automated synthesis of C-terminally labeled peptides

The procedures described so far require the fluorescent derivatization of peptides after automated SPPS. In order to accelerate the generation of carboxyfluorescein-labeled peptides and guarantee uniform labeling yields for all peptides, we decided to establish a resin already carrying a fluorescein moiety. Such a preloaded resin should be compatible with automated parallel peptide synthesis.

Rink amide resin was loaded with Fmoc-Lys(Dde)-OH, followed by deprotection of the N_α-amino group and coupling of 5(6)-carboxyfluorescein, as described. Following tritylation of the fluorescein moiety and removal of the Dde protecting group, the N_α-group was available for further peptide synthesis (Fig. 3.6).

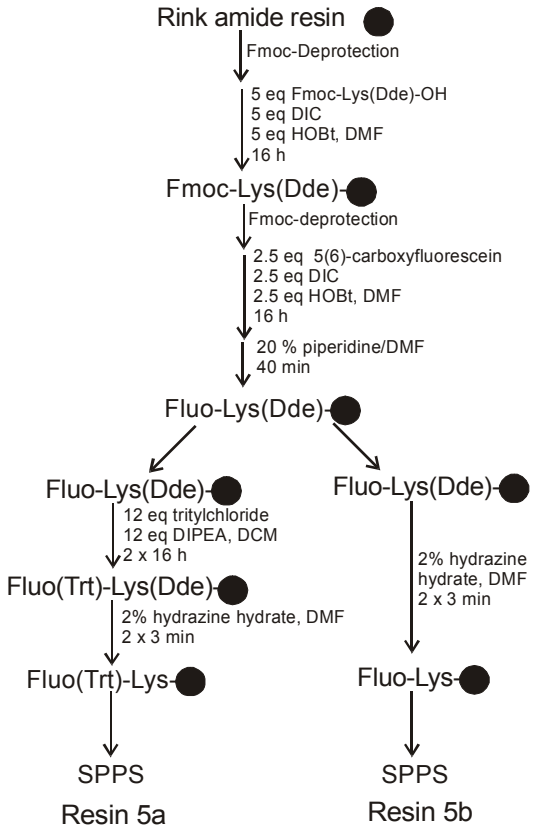

Figure 3.6 Preparation of the N_α-carboxyfluorescein-labeled lysyl-Rink amide resins 5a and 5b with a free ε-amino group for peptide assembly.

A set of four peptides was synthesized by automated parallel peptide synthesis on this resin (resin 5a, Fluo(Trt)-Lys-Rink amide resin) and compared with the peptides synthesized on a resin carrying a non-tritylated carboxyfluorescein moiety (resin 5b, Fluo-Lys-Rink amide resin). Tritylation of the fluorescein moiety increased the purity of all peptides significantly (Tab. 3.1).

Table 3.1 Analytical data for the peptides synthesized on resins 5a and 5b.

Peptide Sequence, calc. $[M+H]^+$	Resin 5a purity, $[M+H]^+$	Resin 5b, purity	Resin 5b, major side product, $[M+H]^+$
Ahx-KGFKGVDAQGTLS-Ahx-εLys(Fluo) 2020.3 Da	90 %, 2019.8 Da	49 %	28 %, 2087.2 Da
DYGIPADH-εLys(Fluo) 1373.4 Da	> 95 %, 1373.2 Da	76%	12 %, 1441.0 Da
APPPEPPP-Pamb-εLys(Fluo) 1420.6 Da	> 95 %, 1420.4 Da	75 %	13 %, 1488.1 Da
Ahx-EQKLISEEDL-Ahx-εLys(Fluo) 1916.2 Da	87 %, 1917.1 Da	48 %	29 %, 1983.6 Da

The purity was increased by about 20% for the two 9mer peptides and by about 40% for the 16 and 13mer peptides. For the non-tritylated resin 5b the ΔM = +14 Da side product (compound 3b) was present, as well as an unidentified side product with a mass surplus of 68 Da (Tab. 3.1). The latter reduced the purity of the peptides most significantly. All peptides synthesized on resin 5b did not exhibit the typical yellow color of fluorescein in aqueous solutions, but a slightly brown color.

3.4 Discussion

This contribution presents optimized coupling procedures and protocols for the generation of fluorescently labeled peptides and particularly doubly-labeled peptides by SPPS. So far no investigator has addressed the chemistry of the introduction of 5(6)-carboxyfluorescein by *in situ* activation in detail. A large excess of fluorophore and coupling reagents for N-terminal labeling of solid-phase bound peptides led to the generation of side products with higher molecular masses which matched multiples of the carboxyfluorescein moiety. Alternative *in situ* activation reagents, such as TBTU, did not affect the formation of these side products (data not shown). Considering the absence of any reactive functional group in the chosen L-phenylalanine model compound, apart from the free α-amino group, the phenolic hydroxy groups of fluorescein are the only available reactive functional groups. In organic solvents, like DMF, fluorescein exists predominantly in its lactonic form (Fompeydie and Levillain, 1980). Evidently, the phenolic hydroxy group of carboxyfluorescein can be acylated by *in situ* activated carboxyfluorescein resulting in the formation of phenolic esters. Moreover, phenolic esters, in particular activated phenyl esters with electron withdrawing groups, are well known to be cleavable by nucleophiles, such as free amino groups of peptides or in basic media. Consistent with this hypothesis, treatment with piperidine readily removed these side products yielding highly pure carboxyfluorescein-labeled peptides.

Completion of removal of the ester bound carboxyfluorescein could be confirmed by the absence of the red color of carboxyfluorescein in piperidine/DMF. It should be noted that using continuous flow-through, the removal of ester bound carboxyfluorescein with 20% piperidine/DMF lasted between 10 and 45 min, depending on the peptide sequence. The use of piperidine for this crucial ester cleavage makes it possible to work with automated parallel SPPS, because piperidine is routinely used for Fmoc-removal during Fmoc/tBu-based SPPS. Moreover, peptide synthesizers are frequently equipped with UV-detection devices in order to monitor Fmoc-removal, which makes it possible to monitor the removal of the carboxyfluorescein molecules.

A considerable reduction of the equivalents of fluorophore and coupling reagents and the extension of the reaction times still ensured a quantitative

turnover. This procedure is especially useful for applications in which the use of isomerically pure carboxyfluorescein is desired, which is far more expensive than the mixture of the two positional isomers (Rossi *et al.*, 1997). Fulop et al. presented the labeling of individual peptides with 1.5 and 3 fold excess and variable coupling times from 4 to 24 h. Here, we validated a 2.5 fold excess and a 16 h coupling time as a general approach yielding complete turn over and high purities of the crude products for a large number of different peptides.

Labeling of resin bound L-phenylalanine with 5-carboxyfluorescein resulted in only one single product peak after piperidine treatment, consistent with a lack of reactivity of the carboxy group in the 2' position. Fluorescein derivatives are known to exist as lactones or free acid tautomers (Anthoni et al., 1995). The lack of reactivity of the 2' carboxy group is indicative of the fact, that fluorescein exists predominantly in its lactonic form in organic solvents, like DMF (Fompeydie *et al.*, 1980).

For further derivatization of fluorescein-labeled peptides, the phenolic hydroxy groups were protected by tritylation. O-tritylation could be monitored by the change of color of the resin from orange to yellow, consistent with a conversion of carboxyfluorescein from the acid into its lactonic form. Completeness of the O-tritylation of the carboxyfluorescein moiety was deduced from on-bead FT-ATR-IR spectroscopy and the resulting chemical inertness. A direct structural confirmation by NMR was not possible due to the failure to release the protected compound from the resin without partial loss of the highly acid labile trityl protecting group.

The availability of a protecting group strategy for carboxyfluorescein compatible with Fmoc/tBu-SPPS and orthogonal side chain protecting groups, such as Dde or allyloxycarbonyl (Alloc) (Loffet and Zhang, 1993), offers highly attractive options for the generation of biological probe molecules carrying a second dye or modification (e.g. a biotin or a lipid moiety) apart from N-terminal carboxyfluorescein. In the absence of tritylation, removal of Dde with hydrazine led to the formation of a side product with a 14 Da mass surplus. While the prevalence of the lactonic form of fluorescein favors the hydrazide as the side product, the formation of the hydrazone with the quinoid carbonyl C-atom of carboxyfluorescein in a residual fraction of the acid form may also be possible.

In spite of the O-tritylation of the Fluo-Phe model compound, minor amounts of the side product were still formed, as shown in Fig. 3.3 B (trace 3a). This residual formation of side product is probably caused by incomplete tritylation and not by the lability of the trityl group. In our hands O-tritylation of carboxyfluorescein has proven to be stable to various conditions of SPPS employing the Fluo(Trt)-Lys-Rink amide resin, i.e. repetitive steps of coupling, piperidine treatment and washing. Methanol was omitted from the washing steps, however, because prolonged exposure to protic solvents led to partial removal of the trityl-protecting group.

O-tritylation enables the efficient synthesis of doubly-labeled peptides because it renders resin bound fluorescein inert towards an activated second dye, which may by itself react with the fluorescein moiety. In contrast to protocols published previously our procedure leads to a major improvement in the purity of the crude peptides and reduces the number of steps required for the generation of a doubly-labeled peptide after automated peptide synthesis from four to only one (Hoogerhout *et al.*, 1999;Kruger *et al.*, 2002).

Finally, the O-trityl-protecting group enabled the development of a Fluo(Trt)-Lys-OH preloaded resin for the generation of C-terminally labeled peptides. This resin eliminates the problem of sequence dependent reaction times necessary for the cleavage of the phenolic esters. Using this resin, carboxyfluorescein-labeled peptides with uniform labeling yields could be obtained by automated procedures. Interestingly, when using non-tritylated carboxyfluorescein for this purpose the major side product was not derived from hydrazine treatment. The major side product accumulated with increasing length of the assembled peptide and showed a mass surplus of 68 Da. This mass difference might be explained by the addition of piperidine under conditions of water condensation. The exact identity of this side product is under investigation.

The Fluo(Trt)-Lys-Rink amide resin is currently used in our laboratory for the parallel-automated synthesis of doubly-labeled peptides, carrying carboxyfluorescein as the C-terminal fluorescent dye and a second fluorophore of choice at the N-terminus. Moreover, we expect that such a resin is of general use in solid-phase synthesis with applications in the generation of fluorescein-labeled combinatorial compound collections.

3.5 Materials and methods

3.5.1 Peptide synthesis

Automated peptide synthesis was performed by solid-phase Fmoc/tBu-chemistry using an automated peptide synthesizer for multiple peptide synthesis (RSP5032, Tecan, Hombrechtlikon, Switzerland) in 2 ml syringes. Fmoc-protected amino acids (twelve fold excess) were activated *in situ* using DIC/HOBt. After 90 min, the Fmoc group was removed by treatment with piperidine/DMF (1:4, v/v) twice for 8 min. The resin was washed with DMF (6x) after each coupling and deprotection step. Side chains of Asp, Glu, Ser, Thr and Tyr were tBu protected, side chains of His and Gln were Trt protected and the side chain of Lys was Boc protected. Fmoc-(4-aminomethyl) benzoic acid (Fmoc-Pamb) was purchased from Neosystem (Strasbourg, France) and Fmoc-Lys(Dde)-OH from Novabiochem (Läufelfingen, Schweiz). 5(6)-carboxyfluorescein (Fluo) and 5(6)-carboxytetramethylrhodamine (Tamra)-N-succinimidylester were from Fluka (Deisenhofen, Germany).

Derivatizations of peptides were performed manually in 2 ml syringes on a shaker at RT. Reactions were stopped by washing the resins 3 times each with DMF, MeOH, DCM and diethyl ether. Completeness of amine acylation was confirmed using the Kaiser-Test (Sarin et al., 1981). Manual Fmoc-deprotection was achieved by treating the resin with piperidine/DMF (1:4, v/v) twice for 10 min. Deprotection of the Dde protecting group was performed using 2% hydrazine monohydrate in DMF (v/v) twice for 3 min.

Unless otherwise stated, peptides were cleaved off the resin using TFA/TIS/H_2O (95:2.5:2.5, v/v/v) for the indicated period of time. Crude peptides were precipitated by adding cold diethyl ether (-20°C). The precipitated peptide was collected by centrifugation and resuspended in cold diethyl ether. This procedure was repeated twice. Finally peptides were dissolved in tBuOH/H_2O (4:1, v/v) and lyophilized.

3.5.2 FT-ATR-IR spectroscopy

On-bead FT-ATR-IR spectroscopy was performed on a Bruker IFS48 Spectrometer (Bremen, Germany). The intensities of the spectra were adjusted according to the intensity of the amide band at 1670 cm^{-1}.

3.5.3 HPLC

Peptides and conjugates were analyzed using analytical RP-HPLC using a water (0.1% TFA) (solvent A)/ACN (0.1% TFA) (solvent B) gradient on a Waters 600 System (Eschborn, Germany) with detection at 214 nm. The samples were analyzed on an analytical column (Nucleosil 100, 250 x 2 mm, C18 column, 5 μm particle diameter; Grom, Herrenberg, Germany), using a linear gradient from 10% B to 100% B within 30 min (flow rate: 0.3 ml/min).

Peptides were purified by preparative RP-HPLC (Nucleosil 300, 250 x 20 mm, C18 column, 10 μm particle diameter; Grom, Herrenberg, Germany) on a Waters 600 Multisolvent Delivery System (flow rate: 10 ml/min). Gradient Systems were adjusted according to the elution profiles and peak profiles obtained from the analytical HPLC chromatograms.

3.5.4 MALDI-MS

One micro liter of DHAP matrix (20 mg of DHAP, 5 mg of ammonium citrate in 1 ml of 80% isopropyl alcohol) was mixed with 1 μl of each sample (dissolved in ACN/water (1:1) at a concentration of 1 mg/ml) on a gold target. Measurements were made using a laser-desorption time of flight system (G2025A, Hewlett-Packard, USA). For signal generation 20-50 laser shots were added up in the single shot mode.

3.5.5 Labeling of peptides with carboxyfluorescein

In all experiments, the isomeric mixture of 5-and 6-carboxyfluorescein (61:39 isomer ratio, purchased from Fluka) was used for labeling, unless otherwise

stated. 5(6)-carboxyfluorescein is also known as 4(5)-carboxyfluorescein (Adamczyk *et al.*, 1997;Rossi *et al.*, 1997).

3.5.6 Fluorescence emission and absorption spectra

Fluorescence emission spectra were recorded from 450 to 750 nm (excitation at 492 nm) at RT in 100 mM Tris/HCl (pH 8.8) using an LS50B spectrofluorometer (Perkin-Elmer, Norwalk, CT, USA). The spectra were corrected for the sensitivity of the detection system. The excitation and emission bandwidths were set to 5 nm. Absorption spectra were acquired using an Ultrospec 2000 (Pharmacia Biotech, Cambridge, England) using 100 mM Tris/HCl (pH 8.8).

3.5.7 Procedures for the synthesis of the different fluorescently labeled compounds

Synthesis of Fluo-Phe-OH (1a and 1b) with high excess of carboxyfluorescein. Fmoc-Phe-Wang resin (14 mg, 10 μmol) was Fmoc-deprotected and treated as described (Weber *et al.*, 1998) for 1 h with 5(6)-carboxyfluorescein (37.6 mg, 100 μmol), DIC (15.5 μl, 100 μmol), HOBt (15.3 mg, 100 μmol) in DMF (130 μl). The resin was divided into two portions of 5 μmol each (1a and 1b). 1a was treated with 20% piperidine/DMF (v/v) in a syringe until the solution was free of excess carboxyfluorescein (15 min). The products (1a and 1b) were cleaved off using TFA/H_2O (97.5:2.5, v/v) over 4 h. After evaporation of the cleavage mixture to dryness, the products were dissolved in ACN/water (1:1), lyophilized and analyzed by HPLC and MALDI-MS.

Synthesis of Fluo-DYGIPADH (2a and 2b) with low excess of carboxyfluorescein. The peptide H-DYGIPADH-OH was synthesized automatically on 2-chlorotrityl resin, which was preloaded with Fmoc-His(Trt)-OH. Resin bound H-DYGIPADH-OH (6 μmol) was allowed to react with 5(6)-carboxyfluorescein (5.6 mg, 15 μmol), DIC (2.3 μl, 15 μmol), HOBt (2.3 mg, 15 μmol) in DMF (150 μl) for 16 h. After washing the resin as described, the resin was

divided into two portions of 3 μmol each (2a and 2b). 2a was treated with 20% piperidine/DMF as described for 1a (45 min).

The carboxyfluorescein-labeled peptides 2a and 2b were cleaved from the resin with TFA/TIS/H_2O (95:2.5:2.5, v/v/v) for 4 h. After precipitation with diethyl ether, both peptides were dissolved in ACN/water, lyophilized and analyzed by HPLC and MALDI-MS.

On-resin introduction of the O-trityl-protecting group to carboxyfluorescein (3). Fluo-Phe-Wang resin (10 μmol) was prepared as described for 1. The resin was then divided into two portions of 5 μmol each (3a and 3b). 3a was treated twice with trityl chloride (16.7 mg, 60 μmol) and DIPEA (10.3 μl, 60 μmol) in DCM for 16 h. Small amounts of resins 3a and 3b were vacuum dried and analyzed by on-bead FT-ATR-IR spectroscopy.

Treatment of 3a and 3b with hydrazine. Resins 3a and 3b were treated twice using 2% hydrazine hydrate in DMF for 3 min and washed thoroughly. Products were cleaved off using TFA/TIS/H_2O (95:2.5:2.5, v/v/v) for 2 h. After evaporation of the cleavage mixture to dryness the products were dissolved in ACN/water, lyophilized and analyzed by HPLC and MALDI-MS.

Synthesis of Fluo-APPPEPPP-Pamb-Lys(Tamra) (4). The peptide amide H-APPPEPPP-Pamb-Lys(Dde)-NH_2 was synthesized by automated solid-phase peptide synthesis on Rink amide resin. H-APPPEPPP-Pamb-Lys(Dde)-NH_2 Rink amide resin (14 μmol) was labeled with 5(6)-carboxyfluorescein as described for 2a and then treated twice with trityl chloride (168 μmol, 46.8 mg) and DIPEA (168 μmol, 28.8 μl) in DCM for 16 h. Subsequently, Dde-deprotection of resin bound Fluo(Trt)-APPPEPPP-Pamb-Lys(Dde)-NH_2 was performed as described. 5(6)-carboxytetramethylrhodamine-N-succinimidyl ester (8 μmol, 4.2 mg) was dissolved in DMF (150 μl) containing DIPEA (20 μmol, 3.4 μl) and the solution was then added to resin loaded with 4 μmol of peptide. After 16 h, the resin was thoroughly washed. Deprotection of the doubly-labeled peptide amide was performed using TFA/TIS/H_2O (95:2.5:2.5, v/v/v) for 4 h. Following ether precipitation, peptide 4 was dissolved in ACN/water, lyophilized and analyzed by HPLC and MALDI-MS.

The peptide was purified as described by preparative HPLC for spectroscopic characterization.

Preparation of Fluo(Trt)-Lys-Rink amide resin (5a, 5b). Fmoc-Rink amide resin (200 μmol, 270 mg) was deprotected and reacted with Fmoc-Lys(Dde)-OH (1 mmol, 533 mg), DIC (155 μl, 1 mmol) and HOBt (153 mg, 1 mmol) in DMF for 16 h. After N_α-Fmoc-deprotection, the N_α-amino group was labeled with 5(6)-carboxyfluorescein as described for 2a, yielding Fluo-Lys(Dde)-Rink amide resin. Immediately afterwards, 50 μmol of the Fluo-Lys(Dde)-Rink amide resin were Dde-deprotected (5a). In a parallel reaction 100 μmol of the Fluo-Lys(Dde)-Rink amide resin was tritylated first as described for 3a and then Dde deprotected (5b). A set of four peptides (as listed in Tab. 3.1) were synthesized by automated peptide synthesis on the ε-lysine side chain of resins 5a and 5b for a comparative study.

4 A quantitative validation of fluorophore-labeled cell-penetrating peptide conjugates: Fluorophore and cargo dependence of import

This chapter was published in Biochimica Biophysica Acta-Biomembranes in 2002. The author of this thesis performed all experiments shown in Figures 1, 2, 5 and 6. Figure 3 was contributed by T. Waizenegger as part of his diploma thesis. Figure 4 gives a comparison between the data obtained by flow cytometry (contributed by R.F.) and FCM (contributed by T. Waizenegger). The author of this work has established FCM for the validation of the cellular import of CPPs during his own diploma thesis. T. Waizenegger has optimized and published these protocols during his diploma thesis (Waizenegger et al. 2002).

4.1 Summary

Cell-penetrating peptides (CPPs) were evaluated for a quantitatively controlled import of small molecules. The dependence of the import efficiency on the fluorophore, on the position of the fluorophore as well as on the nature of the cargo was addressed. Cellular uptake was quantified by flow cytometry and fluorescence correlation microscopy (FCM). Fluorophores with different spectral characteristics, covering the whole visible spectral range were selected in order to enable the simultaneous detection of several cell-penetrating peptide constructs. The transcytosis sequences were based either on the sequence of the Antennapedia homeodomain-derived Penetratin peptide (Antp) or the Kaposi bFGF-derived MTS-peptide. In general, the Antp-derived peptides had a three to four fold higher import efficiency than the MTS-derived peptides. In spite of the very different physicochemical characteristics of the fluorophores, the import efficiencies for analogues labeled at different positions within the sequence of the import peptides showed a strong positive correlation. However, even for peptide cargos of very similar size, pronounced differences in import efficiency were observed. The use of CPP/cargo constructs for intracellular analyses of structure-function relationships therefore requires the determination of the intracellular concentrations for each construct, individually.

4.2 Introduction

Many CPPs were originally considered to cross the plasma membrane in a receptor and energy-independent manner (Derossi et al., 1994;Derossi et al., 1996). More recent data demonstrated, that earlier interpretations of cell-biological experiments, may have suffered from artifactual uptake of CPPs caused by fixation of cells. Endocytosis is currently implicated in the internalization of the HIV-1 Tat peptide (Richard et al., 2003). CPPs represent a structural diverse class of substances. Some CPPs are derived from hydrophobic sequences of signal peptides, such as the Kaposi basic fibroblast growth factor-derived membrane translocating sequence (MTS) (Lin et al., 1995), or from insect proteins, such as the third helix of the DNA-binding domain of the Antennapedia homeodomain protein (Antp) (Derossi et al., 1994). While the former is a highly hydrophobic sequence with 8 out of 16 amino acids being valine and leucine residues and the remainder either alanine or proline, the latter is basic with 7 out of 16 residues being arginine or lysine.

Covalent or non-covalent (Dokka et al., 1997) linkage of CPPs to other molecules mediates the non-invasive import of these cargo molecules into cells *ex vivo*, as well as in whole animals (Schutze-Redelmeier et al., 1996;Schwarze et al., 1999). Such cargo have been peptides (Prochiantz, 1996;Hawiger, 1999), oligonucleotides (Dokka et al., 1997), as well as proteins as large as 120 kDa (Rojas et al., 1998;Schwarze *et al.*, 1999). The capacity to mediate entry of impermeable molecules into cells renders CPPs a valuable tool in the early stages of the drug development process. Import of inhibitors may serve to identify and validate intracellular molecules as targets for achieving a desired therapeutic outcome (Wallace, 1997). Substances exhibiting biological activity for isolated molecules *in vitro*, but unfavourable pharmacokinetic properties for *in vivo* tests may be rendered cell-permeable. Fusion of CPPs to antisense-oligonucleotides has been employed for suppressing the expression of certain proteins (Pooga *et al.*, 1998b). Peptide conjugates have served as pseudo-substrates, competitive inhibitors of the enzyme active site (Rojas et al., 1996) or structural mimics of the interaction domain. The advantages of peptide-based approaches are the accessibility of large collections of different compounds by well-established

automated procedures, as well as the generation of active compounds based on available structural information of interaction domains. Structure-function relationships of intracellular interaction domains have been analysed by testing a series of different peptides fused to a CPP moiety (Liu et al., 1996).

If the import efficiency of CPP-constructs is cargo-dependent, the determination of the intracellular concentrations for each of the CPP/cargo constructs is mandatory, particularly in the analysis of structure-function relationships. Otherwise differences in a biological response may simply reflect differences in uptake efficiency. Fluorescent derivatization of CPPs provides a sensitive and specific quantitative read-out on intracellular peptide concentration using established techniques such as flow cytometry. In addition, the analysis of the subcellular distribution of CPP/cargo constructs by fluorescence microscopy enables the identification of cellular compartments targeted by a cell-penetrating construct. Attaching the fluorescent reporter group to the CPP moiety minimizes the risk of interference of the fluorescent label with the activity of the cargo. By means of chemical ligation (Zhang et al., 1998) or disulfide linkage (Schulz et al., 2000), CPPs or fluorescent analogues of these peptides may be used as building blocks for rendering molecules cell permeable.

To date, however, fluorescent labeling of CPPs has been limited to N-terminal derivatization of peptides either with fluorescein (Scheller et al., 2000;Fischer et al., 2000) or NBD (7-nitrobenz-2-oxo-1,3-diazol-4-yl) (Drin et al., 2001). The import of CPP constructs into cells expressing GFP fusion proteins, as well as the simultaneous detection of several different CPP constructs requires the identification of spectrally distinct fluorophores compatible with import. For this purpose, it needs to be determined to which degree reporter groups with different physicochemical characteristics influence the import characteristics of the CPP constructs. A fluorescein reporter group, for example, carries negative charge, while a tetramethylrhodamine (Tamra) reporter group is zwitterionic. Positive charge as well as hydrophobicity were identified as important physicochemical determinants for import efficiency for the AntpHD peptide (Derossi *et al.*, 1994;Futaki et al., 2001). It was therefore to be expected that the import efficiency of the transcytosis sequences should be affected by the physicochemical characteristics of the fluorophore. Furthermore, fluorescent analogues carrying the fluorophore at a residue within the peptide sequence rather than at the N-terminus

are still missing. Such analogues would enable the N-terminal modification of CPPs with cargo molecules by solid-phase synthesis. In addition, the introduction of one fluorophore within the transcytosis peptide and a second reporter group within the cargo would enable the tuning of the spectral characteristics of double labeled constructs for fluorescence resonance energy transfer (FRET) (Clegg, 1995). Such molecules are valuable tools for the intracellular monitoring of e. g. kinase (Nagai et al., 2000) or protease activity (Jones et al., 2000).

In order to establish fluorescently labeled CPPs as pharmacokinetic modifiers for small molecules, the impact of a fluorescent tag on the ability of the CPPs to enter cells was addressed. For this purpose, sets of analogues labeled with different fluorophores were generated by solid-phase peptide synthesis. Fluorophores were attached to the side chains of lysine residues introduced at different positions within the peptide sequence, and the effect of different fluorophores on import was compared.

For both, the Antp and the MTS peptides, internally labeled analogues were identified with import efficiencies equivalent to the N-terminally labeled peptides. Surprisingly, the relative import efficiencies of peptides labeled either with fluorescein or Tamra at the N-terminus or within the peptide showed a strong positive correlation. This correlation of import efficiencies for fluorescein and Tamra-labeled CPP analogues demonstrates that the capacity for import resides within the structure of the peptide, and is little affected by the physicochemical characteristics of the fluorophore. This finding was confirmed by fluorescence correlation microscopy (FCM) (Brock et al., 1999) of fluorescein and Tamra-labeled peptides at lower nanomolar concentrations. The spectral range was extended to the near infrared by conjugation of an indocyanine dye with Cy5-like (Southwick et al., 1990;Mader *et al.*, 2004) spectral characteristics. Import of three different CPP analogues was simultaneously detected by confocal laser scanning microscopy of living cells.

Finally, the dependence of import on the cargo was addressed for small peptide cargos. Perez et al. have presented one example, in which for one out of three structurally related constructs, import was completely abrogated (Perez et al., 1994). A thorough quantitative analysis of import efficiencies for small peptide cargos has been missing, however. For this purpose a panel of different cargo

peptides of eight to ten amino acids in length, as well as peptides with free or amidated C-termini were synthesized. The intracellular concentrations of these molecules differed by factors of up to eight. These findings underscore the need for an individual determination of intracellular concentrations in applications, such as the intracellular analysis of structure-function relationships and target validation. The results presented in this paper validate fluorescence as the analytical method of choice for these measurements.

4.3 Results

Fluorescently labeled CPPs were established as pharmacokinetic modifiers in intracellular target validation. For this purpose, the import capacity was compared for CPP analogues labeled with fluorophores at different positions along the peptide. Moreover, the dependence of import on the peptide cargo was determined. All peptides were generated by solid-phase peptide synthesis and purified by preparative HPLC. Import of peptides into the human melanoma cell line SKMel37 was quantified in living cells after trypsinization by flow cytometry. Fluorescence correlation microscopy (FCM), as well as confocal laser scanning microscopy was employed to fully interpret the results obtained by flow cytometry.

4.3.1 Internally labeled fluorescent analogues

To this end, import of CPPs had only been observed for peptides labeled with fluorophores at their N-terminus. In order to extend the range of fluorescently labeled CPPs, analogues derivatized with a fluorophore within the peptide sequence were generated.

Table 4.1 Name and sequence of carboxyfluorescein-labeled Antp and MTS analogues. Those peptides marked with an asterisk were also synthesized as carboxytetramethylrhodamine-labeled analogues. “Ac” denotes an N-terminal acetylation, “Ado” represents a hydrophilic 8-amino-3,6-dioxaoctanoic acid building block. All peptides were synthesized as peptide carboxylic acids.

Abbreviation	Amino acid sequence
Antp WT(Fluo)*	Fluo-RQIKIWFQNRRMKWKK-COOH
Antp W6K(Fluo)	Ac-RQIKIK(Fluo)FQNRRMKWKK-COOH
Antp F7K(Fluo)*	Ac-RQIKIWK(Fluo)QNRRMKWKK-COOH
Antp Q8K(Fluo)	Ac-RQIKIWFK(Fluo)QNRRMKWKK-COOH
Antp N9K(Fluo)*	Ac-RQIKIWFQK(Fluo)NRRMKWKK-COOH
MTS WT(Fluo)*	Fluo-AAVALLPAVLLALLAP-Ado-A-COOH
MTS V9K(Fluo)	Ac-Ado-AAVALLPAK(Fluo)LLALLAP-Ado-A-COOH
MTS L10K(Fluo)*	Ac-Ado-AAVALLPAVK(Fluo)LALLAP-Ado-A-COOH
MTS L11K(Fluo)	Ac-Ado-AAVALLPAVLK(Fluo)ALLAP-Ado-A-COOH
MTS A12K(Fluo)*	Ac-Ado-AAVALLPAVLLK(Fluo)LLAP-Ado-A-COOH

The availability of such compounds would (i) significantly increase the options for the generation of doubly-labeled CPP constructs and (ii) enable the N-terminal extension of fluorescently labeled CPPs with cargo. Analogues were generated for both, the Antp and the MTS peptide. The uptake efficiencies were compared and the effect of different fluorophores on uptake properties addressed.

For both transcytosis peptides, series of analogues were synthesized in which one of four consecutive residues in the central portion of the peptide was replaced by a lysine residue derivatized with carboxyfluorescein via its ε-amino group (Tab. 4.1). Relative import efficiencies into adherently growing SKMel37 cells were determined by flow cytometry. As reported earlier for measurements by fluorescence correlation microscopy (Waizenegger et al., 2002), import of the N-terminally labeled Antp analogue was about 2.5 times that of the corresponding MTS analogue (Fig. 4.1).

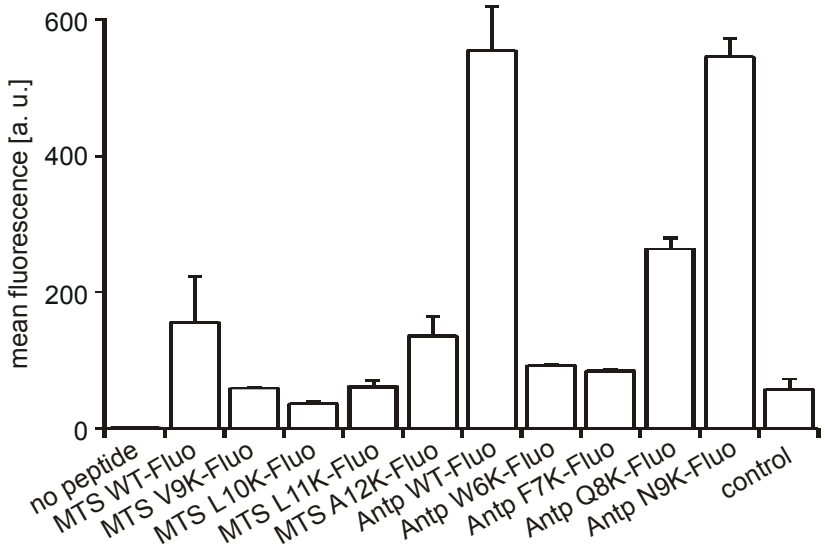

Figure 4.1 Relative import efficiencies of carboxyfluorescein-labeled CPPs. Given are the means for two independent experiments. The experiments were normalized based on the total fluorescence of both experiments. As a control for unspecific peptide binding, the amidated peptide Fluo-Ahx-SFHTMSAAKLI was used. Adherently growing SKMel37 cells were incubated with peptides at a concentration of 4 μM at 37°C for 2 h followed by trypsinization and flow cytometry.

The relative import efficiencies were highly reproducible. Except for the fluorescein-labeled A12K(Fluo) MTS analogue, fluorescent derivatization within the MTS peptide reduced the import efficiency to the levels of unspecific binding and uptake of a fluorescein-labeled control peptide. The import efficiency of the

A12K(Fluo) analogue was about 85% that of the N-terminal analogue. For the Antp peptide, as well, one analogue (N9K(Fluo)) was imported as efficiently as the N-terminal analogue, while the other three fluorescein derivatives showed greatly reduced import efficiencies. For the Q8K(Fluo) analogue, import was reduced by 50% and nearly completely abolished for the other two analogues.

4.3.2 Effect of the fluorophore on import efficiency

So far, fluorescent labeling of CPPs has been limited to the introduction of fluorophores emitting in the short-wavelength visible part of the spectrum. Fluorophores emitting in the orange to far red spectral range are highly desirable for the elimination of autofluorescence (Aubin, 1979) and for the detection of CPPs in the presence of GFP-fusion proteins. The fluorophore tetramethylrhodamine (Tamra) was selected based on its compatibility with solid-phase peptide synthesis, price, high photostability and spectral compatibility with fluorescein and Cy5-like dyes for simultaneous detection. A subset of Tamra-labeled analogues was synthesized and import quantified by flow cytometry (Fig. 4.2 A).

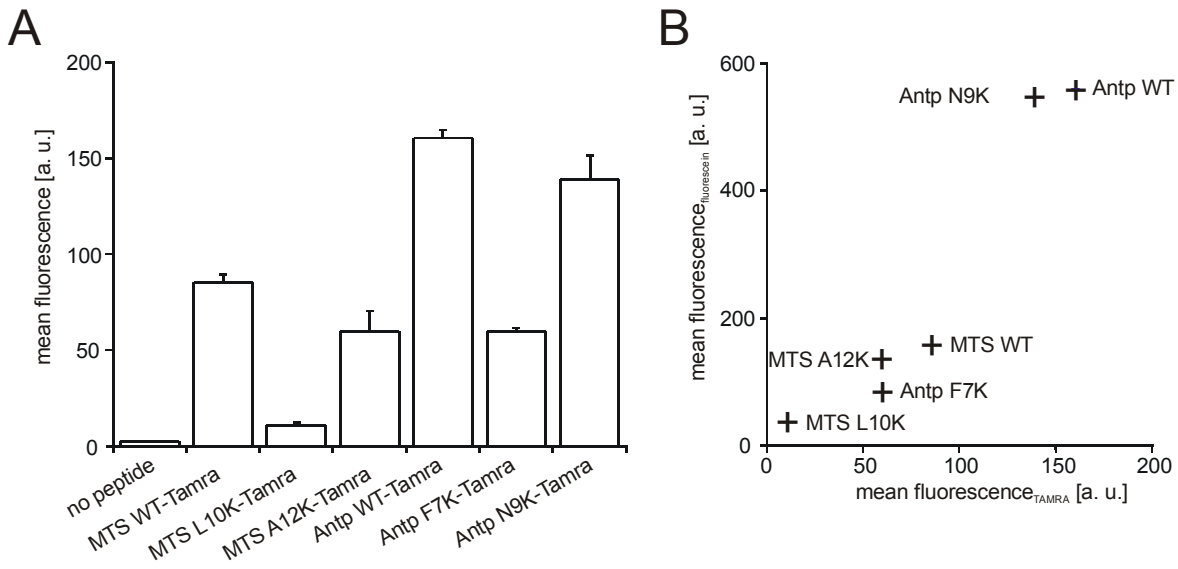

Figure 4.2 Comparison of import efficiencies of carboxyfluorescein and Tamra-labeled CPP analogues. (A) Relative import efficiencies of Tamra-labeled peptide analogues. Adherent SKMel37 tissue culture cells were incubated with peptide at a concentration of 4 μM for 2 h, trypsinized and fluorescence measured by flow cytometry. (B) Correlation of import efficiencies of Tamra and carboxyfluorescein-labeled peptide analogues.

In contrast to fluorescein carrying one negative charge at neutral pH, Tamra is a zwitterionic compound with a neutral net charge. Earlier analyses of structure-function relationships of CPPs had stressed the significance of the physicochemical characteristics of the transcytosis sequence (Fischer et al., 2000). Negative charge, in particular, was shown to be incompatible with import (Scheller et al., 1999). In comparison to fluorescein, it was therefore suspected that Tamra would significantly promote import.

As for the fluorescein analogue, full import capacity was observed for the MTS A12K(Tamra) and Antp N9K(Tamra) variants, while import was abolished for the MTS L10K(Tamra) analogue. In contrast to the fluorescein derivatives, import of the Antp F7K(Tamra) was reduced by only 50%. The relative import efficiencies for the fluorescein-labeled constructs showed a strong positive correlation with those of the Tamra-labeled constructs (Fig. 4.2. B). In spite of the differences in the physicochemical characteristics of the dyes, derivatization of individual residues affected import in a similar way, independent of the dye. Measurements of intracellular concentrations by fluorescence correlation microscopy (see below), revealed that import of the N-terminally labeled Tamra-labeled peptides was more efficient by a factor of 1.5 than that of the respective fluorescein-labeled peptides. Considering the positive correlation of import efficiencies, the Tamra reporter group affected import of all analogues in a similar fashion.

4.3.3 Concentration independence of peptide import

The concentration independence of import is a vital prerequisite for the analysis of intracellular dose-response characteristics using CPP/cargo constructs. To date, however, the analysis of import has been limited to the micromolar range. Recently, we presented intracellular concentration measurements of fluorescein-labeled CPPs in the nanomolar range by fluorescence correlation microscopy (Waizenegger et al., 2002). In contrast to other techniques, FCM allows for a direct determination of molecule numbers. Due to the minuteness of the confocal detection volume (sub-femtoliter), intracellular measurements can be conducted with peptide present in the incubation buffer outside the cell.

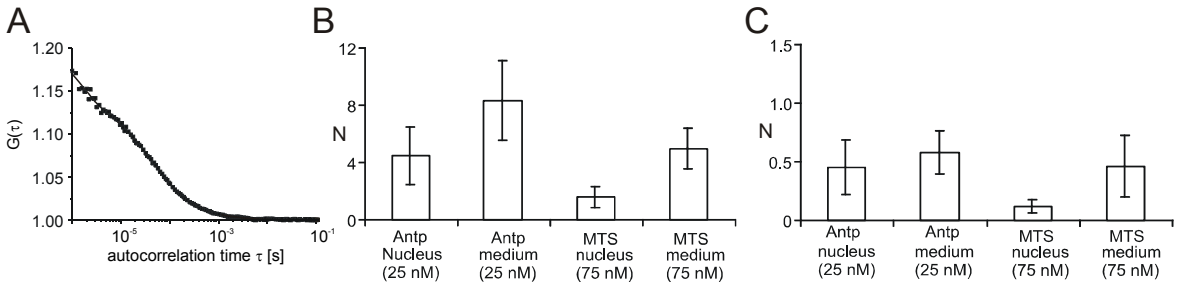

Figure 4.3 Intracellular concentration measurements of CPPs labeled at the N-terminus with either fluorescein or Tamra by fluorescence correlation microscopy. (A) Intranuclear autocorrelation measurement of Fluo-Antp at a concentration of peptide in the buffer of 75 nM. The amplitude of the autocorrelation function at τ=0 s is inversely related to the number of molecules in the confocal detection volume. (B, C) FCM measurements of MTS and Antp peptides labeled at the N-terminus with either carboxyfluorescein (B) or Tamra (C). The number of molecules were derived from two-component fits to the autocorrelation functions and corrected for fluorescence originating from molecules adsorbed to the bottom of the measurement chambers. For MTS peptides as well as for Tamra-labeled Antp peptides the molecule numbers in the buffer were lower than those of the fluorescein-labeled Antp peptide due to stronger absorption of the peptides to the walls and the bottom of the measurement chamber.

Cellular import of analogues labeled at the N-terminus was measured by FCM at lower nanomolar concentrations. Import of peptides was compared by calculating the partition coefficients as the ratio of the number of molecules in the nucleus and in the incubation buffer (Fig. 4.3).

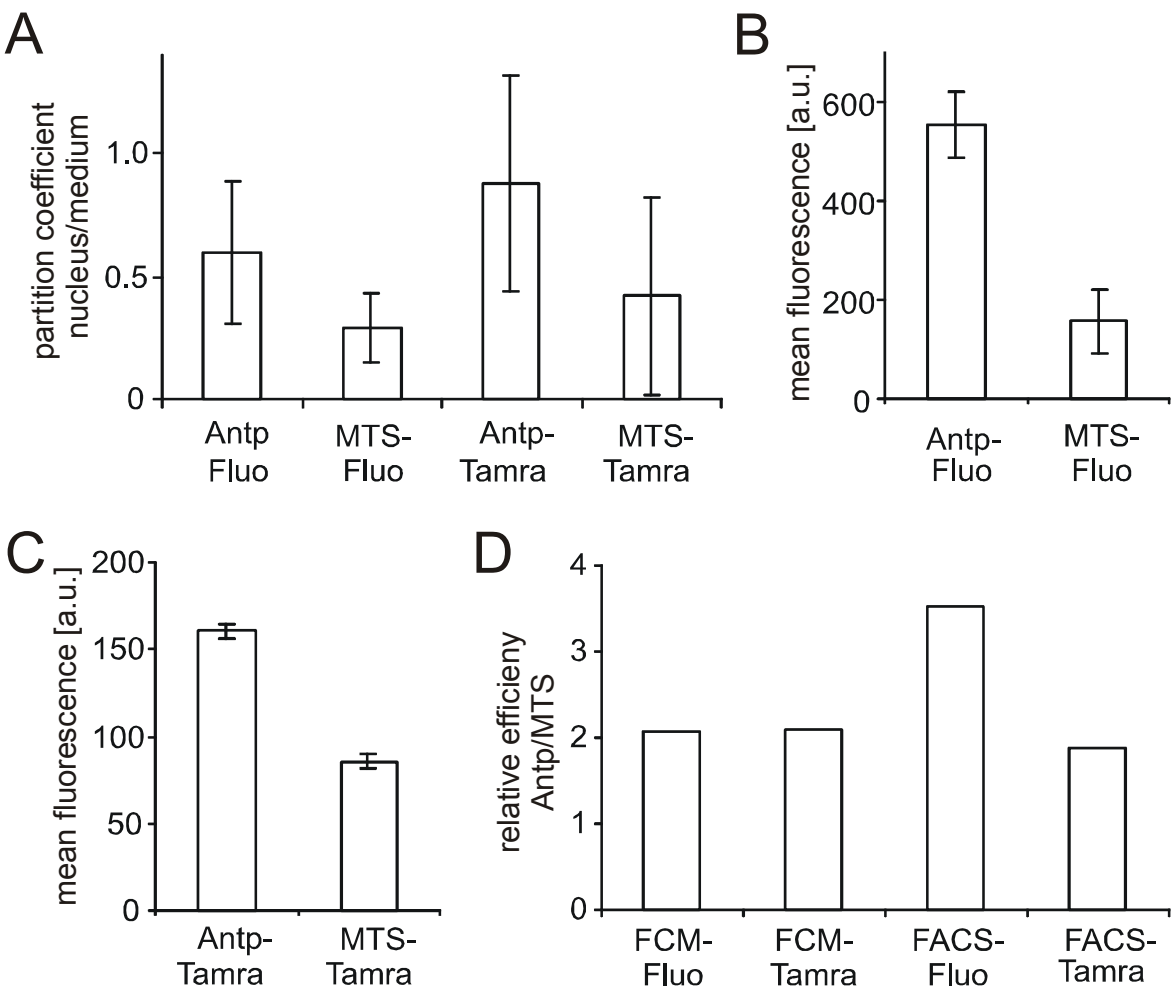

Figure 4.4 Concentration-independence of import. (A) FCM-derived partition coefficients of cellular uptake calculated by dividing the number of molecules in the nucleus by the number of molecules in the incubation buffer (see Fig. 4.3). (B, C) Import efficiencies for Antp and MTS peptides N-terminally labeled with either carboxyfluorescein or Tamra. (D) Comparison of relative import efficiencies of carboxyfluorescein and Tamra-labeled peptides determined by FCM and flow cytometry. For FCM measurements, peptide concentrations were 75 nM for carboxyfluorescein and 25 nM for Tamra-labeled peptides, and 2 μM and 4 μM for flow cytometry. In spite of these very different concentrations, the relative import efficiencies for Antp and MTS labeled peptides agreed with each other.

The Tamra-labeled peptides were internalized more efficiently than the fluorescein-labeled peptides by a factor of 1.5 (Fig. 4.4 A). The application of FCM is limited to the subnanomolar to lower nanomolar concentration range. For this reason, it was impossible to compare the import efficiencies at nanomolar concentrations directly with those at micromolar concentrations. Instead, the relative import efficiencies of fluorescein and Tamra-labeled MTS and AntpHD

peptides determined by flow cytometry (Fig. 4.4 B and C) were compared with those determined by FCM (Fig. 4.4 D).

The larger standard deviations of the FCM data result from the fact that this number is the ratio of the number of molecules outside and inside the cell. A total of at least 30 measurements in eight different cells were included for each condition. The higher standard deviations of the MTS peptides are explained by the stronger absorption to the bottom of the measurement chamber which had to be compensated for in order to determine the intracellular molecule number. A detailed presentation of these intracellular concentration measurements can be found in the publication by Waizenegger et al. (Waizenegger et al., 2002). The relative import efficiencies determined by both methods closely matched one another. If import for either one peptide was concentration dependent, this correspondence of import efficiencies would be very unlikely. This result, therefore, strongly supports a concentration independence of import covering the lower nanomolar to the lower micromolar range. Except for the Tamra-labeled Antp analogue, all partition coefficients were significantly smaller than one (Fig. 4.4 A), i. e. the concentration of the peptide inside the cells was lower than the concentration outside. The peptide concentration in the buffer therefore does not reflect the intracellular concentration; the latter depends on the peptide in each individual case.

4.3.4 Cargo-dependence of import

In order to address the cargo-dependence of import for small peptide cargos in detail, N-terminally labeled Antp analogues with C-terminal peptide cargos of similar size were synthesized. Cargos were representative for primary applications of CPP constructs. These were the Myc-tag peptide EQKLISEEDL, a recently reported peptide inhibitor of the tyrosine kinase ZAP-70 KLILFLLL (Nishikawa et al., 2000), as well as the MHC class I-binding T-lymphocyte epitope SIINFEKL (Rötzschke et al., 1991). The latter two have already been employed in combination with CPPs (Nishikawa *et al.*, 2000;Pietersz et al., 2001).

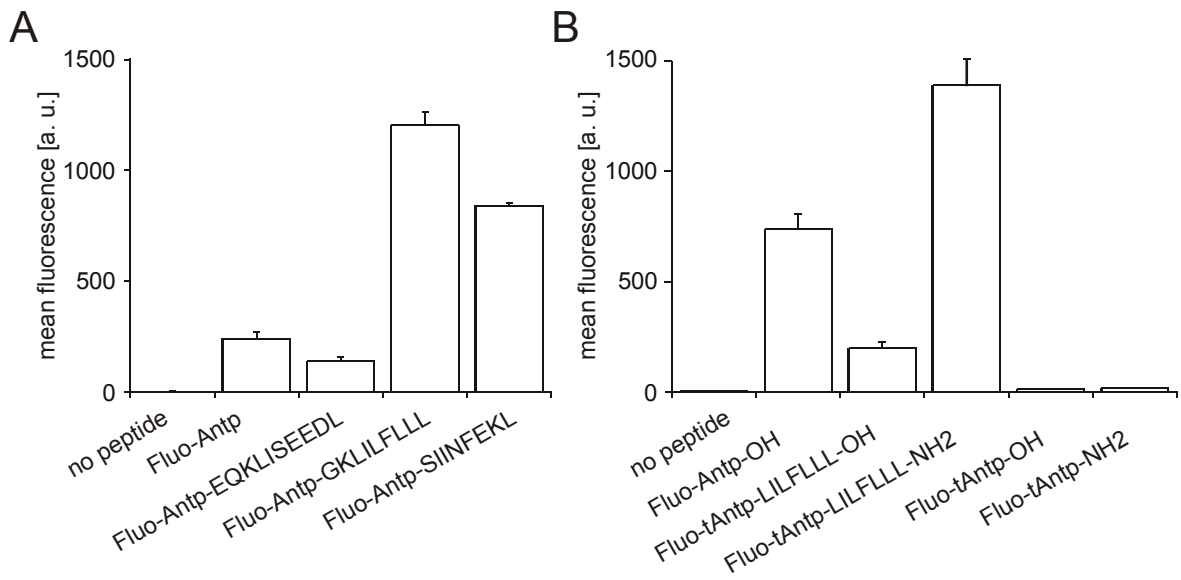

Figure 4.5 Cargo-dependence of import. (A) Import of Antp-based constructs labeled with carboxyfluorescein at the N-terminus. All peptides were synthesized as C-terminal peptide acids (-COOH). The N-terminal glycine residue for the ZAP-70 inhibitor peptide KLILFLLL was introduced as a spacer amino acid. (B) Dependence of import on C-terminal amidation. Constructs were based on a truncated form of the Antp-sequence (tAntp) (Fischer *et al.*, 2000) and the import of these peptides was compared with the import efficiency of the full length Antp peptide. For the inhibitor constructs, the C-terminal lysine residue of the tAntp peptide served as the first residue of the inhibitor. Cells were incubated with 2 μM peptide for 2 h.

Intracellular fluorescence of cells incubated with the Antp-ZAP-70 inhibitor peptide for 2 h was five times that of cells incubated with the Antp peptide alone (Fig. 4.5 A). In contrast to this, the C-terminal extension of the Antp peptide with the Myc-tag peptide decreased the intracellular signal in comparison with the Antp peptide by more than 50%. For the MHC epitope, the intracellular signal was 3.5 times that of the Antp peptide.

The impact of minimal structural differences on import was addressed by quantifying intracellular fluorescence for pairs of peptides with either a free or amidated C-terminus. The constructs were based on a recently described truncated form of the Antp peptide comprising the C-terminal eight amino acids NRRMKWKK only (Fischer et al., 2000). C-terminal amidation had a great impact on import efficiency. Import of the amidated inhibitor construct was seven-times that of the construct with the free carboxy terminus, import of the amidated truncated peptide alone was 1.5 times that of the free acid. In contrast to the initial report on the truncated peptide, in our hands this molecule only translocated weakly. The truncated Penetratin peptides conjugated to the inhibitor peptide,

however, exhibited an internalization efficiency similar to the efficiency of the full length Penetratin.

4.3.5 Triple labeling

The availability of CPPs labeled with spectrally distinct fluorophores affords the use of combinations of different CPP/cargo constructs. In this way, several molecular interactions may be addressed simultaneously. To this end, only one CPP/cargo construct carrying one specific fluorophore has been used at a time. To explore the possibility of simultaneously detecting three CPP constructs in one cell, a further fluorescent analogue emitting fluorescence in the near infra-red part of the spectrum was generated. Cells were incubated with fluorescein-labeled, Tamra-labeled and S0387-labeled Antp (Mader et al., 2004) peptides and fluorescence detected by triple-channel confocal laser scanning microscopy (Fig. 4.6). The cellular localization was very similar for all peptides, with a homogeneously distributed fluorescence present in the cytoplasm and in the nucleus and a vesicular pattern of fluorescence in the extra-nuclear region of the cell. In comparison to the fluorescein- and S0387-labeled peptides, the Tamra-labeled peptide exhibited a stronger tendency to accumulate in vesicular structures.

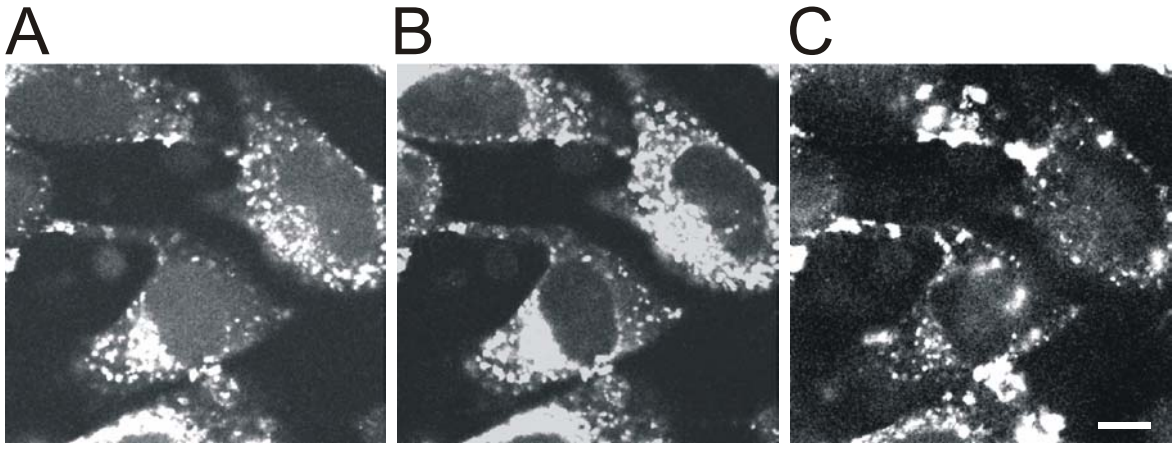

Figure 4.6 Simultaneous internalization of three different CPPs. Carboxyfluorescein- (A), carboxytetramethylrhodamine- (B), and S0387-labeled (C) Antp peptides were detected by multichannel confocal laser scanning microscopy of living cells. Cells were incubated with peptide at concentrations of 4 μM, 1 μM, and 2 μM for the fluorescein-, Tamra-, and S0387-labeled peptides, respectively, for 2 h at 37°C. The rhodamine and S0387 channel were virtually free of cross-talk as determined from control samples loaded with either fluorescein- or Tamra-labeled peptides, alone. The bar denotes 10 μm.

4.4 Discussion

4.4.1 Import efficiencies of fluorescent derivatives

For both the Antp and the MTS peptide, an internally labeled analogue was identified with an import efficiency comparable to the efficiency of the respective N-terminally labeled peptide. All peptides were generated by solid-phase peptide synthesis. The internal label was coupled to a lysine ε-amino-group with the fully side-chain protected peptide still attached to the polymeric support. For this reason, once the peptide moiety is synthesized, the N-terminus of a fully side-chain protected peptide is available for extension with a peptide cargo or non-peptide cargo molecule. Based on this labeling strategy, we anticipate that fluorescently labeled CPPs will gain significance as pharmacokinetic modifiers for small molecules that otherwise do not penetrate the plasma membrane. The fluorophore serves as the reporter group to quantify import of the small molecule.

Import of Antp analogues was more efficient than import of MTS analogues by a factor of about three. So far only few reports exist in which the import competence of different sequence motifs were compared relative to each other. To our knowledge, no direct comparison of a purely aliphatic motif, such as the MTS peptide, and a cationic motif such as the Antp peptide, has been presented so far. One should note, however, that in our case a hydrophilic building block (Ado) was introduced at the C-terminus of the MTS peptide in order to increase the solubility in aqueous buffers. In our hands, Antp is the preferred CPP moiety because of the higher import efficiency, higher solubility in aqueous buffers and comparatively less adsorption to the walls of the measurement chambers (Waizenegger et al., 2002).

By introduction of fluorophores within the central part of the peptide sequence, constructs carrying a second fluorophore either within the cargo or at the N-terminus of the cargo may be generated. Such constructs may serve as cell-permeable probes for intracellular protease activity by detection of fluorescence resonance energy transfer (FRET, (Clegg, 1995)) with optimized FRET characteristics.

The abrogation of import of the Antp W6K(Fluo) construct further substantiates the role of this specific amino acid side chain for import (Derossi et al., 1994).

Interestingly, replacement with the large aromatic fluorophore moiety had the same effect as replacement with alanine (Drin *et al.*, 2001). While import competence may be conveyed by the general physicochemical characteristics of the whole peptide (Scheller et al., 2000), efficient uptake is strongly dependent on the presence of structural determinants at specific positions of the CPP. The finding that only one out of four analogues derivatized with bulky fluorophores at consecutive positions entered cells efficiently supports the view that these peptides associate to a biological membrane in a well-defined orientation (Du et al., 1998;Drin *et al.*, 2001).

The import efficiencies for Antp as well as MTS peptides labeled with the negatively charged carboxyfluorescein strongly correlated with those labeled with the zwitterionic Tamra fluorophore. This finding supports the notion that for these two CPP motifs, efficient uptake is a function of the peptide structure rather than the overall physicochemical characteristic. Surprisingly, the introduction of the negatively charged fluorescein moiety in the central part of the strongly basic Antp peptide was compatible with efficient import. Recently, we introduced fluorescence correlation microscopy for a direct determination of intracellular peptide concentrations (Waizenegger et al., 2002). The determination of partition coefficients for cellular uptake by FCM revealed that import of the Tamra-labeled analogues was slightly more efficient than that of the fluorescein-labeled analogues. From the correlation of import efficiencies we conclude, however, that this effect must be very similar for all Tamra derivatives. Comparison of the cellular distribution of fluorescein and Tamra-labeled peptides having no intrinsic transcytosis capacity has shown that the Tamra label may promote accumulation of these peptides in vesicular structures by itself (own unpublished data). This dye-dependent contribution may provide an explanation for the generally higher import efficiency of Tamra over fluorescein-labeled peptides. One should note that fluorescence correlation microscopy is the only technique capable of comparing import efficiencies for cell-permeable substances labeled with different fluorophores that does not depend on cumbersome calibration procedures to normalize on the detection efficiencies for different spectral ranges.

Comparison of import efficiencies determined by FCM and flow cytometry demonstrated a concentration independence of import from the lower micromolar

to the lower nanomolar range. So far, the analysis of the concentration dependence of import has been limited from the higher nanomolar to the mean micromolar range (Derossi *et al.*, 1996;Mitchell et al., 2000;Fischer *et al.*, 2000). That large of a concentration range could only be covered by combination of these two analytical techniques. Flow cytometry is too insensitive to quantify import in the lower nanomolar range, while FCM can only be used at lower nanomolar concentrations.

To further expand the spectral range of fluorescent CPP derivatives, an N-terminal analogue of Antp labeled with the indocyanine dye S0387 (Mader *et al.*, 2004) was generated and the intracellular distribution investigated with confocal laser scanning microscopy. In this way we were able to demonstrate the simultaneous detection of three different CPP constructs. In all cases, a vesicular staining was present that was most pronounced for the Tamra-labeled derivative. So far the nature of the vesicles has not been addressed. The vesicular accumulation of the CPPs will present some limitation in the analysis of a cargo driven subcellular targeting of CPP constructs, e. g. to target molecules present in specific cellular compartments. Our data indicate that Tamra will be the least suited fluorophore for this kind of application.

4.4.2 Cargo-dependence of import

The independence of import on the nature of the fluorophore was contrasted by a marked dependence on the peptide cargo. Even though all peptides investigated were very similar in size, ranging from eight to ten amino acids, import efficiencies varied by as much as a factor of eight for the Myc-tag peptide and for the ZAP-70 inhibitor peptide. While the Myc-tag peptide is characterized by a negative charge surplus, the Antp-conjugated SIINFEKL-epitope carries one negative net charge, and the ZAP-70 inhibitor peptide is strongly hydrophobic with a neutral net charge. Apparently, a strong negative correlation exists between the negative charge of the cargo and the import efficiency. So far, this observation has only been reported for the transcytosis sequence, alone (Scheller et al., 1999). The effect that subtle structural changes may have on uptake was addressed using a truncated analogue of the Penetratin peptide. For the import peptide alone, as much as for a conjugate with the ZAP-70 inhibitor peptide, C-terminal amidation greatly affected

the import efficiency. Interestingly, the truncated peptide alone was very inefficient in cellular import when compared with the full-length Penetratin peptide. Previously, this peptide was shown to possess about 60% of the translocation efficiency of the full length Antennapedia peptide (Fischer et al., 2000). This discrepancy may result from the differences in assay conditions. In the initial report, a biotinylated analogue was employed and cells were labeled with fluorescently labeled streptavidin after fixation. Fixation, however, may lead to a loss of small molecules due to poor crosslinking. It cannot be excluded that only a fraction of molecules, e. g. those present in vesicular structures, were retained in the cells while the major part of those present in the cytoplasm and nucleus were lost. For this reason, all analyses in our report were based on fluorescence in living cells. In one of the initial analyses of the structure-activity relationship of the Antp-peptide, Derossi et al., reported that removal of only two amino acids from either the N- or C-terminus abolished import (Derossi et al., 1994). For the truncated peptide, import competence was rescued by conjugation of the highly hydrophobic cargo KLILFLLL. It seems that in this case, the cargo complements the cell-permeable moiety.

In summary, attachment of fluorophores that differed markedly in their physicochemical characteristics was tolerated surprisingly well. Import depended much more on the cargo than on the nature of the fluorophore. Analysis of import by FCM revealed that the concentrations in the buffer did not reflect the concentrations of these molecules inside the cells. Both findings stress the need for a detailed monitoring of intracellular peptide concentrations in applications such as the analysis of structure function relationships and quantitatively controlled inhibition of intracellular processes. The fluorescent peptide analogues identified in this study provide the tools for that purpose.

4.5 Materials and methods

4.5.1 Peptide synthesis

Peptides were synthesized in a 15 μmol scale by solid-phase Fmoc-chemistry on an automated peptide synthesizer for multiple peptide synthesis (RSP5032, Tecan, Hombrechtlikon, Switzerland). Fmoc-amino acids were purchased from Novabiochem (Heidelberg, Germany) and Fmoc-protected 8-amino-3,6-dioxaoctanoic acid (Ado) from Neosystem (Strasburg, France). Standard chemicals in peptide chemistry were obtained from Fluka (Deisenhofen, Germany) and Merck (Darmstadt, Germany), solvents were p.a. grade. Peptides were synthesized as free acids on a 2-chlorotrityl resin (capacity 0.5 mmol/g; Senn Chemicals, Dielsdorf, Switzerland) and as peptide amides on Rink amide resin (Rapp Polymere, Tübingen). The amino acid sequence of the Antp peptide was RQIKIWFQNRRMKWKK and of the MTS peptide AAVALLPAVLLALLAP. The MTS peptide was extended at its N- and/or C-termini with one Ado-building block to increase its water solubility.

The resin bound peptides were labeled at the N-terminus with 5(6)-carboxyfluorescein as described (Fischer et al., 2003). Labeling with 5(6)-carboxytetramethylrhodamine was accomplished using 5 eq each 5(6)-carboxytetramethylrhodamine, HOBt and DIC in DMF twice for 20 h. N-terminal labeling of the resin bound Antp-peptide with the free carboxylic acid of the S0387 fluorophore was carried out in the presence of 2 eq of S0387 (FEW, Wolfen, Germany), 5 eq HOBt and 5 eq DIC in DMF twice for 20 h. Conjugation of fluorophores to the ε-amino group of lysine side chains was carried out via incorporation of Fmoc-Lys(Dde)-OH (Novabiochem, Läufelfingen, Switzerland) as building block in peptide synthesis. After Fmoc-deprotection of the N-terminus of the resin bound peptide with piperidine/DMF, the N-terminal amino group was acetylated (Ac_2O/DIPEA/DMF (1:1:8, v/v/v), 2 x 30 min). Removal of the Dde protecting group was performed by treatment with 2% hydrazine monohydrate in DMF (v/v) twice for 3 min. The coupling of the fluorophore followed the same protocol as the one for N-terminal labeling.

The peptides were cleaved off the resin by treatment with TFA/TIS/EDT/H_2O (92.5:2.5:2.5:2.5, v/v/v/v) twice for 2 h each. Peptides were precipitated by addition of diethyl ether (-20°C). Precipitated peptides were washed twice with cold ether. Finally the peptides were dissolved in tBuOH/H_2O (4:1, v/v) and lyophilized.

The peptides were analyzed by analytical reverse phase chromatography RP-HPLC using an H_2O (0.1% TFA)/ACN (0.1% TFA) gradient on a Waters 600 System (Eschborn, Germany) with detection at 214 nm and by MALDI-TOF-MS (Hewlett-Packard G2025A). Peptides were purified by preparative RP-HPLC (Nucleosil 300 C18 column, 10 µm particle diameter, 250 x 20 mm; Grom, Herrenberg, Germany) on a Waters 600 Multisolvent Delivery System using the same gradient system as used for analytical HPLC.

4.5.2 Determination of concentrations of fluorescently-labeled peptides by UV/VIS-spectroscopy

Peptides were dissolved in DMSO at a concentration of 20 mg/ml. These stock solutions were further diluted 1:10 in H_2O. This solution was further diluted 1:100 in 0.1 M Tris/HCl pH 8.8 and the absorbance at the wavelength of 492 nm measured. The concentrations of the stock solutions were calculated assuming $\varepsilon_{carboxyfluorescein,\ 492\ nm}$ = 75,000 l/(mol·cm). Tamra-labeled peptides dissolved in DMSO to about 20 mg/ml were diluted 1:10 in H_2O followed by a 1:100 dilution in methanol. The absorbance of these solutions was measured at 540 nm. The concentrations of the solutions were calculated assuming $\varepsilon_{Tamra,\ 540\ nm}$ = 95,000 l/(mol·cm).

4.5.3 Cell culture

The adherent SKMel37 cell line was grown in a 5% CO_2 humidified atmosphere at 37°C in DMEM with GLUTAMAX I, 25 mM HEPES, 4500 mg/l D-glucose, pH 7.2 (Invitrogen, Karlsruhe, Germany), supplemented with 10% fetal calf serum (PAN Biotech, Aidenbach, Germany), 100 U/ml Penicillin, and 0.1 mg/ml Streptomycin (Biochrom, Berlin, Germany). Cells were passaged by trypsinization

with trypsin/EDTA 0.05/0.02% (w/v) in PBS (Biochrom) every third to fourth day. For growth in chambered cover glasses (Nunc, Wiesbaden, Germany), cells were seeded at a density of 25,000/cm^2 and used for FCM measurements at a confluency of approximately 75%.

4.5.4 Flow cytometry

SKMel37 cells were seeded at a density of 80,000 per well in 24 well plates (Sarstedt, Nümbrecht) in 400 µl serum-containing medium. One day later, the cells were washed with serum-free medium and incubated in 200 µl serum-free medium. After 2 h, peptides were added in concentrations as indicated in the results section. Each condition was tested in duplicate. After 2 h incubation, cells were washed with PBS and trypsinized. The cells were suspended in PBS containing 0.1% (w/v) BSA and 5 mM glucose. Samples were kept on ice and measured immediately. The fluorescence of 5000 vital cells was acquired. Vital cells were gated based on sideward scatter and forward scatter. For the determination of non-specific uptake of fluorescein-labeled peptides, the peptide Fluo-Ahx-SFHTMSAAKLI-$CONH_2$ was added in the same concentration as were the MTS or Antp analogues. This peptide was previously designed as a peptide ligand for the HLA-DRB1*1501 MHC class II molecule (Fleckenstein et al., 1999). It was selected because of the different physicochemical side-chain characteristics and its very different biological relevance.

4.5.5 FCM

FCM measurements were carried out on a ConfoCor2 fluorescence correlation microscope (Carl Zeiss, Jena), equipped with a SensiCam cooled 12-bit CCD camera (PCO Computer Optics, Kelheim, Germany). For image acquisition by whole-field epifluorescence microscopy a filter set consisting of an HQ470/40 excitation filter, a Q495LP beam splitter and an HQ525/50 detection filter (AHF Analysentechnik, Tübingen, Germany) was used for imaging of fluorescein. A combination of an HQ548/10 excitation filter, a Q565LP beam splitter and an HQ610/75 detection filter were employed for imaging of Tamra-labeled samples. For FCS measurements of fluorescein-labeled peptides, the 488 nm line of an

argon ion laser was reflected into the sample via an HFT488 beam-splitter and fluorescence detected with a 500-550 nm band-pass filter. Fluorescence of Tamra-labeled peptides was excited with a 543 HeNe-laser and detected with an HFT 488/543 beam-splitter in combination with a BP 560-615 detection filter. For positioning along the optical axis, the z-scan option of the ConfoCor2 software was employed. Profiles of fluorescence along the optical axis were acquired at 0.4 kW/cm^2 (for both laser lines) at a resolution of 0.5 μm per step. Z-scans were saved by screen capture from the computer screen. The position of the detection volume in the x- and y-dimensions was determined by bleaching a film of fluorescein adsorbed to the surface of a microscopy slide and determining the position of the bleached spot in an epifluorescence image. Positioning in x and y was based on real-time transmission images acquired by the CCD camera using a motorized stage. A series of five subsequent autocorrelation measurements was carried out over 30 s each, for every data point. Laser intensities were 40 kW/cm^2 for fluorescein and 16 kW/cm^2 for Tamra. The individual autocorrelation functions were fitted one-by-one and those unaffected by initial photo bleaching included for averaging.

Reference measurements were carried out for carboxyfluorescein, Tamra, Fluo-Antp, Fluo-MTS and the corresponding Tamra-labeled peptides at concentrations of 25 nM and 75 nM in HBS (135 mM NaCl, 10 mM KCl, 0.4 mM $MgCl_2$, 1 mM $CaCl_2$, 10 mM Na-HEPES, pH 7.4), supplemented with 0.1% BSA and 5 mM glucose in chambered cover glasses without cells in a volume of 400 μl.

For the determination of import efficiencies, the cells were incubated with the fluorescently-labeled peptide in HBS, 0.1% BSA, 5 mM glucose in a volume of 400 μl. The respective concentrations were as indicated. After 1 h incubation at 37^{o}C, FCM measurements were started at RT. Autocorrelation functions were recorded in the nucleus and in the buffer next to each cell. A minimum of eight cells was analysed for each condition. Autocorrelation functions were fitted with the built-in routines of the ConfoCor2 software.

4.5.6 Confocal laser scanning microscopy

Confocal laser scanning microscopy was performed on an inverted LSM510 laser scanning microscope (Carl Zeiss, Göttingen, Germany) fitted with a Plan-Apochromat 63 x 1.4 N. A. lens. Triple detection of fluorescein, Tamra and S0387-labeled peptides was performed using a filter set consisting of an HFT UV/488/543/633 beam splitter in combination with an NFT 545 beam splitter and a BP 505-530 band pass filter for fluorescein detection, an NFT 635 VIS beam splitter and a BP 560-615 detection filter for Tamra detection, and an LP650 long pass filter for S0387-detection. To avoid cross-talk detection, the multi-track modality of the LSM was employed for image acquisition. Live cells were measured in chambered cover slips as in FCM measurements.

5 A stepwise dissection of the intracellular fate of cationic cell-penetrating peptides

This chapter was published in Journal of Biological Chemistry in 2004. The author of this thesis performed all experiments shown.

5.1 Summary

The role of endosomal acidification and retrograde transport for the uptake of the highly basic cell-penetrating peptides Penetratin, Tat and oligo-arginine was investigated. The effect of a panel of drugs that interfere with discrete steps of endocytosis or Golgi-mediated transport on uptake and cellular distribution of fluorescein-labeled peptide analogues was probed by confocal microscopy, flow cytometry and fluorescence spectroscopy of whole-cell lysates. The analyses were carried out in MC57 fibrosarcoma cells and in HeLa cells. While MC57 fibrosarcoma cells showed some vesicular fluorescence and a pronounced cytoplasmic fluorescence, in HeLa cells little cytoplasmic fluorescence was observed. In MC57 cells the inhibitors of endosomal acidification chloroquine and bafilomycin A1 abolished the release of the peptides into the cytoplasm. Release into the cytosol preserved endosomal integrity. In addition, cellular uptake of the peptides was inhibited by brefeldin A, a compound interfering with trafficking in the *trans*-Golgi network. In contrast, nordihydroguaiaretic acid, a drug that stimulates the rapid retrograde movement of both Golgi stacks and *trans*-Golgi network to the ER, promoted a cytoplasmic localization of Tat-peptides in peptide pulsed HeLa cells. The effects of these drugs on trafficking shared characteristics with those reported for the trafficking of plant and bacterial toxins, such as cholera toxin, which reach the cytoplasm by means of retrograde transport. A sequence comparison revealed a common stretch of 8-10 amino acids with high sequence homology to the Tat-peptide. The structural and functional data therefore strongly suggest a common mechanism of import for cationic cell-penetrating peptides and the toxins.

5.2 Introduction

The introduction of membrane-impermeable molecules into mammalian cells has become a key strategy for the investigation of intracellular processes (Stephens *et al.*, 2001). Peptide-mediated import has been attracting growing attention as a delivery technology during the last decade (for reviews see (Fischer et al., 2001;Langel, 2002)). Linkage of CPPs to other molecules mediates the non-invasive import of these cargo molecules into cells *ex vivo* as well as in whole animals (Schutze-Redelmeier et al., 1996;Schwarze et al., 1999). Cargos have been peptides (Prochiantz, 1996;Hawiger, 1999), proteins as large as 120 kDa (Rojas et al., 1998;Schwarze *et al.*, 1999), oligonucleotides (Astriab-Fisher et al., 2002), plasmids (Singh et al., 1999), peptide nucleic acids (PNAs) (Pooga *et al.*, 1998b) and even nanoparticles (Lewin et al., 2000).

Peptide cargos delivered by conjugation to CPPs included pseudo-substrates (Theodore et al., 1995), competitive inhibitors of an enzyme active site (Nishikawa et al., 2000), compartment-specific localization sequences (Lin et al., 1995), structural mimetics of interaction domains (Horng et al., 2001) and epitopes for presentation by MHC class I molecules (Schutze-Redelmeier *et al.*, 1996;Pietersz et al., 2001). The advantages of peptide-based functional analyses in cell biology are the accessibility of large collections of different compounds by well-established automated procedures (Jung *et al.*, 1992) as well as a rational approach to the generation of biologically active compounds based on available structural information of interaction domains. Structure-function relationships of intracellular interaction domains have been analysed by testing a series of different peptides fused to cell-penetrating peptides (Liu et al., 1996). The delivery of exogenous antigens into the MHC class I processing pathway using CPPs has been presented *in vitro* and in whole animals (Schutze-Redelmeier *et al.*, 1996;Pietersz *et al.*, 2001). On dendritic cells CPP-epitope constructs were shown to enable prolonged antigen presentation (Wang *et al.*, 2002). CPPs therefore have the promise to represent a widely applicable means to enhance immune responses against cancer and infectious diseases.

A total of about 20 different peptide delivery vectors have been described so far, the majority of which were identified as structural determinants mediating cellular internalization of proteins (Fischer *et al.*, 2001). While some of these peptides are

purely cationic, others are amphipathic with a large fraction of basic residues and again others are fully hydrophobic. These peptides vary in length from about 9 to more than 30 amino acids (Fischer *et al.*, 2001).

Three highly basic import peptides, the *Drosophila* Antennapedia homeodomain derived Penetratin peptide (Derossi et al., 1994), the HIV-1 Tat derived peptide (Vives *et al.*, 1997) and the oligo-arginine peptides (Futaki, 2002) have been used widely in many of the applications described above. The Penetratin peptide and the HIV-1 Tat peptide have been identified as protein transduction domains (PTDs) of their respective proteins, while the oligo-arginine peptides (among them the nona-arginine peptide R9) have been developed based on structure-activity relationships of the HIV-1 Tat peptide.

Despite their broad acceptance as molecular carriers, the mechanism of internalization of CPPs and CPP/cargo constructs is not well understood. The uptake of the Penetratin and the HIV-1 Tat peptide had originally been described to be insensitive to low temperature (Derossi *et al.*, 1994;Vives *et al.*, 1997;Futaki *et al.*, 2001) and to inhibitors of endocytosis (Vives *et al.*, 1997;Suzuki *et al.*, 2002). Penetratin was also demonstrated to traverse a pure lipid bilayer (Thoren et al., 2000) without forming pores (Thoren *et al.*, 2000;Persson et al., 2003). In summary, these results were consistent with the theory of a direct translocation of the cationic peptides through the plasma membrane (Derossi *et al.*, 1994;Vives *et al.*, 1997;Futaki *et al.*, 2001).

Recent data demonstrated, however, that earlier interpretations of cell-biological experiments, may have suffered from artifactual uptake of CPPs caused by fixation of cells. Endocytosis is clearly involved in the internalization of the HIV-1 Tat peptide (Richard et al., 2003). For Tat fusion proteins it was demonstrated that cellular internalization occurs through a temperature-dependent endocytic pathway that originates from lipid rafts and follows caveolar endocytosis (Fittipaldi et al., 2003). Inhibitors of metabolism or endocytosis, such as cytochalasin D were demonstrated to impair uptake of Penetratin (Drin et al., 2003). Recently, the Penetratin and the Tat peptide were shown to promote endocytosis of high molecular weight cargo upon binding to cell surface glycosaminoglycans (Console et al., 2003).

With a picture of an endocytic uptake mechanism emerging, the implications of the endosomal pathway for functional cell-biological studies using CPPs need to

be readdressed. The biological activity exhibited by CPPs in cell-biological applications (Prochiantz, 1996) is fully consistent with intact CPP-constructs reaching the cytosol. However, the accumulation of CPPs in the endocytic compartment (Richard *et al.*, 2003;Fittipaldi *et al.*, 2003;Drin *et al.*, 2003) raises the question to which degree and by which mechanism internalized CPPs reach the cytosol. A rational design of more effective CPPs can only be achieved if the mechanism of uptake is fully understood.

In this contribution we address these questions by investigating the effect of drugs that interfere with distinct steps of the endosomal pathway and Golgi trafficking. In order to study a potential cell-type dependence of the peptide trafficking, adherently growing MC57 fibrosarcoma cells and HeLa cells were examined. Both cell lines showed marked differences in the intracellular distribution of fluorescein-labeled CPPs.

5.3 Results

5.3.1 Cellular uptake of Penetratin, R9 and Tat peptides

Considering two recent studies demonstrating the involvement of endocytosis in the uptake of the R9-peptide, the HIV-1 Tat peptide (Richard *et al.*, 2003), and Tat fusion proteins (Fittipaldi *et al.*, 2003), we intended to dissect in detail the cellular mechanisms involved in the uptake of cationic CPPs and their release into the cytosol. Initially, the effect of wortmannin, bafilomycin A1 and chloroquine as inhibitors of endocytosis and endosomal acidification on the uptake of fluorescently labeled CPPs was assessed by flow cytometry of living cells. While wortmannin affects early endosome fusion by inhibition of the phosphatidylinositol-3-OH kinase (PI3K) (Simonsen et al., 1998), chloroquine (de Duve et al., 1974;Kozak et al., 1999) and bafilomycin A1 (Bowman et al., 1988;Clague et al., 1994) inhibit endosomal acidification. While chloroquine diffuses across membranes and binds protons, bafilomycin A1 is a highly potent and selective inhibitor of vacuolar H^+-ATPases (Bowman *et al.*, 1988). In addition to R9 and the Tat peptide, the Penetratin peptide was included in this comparison.

Table 5.1 Primary structures of the cell-penetrating peptides used in this study. All peptides were synthesized as peptide amides. Fluo represents an N-terminal fluorescein moiety.

Peptides	Sequences
Fluo-Antp	Fluo-RQIKIWFQNRRMKWKK-$CONH_2$
Fluo-R9	Fluo-RRRRRRRRR-$CONH_2$
Fluo-Tat	Fluo-YGRKKRRQRRR-$CONH_2$

The distortion of uptake experiments by peptides that were only associated with the plasma membrane, but had not been internalized by the cells, was avoided by treating the cells with trypsin prior to flow cytometry (Richard *et al.*, 2003). While Fluo-R9 and Fluo-Antp were taken up efficiently to comparable levels, the intracellular fluorescence of Fluo-Tat was less than 10% of the one of cells treated with the other two peptides (Figure 5.1).

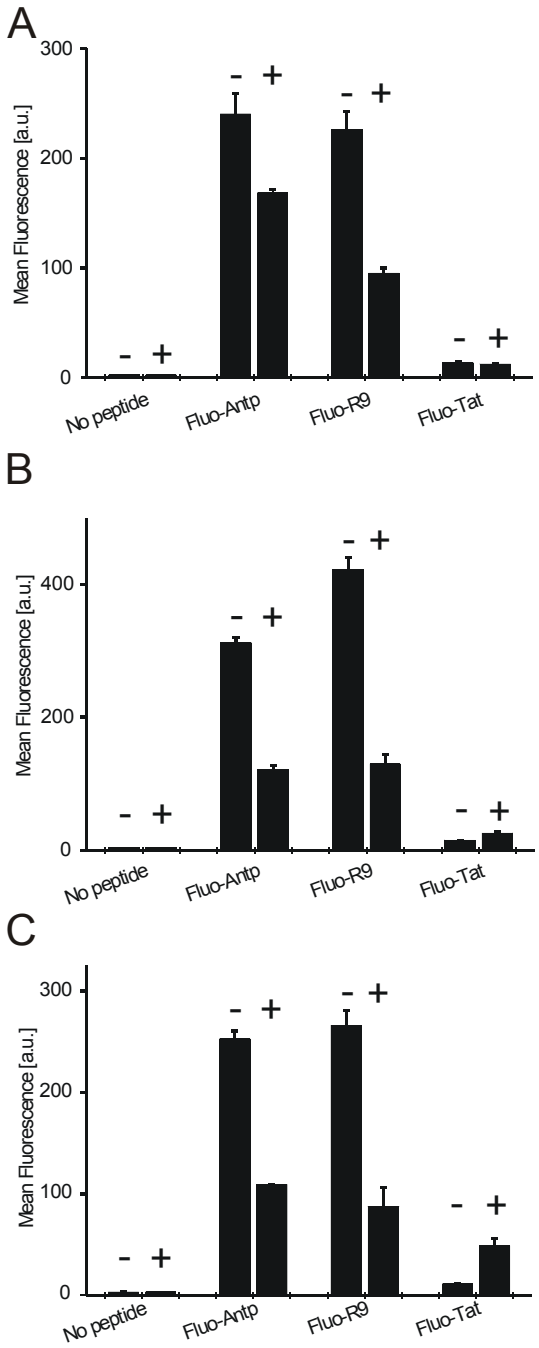

Figure 5.1 Influence of inhibitors of endocytosis on uptake of cell-penetrating peptides. MC57 cells were incubated with carboxyfluorescein-labeled cell-penetrating peptides (1 μM) for 2 h in serum-free medium in the absence (-) or presence (+) of 100 nM wortmannin (A), 300 nM bafilomycin A1 (B), and 100 μM chloroquine (C), washed, trypsinized and analyzed by flow cytometry. The inhibitors were added 30 min prior to the peptide. Each condition was tested in duplicate; error bars represent the absolute deviations from the mean value.

For Fluo-R9 and Fluo-Antp, all three inhibitors led to a reduction of the cellular fluorescence by about 50%. In contrast, for the Fluo-Tat peptide only little effect of

wortmannin was observed while for chloroquine and bafilomycin A1 intracellular fluorescence increased.

5.3.2 Impact of bafilomycin A1 on the cellular distribution of fluorescently labeled CPPs

In order to explain the contrasting results for Fluo-Tat and the other two peptides obtained by flow cytometry, the effect of bafilomycin A1 on the intracellular localization of the peptides was addressed using confocal laser scanning microscopy. Live cell confocal microscopy was performed after 2 h incubation with peptides at 37°C. Images were acquired in the presence of peptide in the medium in order to avoid loss of cellular fluorescence due to wash out (Scheller et al., 2000). In order to compensate for the lower cellular fluorescence of Fluo-Tat, this peptide was applied at a five-fold higher concentration (5 μM). For all three CPPs, both a distinct vesicular staining and cytoplasmic localization were detected (Figure 5.2 A, B, C, upper panels). Cytoplasmic fluorescence was weakest for the Fluo-Tat peptide. For the Fluo-R9 peptide a slight nuclear enrichment of fluorescein fluorescence in MC57 cells could be observed (Fig. 5.2 C).

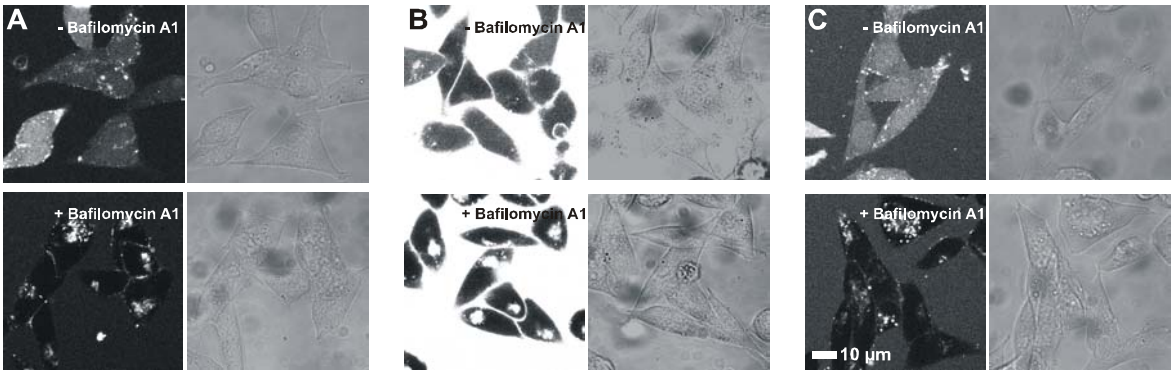

Figure 5.2 Lack of cytosolic fluorescence by inhibition of endosomal acidification. MC57 cells were incubated with serum-free medium containing 1 μM Fluo-Antp (A), 5 μM Fluo-Tat (B), and 1 μM Fluo-R9 (C) for 2 h and analyzed by confocal laser scanning microscopy in the presence of peptide in the medium. Bafilomycin A1 (300 nM) was added 30 min prior to the peptide. Fluorescence images are shown in the left panels, transmission images in the right panels. The bright fluorescence outside the cells for the Fluo-Tat peptide is explained by the five-fold higher concentration used for this peptide in order to compensate for the less efficient intracellular accumulation of this peptide.

When bafilomycin A1 was added to the incubation medium, no cytoplasmic fluorescence was present for any of the three CPPs. Instead, the vesicular staining was enhanced for all three peptides. Using chloroquine as an inhibitor of endosome maturation, essentially the same effect was observed. However, this inhibitor led to the formation of large vesicular structures (data not shown).

5.3.3 Exit of Fluo-Tat from the cytosol

While bafilomycin A1 and chloroquine led to a reduced uptake of Fluo-Antp and Fluo-R9, for Fluo-Tat cellular fluorescence increased. This result is in apparent disagreement with a common internalization mechanism of Tat and R9 (Suzuki *et al.*, 2002). Bafilomycin A1 leads to the accumulation of both peptides in vesicular structures thereby inhibiting their release into the cytoplasm. For this reason the increase in cellular Fluo-Tat fluorescence caused by bafilomycin A1 as observed by flow cytometry (Fig. 5.1 B) might be due to the ability of Fluo-Tat or fluorescent proteolytic fragments to leave the cells rapidly after entry into the cytosol in the absence of bafilomycin A1. In order to test this, MC57 cells were pulsed with the three fluorescently-labeled CPPs for 2 h, washed and then incubated with peptide-free medium for an additional 3 h (Scheller *et al.*, 2000). The Fluo-Tat peptide was again applied at a five-fold higher concentration (5 μM). Cellular fluorescence of MC57 cells after pulse and pulse-chase was determined by flow cytometry (Fig. 5.3 A). Both, the Fluo-Antp and the Fluo-R9 peptides were not chased out of the cells efficiently. However, for Fluo-Tat after a 3 h chase period, only very little fluorescein fluorescence remained associated with the MC57 cells. Two different explanations were considered as the basis for this experimental outcome. First, in contrast to Penetratin and oligo-arginine, the Tat peptide itself could possess the ability to exit the cells by crossing the plasma membrane. Second, instead of the intact full-length peptide, fluorescent fragments generated by proteolytic break-down could leave the cell by diffusion through the plasma membrane. In order to answer this question, supernatants of MC57 cells after the chase period were desalted, concentrated and analyzed by mass spectrometry (Fig. 5.3 B). Peptide fragments bearing an N-terminal carboxyfluorescein and one to six amino acids were specifically detected in chase-supernatants of peptide-pulsed cells. Intact Tat-peptide could not be detected. This data strongly supports that the loss of fluorescence is due to exit of fluorescent peptide fragments during the 3 h chase period.

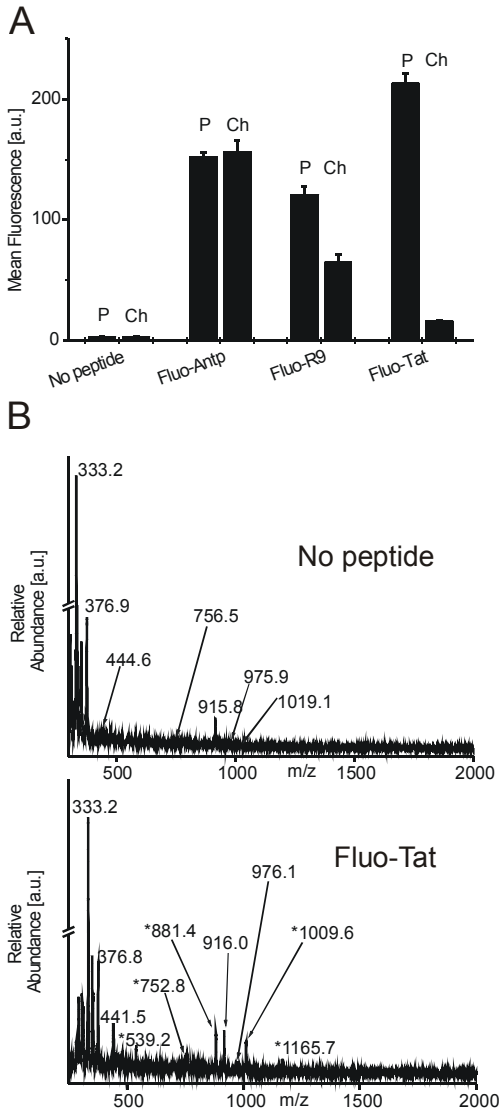

Figure 5.3 Pulse/chase experiments. (A) MC57 cells were incubated with Fluo-Antp (1 μM), Fluo-R9 (1 μM) or Fluo-Tat (5 μM) for 2 h. Internalization was monitored by flow cytometry (P, pulse). For the chase value, aliquots of peptide-loaded cells were washed and incubated with peptide-free medium for additional 3 h. The remaining cellular fluorescence was determined by flow cytometry (Ch, chase). The Fluo-Tat peptide was applied in a five-fold higher concentration in order to compensate for the less efficient intracellular accumulation of this peptide. Each condition was tested in duplicate; error bars represent the absolute deviations from the mean value. (B) MC57 cells were incubated -/+ 30 μM Fluo-Tat for 2 h. After 2 h the cells were detached, washed, resuspended in serum-free medium and incubated for additional 3 h. The supernatants were desalted, concentrated and subjected to MALDI-TOF-MS-analysis (B). Fluo-Tat derived signals are highlighted with an asterisk. Calculated $[M + H]^+$: Fluo-Y-OH, 540.5 Da; Fluo-YG-OH, 597.6 Da; Fluo-YGR-OH, 753.7 Da; Fluo-YGRK-OH, 881.9 Da; Fluo-YGRKK-OH, 1010.1 Da; Fluo-YGRKKR-OH, 1166.3 Da.

5.3.4 Effect on endosomal integrity and intracellular peptide stability of CPPs

Having shown that inhibitors of endosomal acidification inhibited the release of cationic CPPs into the cytosol, we next asked whether entry into the cytoplasm involves destabilization of endosomal membranes after endosomal acidification. Such a mechanism has been described e.g. for peptides containing the N-terminal sequence of influenza virus hemagglutinin HA-2 (Plank et al., 1994). MC57 cells were incubated with medium containing high molecular weight (10,000 Da) AlexaFluor 647-dextran in the absence or presence of Fluo-Antp for 2 h. Dextrans are internalized by fluid-phase endocytosis and accumulate in vesicles that appear as bright spots (Plank *et al.*, 1994) (Fig. 5.4 B). When MC57 cells were co-incubated with AlexaFluor 647-dextran and Fluo-Antp the AlexaFluor 647 dextran partially co-localized with Fluo-Antp in vesicular structures. However, the morphology of the AlexaFluor dextran-spots did not change, even though the Fluo-Antp peptide clearly localized to the cytoplasm (Fig. 5.4 F and G), indicating that Fluo-Antp does not disrupt endosomal membranes. In order to address cellular peptide integrity, after 2 h peptide incubation, cell lysates were prepared and subjected to MALDI-TOF-MS analysis, essentially as described previously (Elmquist and Langel, 2003). Comparison of isolates from peptide-loaded and peptide-free cells revealed two peptide-specific signals ($[M + H]^+$ = 2605.3 Da and $[M + H]^+$ = 531.3 Da). The former corresponds to the intact Fluo-Antp peptide with a calculated $[M + H]^+$ of 2605.1 Da and the latter most likely to Fluo-R-OH with a calculated $[M + H]^+$ of 533.5 Da (Fig. 5.4 I).

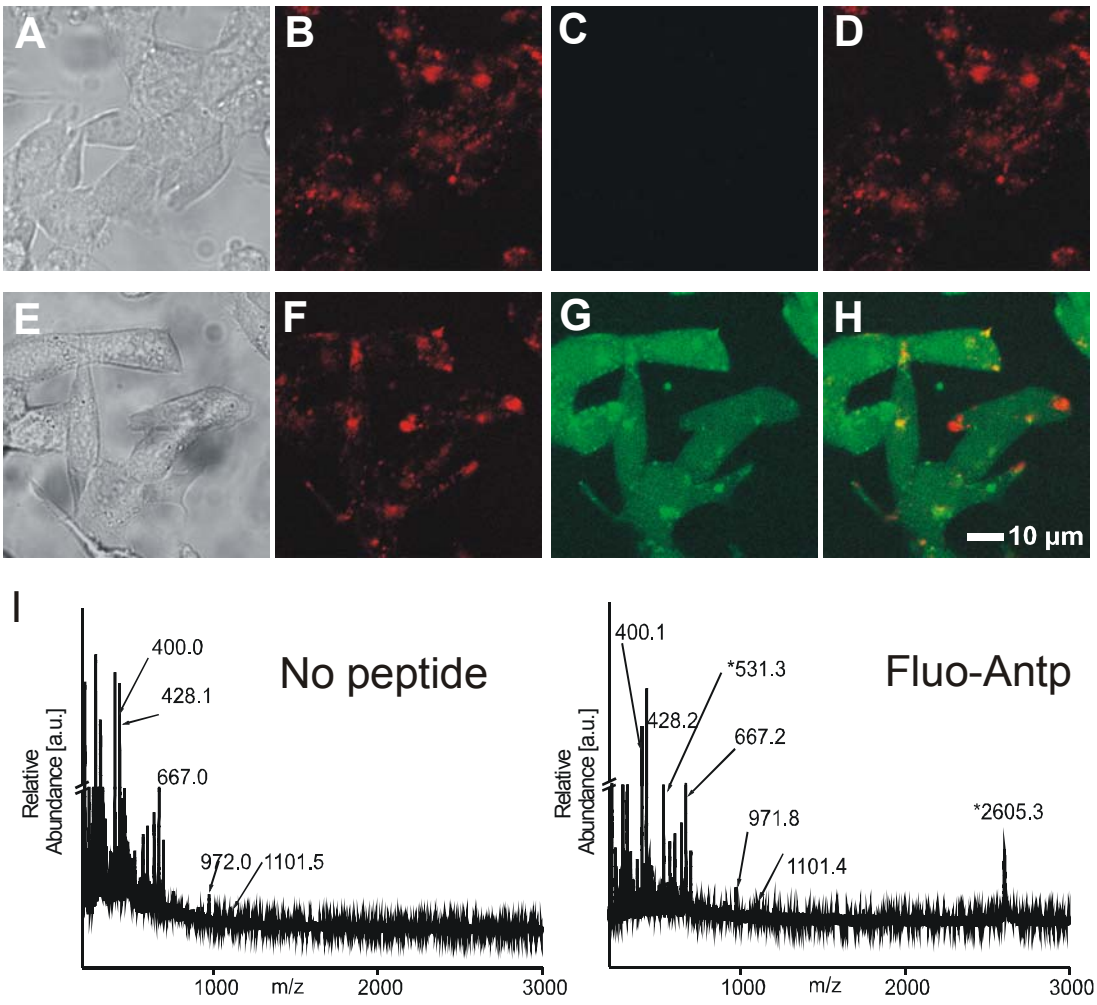

Figure 5.4 Pulse/chase experiments and preservation of endosomal integrity in the presence of Fluo-Antp and intracellular stability of Fluo-Antp. MC57 cells were incubated with serum-free medium containing 5 µM of AlexaFluor 647-dextran alone (A-D), or a combination of 5 µM of AlexaFluor 647-dextran and 1 µM Fluo-Antp (E-H) for 2 h, washed and analyzed by multi-channel confocal laser scanning microscopy. Panels A and E show transmission pictures, panels B and F the AlexaFluor 647-dextran fluorescence, panels C and G the fluorescein fluorescence and panels D and H the superposition of both fluorescence channels.

(I) MC57 cells were incubated -/+ 15 µM Fluo-Tat for 2 h. After 2 h the cells were trypsinized, washed and lysed. The lysates were desalted, concentrated and subjected to MALDI-TOF-MS-analysis. Fluo-Antp derived signals are highlighted with an asterisk. Calculated $[M + H]^+$: Fluo-R-OH, 533.5 Da; Fluo-RQIKIWFQNRRMKWKK-NH_2, 2605.1 Da.

5.3.5 The subcellular distribution of CPPs is cell-type dependent

CPPs have been applied for loading of molecules into a variety of different cell lines, including tissue culture cells and primary cells growing adherently as well as in suspension. A limited number of studies have demonstrated that for a given CPP-containing molecule uptake efficiency is cell-type dependent (Mai et al., 2002;Violini et al., 2002). In these previous studies whole cell read-outs (Mai *et al.*, 2002) or microscopy of fixed cells (Mai *et al.*, 2002;Violini *et al.*, 2002) were employed for comparison of uptake efficiencies. Using confocal microscopy of living cells, we determined whether a cell-type dependence could be observed for the subcellular distribution of fluorescein-labeled CPPs. HeLa cells were chosen as a second cell line, because in the study of Richard et al. (Richard *et al.*, 2003) this cell line was also investigated. In contrast to MC57 cells (Fig. 5.5 A, upper panels) at a concentration of 1 μM, in HeLa cells the Fluo-Antp peptide was only detectable in vesicular structures (Fig. 5.5 A, center panels), as was the case for the Fluo-R9 peptide (data not shown). The same difference in localization was observed when both cell lines were co-cultivated and co-incubated with the Fluo-Antp peptide in order to rule out any artifacts from cultivation conditions (Fig. 5.5 A, lower panels).

At this point two possibilities were considered as the basis for this observation. First, uptake into HeLa cells may be less efficient than uptake into MC57 cells. Second, intracellular trafficking may be different in both cell lines. Analysis of cellular fluorescence of Fluo-Antp by flow cytometry yielded comparable intracellular fluorescence for both cell lines (Fig. 5.5 B). However, vesicular accumulation of fluorescein labeled peptides may lead to concentration quenching of fluorescein fluorescence (Chen and Knutson, 1988). Moreover, the fluorescence of fluorescein is strongly pH dependent, compromising a quantitative comparison of the amounts of peptide localized in acidic vesicles with that localized in the cytoplasm. For this reason, whole cell lysates of MC57 and HeLa cells loaded with peptide were prepared and the amount of fluorescein was determined by fluorescence emission spectroscopy (Fig. 5.5 C). In spite of the very similar cellular fluorescence observed by flow cytometry, analysis of lysates revealed that HeLa cells internalized three times more peptide than MC57 cells (Fig. 5.5 C). For

this reason, the differences in the distribution of cellular fluorescence do indeed reflect differences in the intracellular trafficking of peptide in these two cell lines. However, for treatment with bafilomycin A1, a similar reduction of cellular fluorescence was observed for both cell lines, indicating that the differences in localization reflect quantitative differences in trafficking rather than a different mechanism.

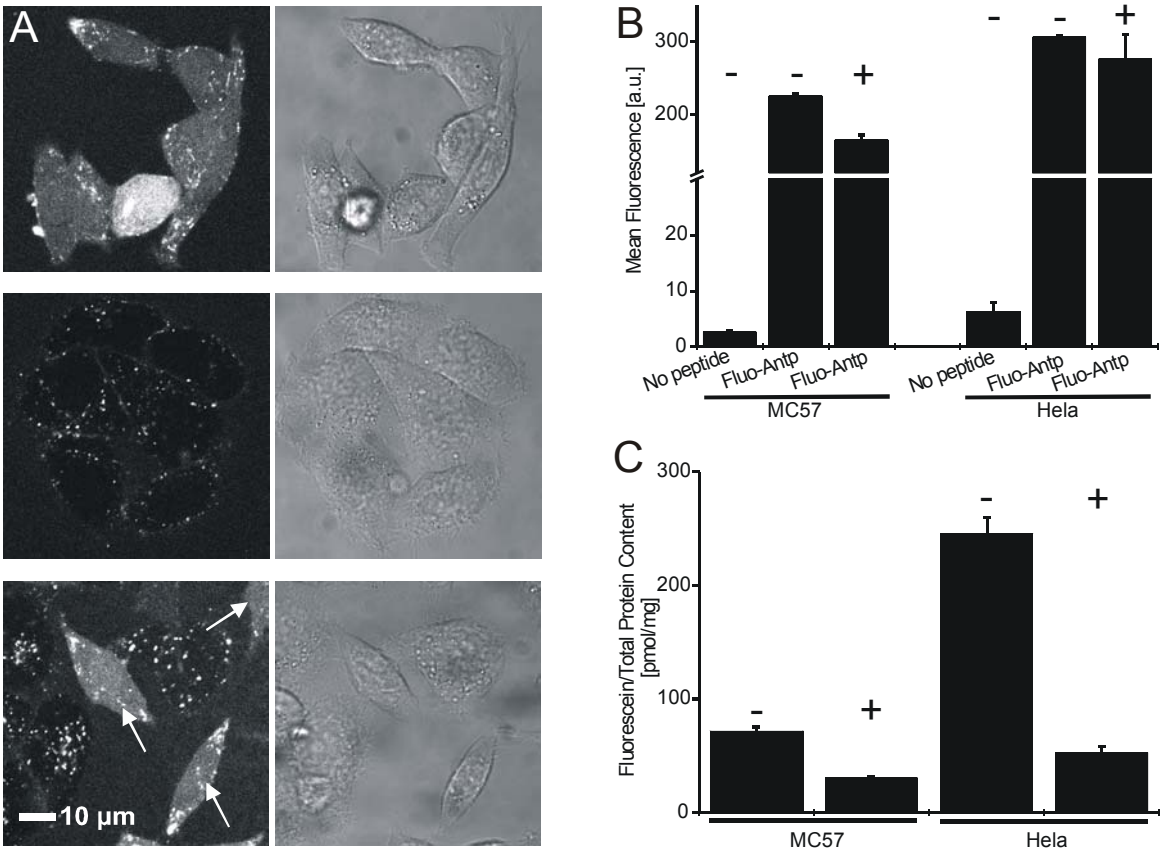

Figure 5.5 Cellular distribution and uptake of CPPs in different cell lines. (A) MC57 (upper panels) and HeLa (center panels) cells were incubated with serum-free medium containing Fluo-Antp peptide (1 µM for 2 h) and then analyzed by confocal laser scanning microscopy in the presence of peptide in the medium. Fluorescence images are shown in the left panels, transmission images in the right panels. In order to exclude incubation conditions as the source of the different peptide distributions, both cell lines were co-cultivated and co-incubated with the Fluo-Antp peptide (lower panels). Arrows indicate MC57 cells, as judged by cell morphology. MC57 and HeLa cells were incubated with 4 µM Fluo-Antp for 2 h. Bafilomycin A1 (300 nM) (+) was added 30 min prior to the peptide, internalization was either determined by flow cytometry (B) or by measuring fluorescein concentrations in whole cell lysates (C). The fluorescence present in the cell lysates was normalized to the protein content to correct for differences in cell number and cell size.

5.3.6 Impact of Golgi-disrupting agents on the uptake and distribution of fluorescently labeled CPPs

Having shown that release of cationic CPPs into the cytosol occurs by a mechanism that depends on endosomal acidification and preserves endosomal integrity, we next addressed a potential involvement of the Golgi complex in the cellular trafficking of cationic CPPs. It was shown recently, that uptake of a Tat fusion protein and Tat-transactivation activity were sensitive to brefeldin A (Fittipaldi *et al.*, 2003). We tested whether brefeldin A and nordihydroguaiaretic acid (NDGA) (Drecktrah et al., 1998), compounds that interfere both with the integrity of the Golgi and the *trans*-Golgi network (TGN), influence the internalization of the cationic CPPs. NDGA is a potent lipoxygenase inhibitor and stimulates the rapid retrograde movement of both Golgi stack and TGN membranes back to the ER, until both organelles are morphologically absent from cells (Drecktrah *et al.*, 1998). Thus NDGA can (i) serve as a Golgi-disrupting drug when added prior to the peptide and (ii) provide a means of inducing retrograde transport.

In a first experiment, cells were incubated with brefeldin A or NDGA for 30 min prior to the addition of peptides. For both drugs, the cellular fluorescence of Fluo-R9 and Fluo-Antp was reduced significantly. In contrast, for Fluo-Tat cellular fluorescence was reduced by brefeldin A and slightly by NDGA (Fig. 5.6), similar to the effects of bafilomycin A and chloroquine on uptake of Fluo-Tat (compare Fig. 5.1 B and C).

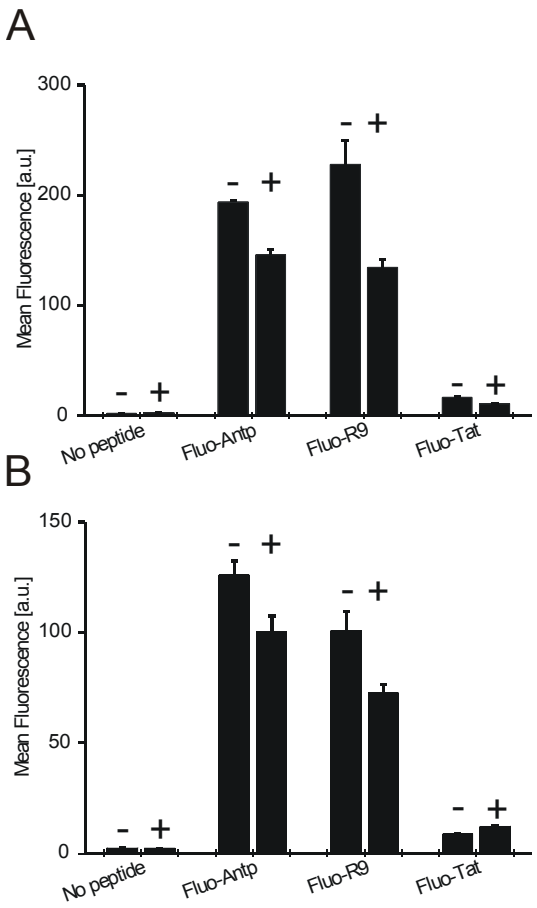

Figure 5.6 Influence of Golgi-disrupting agents on uptake of cell-penetrating peptides. MC57 cells were incubated with carboxyfluorescein-labeled cell-penetrating peptides (1 μM) for 2 h in serum-free medium in the absence (-) or presence (+) of 20 μM brefeldin A (A) or 25 μM nordihydroguaiaretic acid (B), washed, trypsinized and analyzed by flow cytometry. The inhibitors were added 30 min before the peptide. Each condition was tested in duplicate; error bars represent the absolute deviations from the mean value.

5.3.7 Induction of retrograde transport of fluorescently-labeled CPPs by NDGA

Since our data suggest that cationic CPPs enter the cytoplasm by means of retrograde transport, we tested whether NDGA is able to affect subcellular localization of Fluo-Tat in peptide-pulsed cells. In this set of experiments we took advantage of NDGA as an inducer of retrograde transport. HeLa cells were pulsed with Fluo-Tat for 2 h followed by 3 h incubation with NDGA in the cell culture medium (Fig. 5.7). HeLa cells incubated with medium alone during this period exhibited only a vesicular fluorescence, whereas in HeLa cells incubated with

NDGA-containing medium a cytoplasmic fluorescence was clearly visible (panels C and G). In order to exclude that this change in cellular distribution was due to a disruption of endosomal compartments by NDGA, cells were co-incubated with AlexaFluor 647-dextran. In contrast to the fluorescein-labeled CPP, NDGA did not affect the localization of the dextran (panels B and F), indicating that the CPPs reach a compartment distinct from endosomal compartments and functionally coupled to the cytosol. Similar data were obtained for the Fluo-Antp peptide.

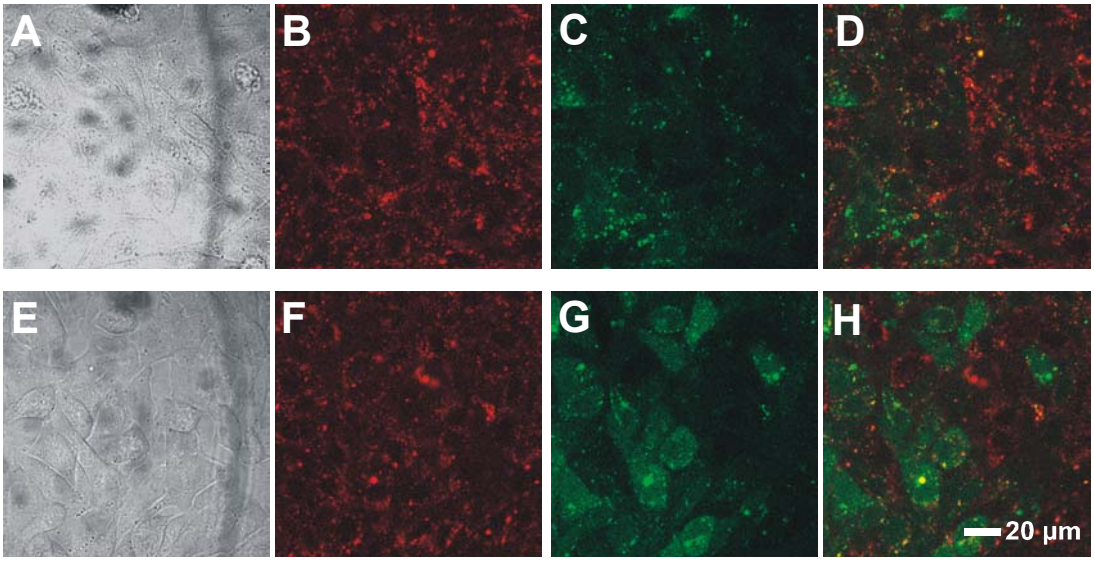

Figure 5.7 Induction of retrograde transport by NDGA. HeLa cells were incubated with 5 µM Fluo-Tat and 10 µM AlexaFluor 647-dextran. After 2 h cells were washed with serum-free medium and then incubated for 3 h in medium with (E-H) or without (A-D) 25 µM NDGA for 3 h. Cellular distribution of both the fluorescein fluorescence and the AlexaFluor fluorescence was followed by confocal laser scanning microscopy. Panels A and E show transmission pictures, panels B and F the AlexaFluor 647-dextran fluorescence, panels C and G the fluorescein fluorescence and panels D and H the superposition of both fluorescence channels.

5.3.8 Co-localization of Fluo-Tat with Golgi-specific fluorescent probes

In order to provide further evidence for the participation of the Golgi-complex in the trafficking of cationic CPPs we finally probed for co-localization of Fluo-Tat with Golgi membranes. The distortion of the distribution of cationic peptides by fixation prohibited an analysis of the co-localization with Golgi-resident proteins by immunofluorescence. Instead, cells were incubated with the cell-permeable Golgi tracer Bodipy TR ceramide. In MC57 cells (Fig. 5.8, panels A to D) vesicular

peptide fluorescence partially co-localized with Golgi-staining, albeit intense peptide staining localized to less intensely stained regions of the Golgi complex. In HeLa cells (Fig. 5.8, panels E to H) peptide fluorescence present in vesicular structures partially co-localized with the cellular regions of Bodipy ceramide staining. Similar results were obtained for the Fluo-Antp peptide.

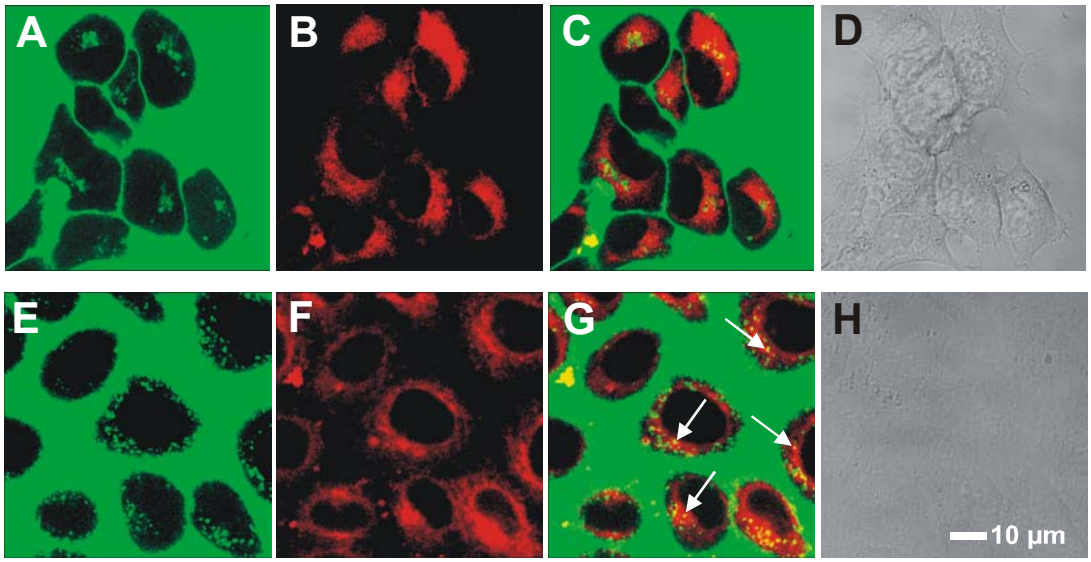

Figure 5.8 Co-localization of Fluo-Tat and Bodipy ceramide. MC57 (panels A to D) and HeLa cells (panels E to H) were incubated with 5 µM Fluo-Tat for 1 h after labeling with Bodipy ceramide. Cells were analyzed by confocal laser scanning microscopy in the presence of peptide in the medium. Panels D and H show transmission pictures, panels A and E the fluorescein fluorescence derived from the Fluo-Tat peptide, panels B and F the fluorescence derived from the fluorescent ceramide derivative and panels C and G the superposition of both fluorescence channels. Arrows indicate areas where peptide-rich structures co-localize with areas of the Golgi complex.

5.4 Discussion

Carboxyfluorescein labeled CPPs in combination with inhibitors of endocytosis and Golgi-disrupting agents were employed in order to elucidate the intracellular fate of cell-penetrating peptides. Artifacts of cellular peptide distribution induced by fixation were avoided by conducting all experiments with fluorescein labeled peptides in living cells. Fluorescein was selected as a reporter group because of minimum impact on the cellular distribution of fluorescently labeled peptides when compared to other fluorescent dyes (own unpublished observations). A vesicular staining could be observed for Tamra-labeled peptides lacking any CPP-motif. For CPPs labeled with the Cy5-like indocyanine dye S0387 a patchy fluorescence at the plasma membrane was observed (Fischer et al., 2002). Moreover, large collections of fluorescein labeled CPPs can be generated in high yield and purity carrying the reporter group at a defined position in the peptide (Fischer *et al.*, 2002;Fischer *et al.*, 2003). These advantages of fluorescein outweigh the limitations imposed by the photophysical characteristics of this dye, i.e. concentration quenching (Chen *et al.*, 1988) and pH-dependence of its fluorescence characteristics. We addressed these potential drawbacks by determining cellular uptake in whole cell lysates. The discrepancies for uptake efficiencies derived from flow cytometry and fluorescence spectroscopy underline the need for such complementary biochemical analyses. This circumstance needs to be considered if quantitative information about molecules entrapped in intracellular vesicles is to be obtained.

MC57 fibrosarcoma cells incubated with Fluo-Tat for 2 h showed a vesicular fluorescence, in accordance with the study by Richard et al. (Richard *et al.*, 2003). In contrast, both Fluo-R9 and Fluo-Antp also exhibited a homogenous cytoplasmic and nuclear fluorescence. This observation is indicative of the escape of these latter two CPPs from endocytic compartments and accumulation in the cytoplasm. The basis for the failure to detect Tat in the cytosol was clarified by pulse/chase experiments and analysis of chase supernatants by mass spectrometry. In contrast to Fluo-R9 and Fluo-Antp, after a 3 h chase period in the absence of peptide, the cellular fluorescence for Fluo-Tat decreased by more than 90% of the value after the peptide pulse. Exit of internalized peptides from the cells into the culture medium has already been reported for amphipathic CPPs (Scheller *et al.*,

2000). However, the MALDI-MS-analysis of the supernatant of Fluo-Tat pulsed MC57 cells provided a different explanation. In the supernatant only carboxyfluorescein-labeled fragments of Fluo-Tat carrying one to six amino acids could be detected. The poor cellular retention of the Fluo-Tat peptide in MC57 cells therefore likely reflects a high susceptibility to intracellular proteases and the ability of the generated fragments to exit the cells.

The effective retention of Fluo-R9 and Fluo-Antp inside the cells demonstrates that this attribute is sequence- and not dye-specific. Moreover, the sequence-dependent retention of cellular fluorescence is indicative of intact peptides leaving the endocytic compartment. Given the detection of proteolytic Fluo-Tat-fragments in the supernatant of Fluo-Tat pulse MC57 cells, the efficient retention of fluorescence for the Fluo-R9 and Fluo-Antp peptides after the 3 h chase period can as well best be explained by a preservation of structural integrity of peptides, reaching the cytosol, in spite of a potential to encounter endolysosomal proteases. Using MALDI-MS analysis (Elmquist *et al.*, 2003) we were able to demonstrate the intracellular integrity of the Fluo-Antp peptide. Apart from this observation, the Fluo-R9 exhibits a nuclear enrichment of fluorescence in MC57 cells in the absence of bafilomycin A1 (s. Fig. 5.2 C), which further supports the notion of intact peptide entering the cytosol. Highly basic peptide stretches are known to serve as conventional nuclear localization sequences (Jans et al., 2000). Identification of peptide fragments by MALDI-TOF-MS demonstrates that the concentrations of peptide required for a direct analysis of peptide integrity and proteolytic degradation are fully compatible with cell biological experiments using fluorescence microscopy. Further experiments using inhibitors of cytosolic and endosomal proteases in combination with the incorporation of protease-specific cleavage motifs, should allow to delineate the basis for the different stabilities of Tat and the other two cationic CPPs and enable a rational design of peptides with increased stability.

Since endocytosis and endosomal acidification are required for the lysosomal escape of complexes consisting of the cationic polymer polyethylenimine and ribozymes (Merdan et al., 2002), we reasoned that cationic CPPs may leave the endosomes via a similar mechanism. In order to assess the role of endocytosis for the uptake of CPPs, cells were incubated with inhibitors of endocytosis and endosomal acidification. In order to exclude inhibitor-dependent artifacts on

cellular uptake, experiments were conducted with wortmannin, chloroquine and bafilomycin A1 that interfere with endocytosis by different mechanisms. For Fluo-Antp and Fluo-R9 all three inhibitors led to a decrease of cellular fluorescence. The increase of cellular fluorescence for Fluo-Tat in the presence of chloroquine and bafilomycin A1 can be explained with the retention of this peptide inside the endosomal compartment thereby inhibiting the rapid exit of its fragments from the cytosol. Together with the microscopy data obtained, it can be concluded that endosomal acidification is required for the delivery of cationic CPPs to the cytoplasm.

Since endocytosis is a well regulated pathway (Gruenberg, 2001), we asked whether a cell-type dependence could also be observed for the localization of CPPs on the subcellular level. Co-cultivation and co-incubation of MC57 fibrosarcoma cells and HeLa cells with the Fluo-Antp and the Fluo-R9 peptide revealed dramatic differences in subcellular distribution. At 1 μM peptide concentration in HeLa cells Fluo-Antp and Fluo-R9 only showed vesicular fluorescence. Almost no cytoplasmic fluorescence could be detected. Comparison of net uptake of both cell types excluded that the vesicular localization of both peptides in HeLa cells resulted from a reduced uptake compared with MC57 cells. Bafilomycin A1 reduced the net uptake in both cell lines significantly, consistent with a similar uptake mechanism, but differences in the intracellular routing after endosomal acidification. The absence of cytoplasmic fluorescence for HeLa cells in the presence of equal amounts of extracellular peptides clearly illustrates that a comparison of biological activities of CPP constructs in different cell types needs to take differences in the subcellular distribution into account.

Next the mechanism by which CPPs leave the endocytic pathway was addressed. Using acidic compartment-specific probes, such as Lysotracker, we tested whether the fluorescein-labeled CPPs reach late endosomes or lysosomes. However, only little or no co-localization was observed for all three CPPs. In order to rule out that the pH-dependent fluorescence properties of fluorescein impaired these co-localization studies, we also performed these experiments with Penetratin labeled with the indocyanine dye S0387 (Fischer *et al.*, 2002), yielding the same results. These data imply that the cationic CPPs leave the endocytic compartment at a rather early stage of endosomal maturation.

In order to assess whether entry into the cytosol involves endosome disruption, cells were co-incubated with CPPs and a fluorescently labeled high-molecular weight dextran. However, the presence of the CPP did not affect the distribution of the dextran. In addition, the low cytotoxicity of the CPPs (Vives *et al.*, 1997) in contrast to agents disrupting endosomes, further supports a mechanism of entry that maintains endosomal integrity.

To this point our observations suggested a mechanism of cellular import that occurs via endocytosis and subsequent translocation of the CPPs via an acidification-dependent passage through endosomal membranes. Such a mechanism would be in line with earlier experiments demonstrating that the Penetratin peptide is able to cross a pure lipid bilayer (Thoren *et al.*, 2000). We therefore asked whether an acidic extracellular pH enabled a direct non-endosomal entry of CPPs from the medium into the cytoplasm. Such a pH-dependent direct passage through the plasma membrane was observed for *Clostridium botulinum* C2 toxin (Barth et al., 2000). This toxin is normally taken up by endocytosis and requires oligomerization and endosomal acidification for release into the cytosol (Barth *et al.*, 2000). Therefore MC57 cells were briefly pulsed with peptide and then incubated with physiological citrate buffer of various acidic pH values (pH 5 – 7). However, during the incubation time tolerated by the cells, no cytosolic fluorescence was observed (data not shown).

The failure to obtain evidence for a direct passage of the CPPs from the endosomal compartment into the cytoplasm prompted us to address an involvement of retrograde transport on cellular trafficking. It was shown that brefeldin A affects uptake and cytosolic biological activity of Tat-GFP-fusion proteins (Fittipaldi *et al.*, 2003). For this reason, we investigated the effects of brefeldin A and NDGA on the net uptake of the fluorescently labeled CPPs in MC57 and HeLa cells. When NDGA or brefeldin A were applied to the cells prior to the addition of the peptide, the net uptake of Fluo-R9 and Fluo-Antp was reduced for both agents, as observed by flow cytometry. However, cellular fluorescence of Fluo-Tat treated MC57 cells was slightly enhanced by NDGA (s. Fig. 5.6 B). This result implies that for Fluo-Tat, disruption of retrograde trafficking traps this peptide in the endosomal compartment thereby preventing its entry into the cytosol and rapid cellular exit of its fragments (as shown in Fig. 5.3). This circumstance led to an enhanced cellular fluorescence in the case of Fluo-Tat in the presence of

NDGA. In the case of Fluo-R9 and Fluo-Antp the absence of TGN and the Golgi complex led to reduced uptake.

In a second series of experiments we utilized the ability of NDGA to induce retrograde transport in cells pulsed with Fluo-Tat or Fluo-Antp for 2 h. The observed increase of cytoplasmic Tat-fluorescence in peptide-pulsed and subsequently NDGA-treated HeLa cells strongly supports an involvement of the Golgi apparatus or the *trans*-Golgi Network (TGN) in the uptake of Tat-peptides (s. Figure 7). Essentially the same result was also obtained for Fluo-Antp (data not shown). The brefeldin A-sensitive transactivation activity of Tat-GFP fusion proteins (Fittipaldi *et al.*, 2003) also supports this hypothesis. The influence of furin, a TGN-resident protease on the processing of Tat-MHC class I constructs (Lu et al., 2001) provides further evidence for a passage of Tat-peptides through the TGN.

Finally, partial co-localization of Fluo-Tat-derived vesicular structures with the Golgi-marker Bodipy ceramide was observed in HeLa cells. Similar co-localization data were obtained for Fluo-Antp (data not shown). The inability to detect bulk quantities of Fluo-Tat and Fluo-Antp in the Golgi-complex in MC57 cells might be due to a rapid passage through this organelle. The plant toxin ricin e.g., which is known to traverse the Golgi complex and the ER, has never been visualized by microscopy in the ER (Sandvig and van Deurs, 2002). For this reason it was initially suggested that ricin A chain translocates from the TGN directly to the cytosol (van Deurs et al., 1988).

For the cationic CPPs, the apparent involvement of the Golgi complex bears striking resemblance with features of some bacterial and plant toxins. A number of well-characterized toxins reach the cytosol of eukaryotic cells after binding to the cell surface, endocytosis by different mechanisms and retrograde transport to the Golgi apparatus and the endoplasmic reticulum (for review see (Lord and Roberts, 1998;Sandvig and van Deurs, 2000)). These toxins, such as ricin and Shiga toxin, consist of a membrane binding subunit (B-subunit) and an enzymatically active moiety (A-subunit) (Sandvig *et al.*, 2000). Interestingly, a sequence comparison with the Tat- and Antp-peptides revealed a highly conserved arginine-rich motif of 8-10 amino acids in the A subunits of several toxins, which are reported to be transported by means of retrograde transport (Tab. 5.2).

Table 5.2 Arginine-rich motifs in plant and bacterial toxins. Primary structures of the arginine-rich motifs with high sequence homology to the HIV-1 Tat peptide. Sequence homologies were identified by visual inspection of the respective proteins. The arginine-rich sequence of the HIV-1 Tat protein is included as entry 5. Sequence information was obtained from http://www.ncbi.nlm.nih.gov/entrez/query.fcgi.

Entry	Protein	Organism	NCBI Accession number	Protein function	Sequence localization	Amino acid sequence
1	Verotoxin-2 variant, subunit A	*Escherichia coli*	AAP37403	Cleavage of glycoside bond within 28S rRNA	192-201	RFRQIQREFR
2	Shiga toxin, subunit A	*Shigella dysenteriae*	AAF28121	Cleavage of glycoside bond within 28S rRNA	192-201	RFRQIQRGFR
3	Cholera enterotoxin, A chain	*Vibrio cholerae*	P01555	ADP-ribosylation of Gsα	159-166	RNRGYRDR
4	Ricin, A chain	*Ricinus communis*	2AAIA	Cleavage of glycoside bond within 28S rRNA	189-207	RTRIRYNRR
5	Tat, transactivating regulatory protein	Human immuno-deficiency virus 1	P04613	Transcriptional regulation	49-57	RKKRRQRRR

In addition to other motifs (e.g. the KDEL sequence) within these toxins, these arginine-rich motifs may therefore represent a common structural basis for a shared route of import along the retrograde pathway of this diverse class of proteins. Another fascinating similarity of both cationic CPPs and Golgi-targeted toxins is the fact that both Shiga toxin subunit A and Tat-MHC class I epitope-constructs are processed proteolytically by furin, a TGN-resident protease (Garred et al., 1995;Lu *et al.*, 2001). Furthermore a recent study on gentamicin, a member of the amino glycoside family of antibiotics, corroborated our findings on the retrograde transport of cationic CPPs. This work provided evidence that amino glycosides and other cationic amino glycoside structural analogues, such as low molecular weight cationic dextrans are transported through the Golgi complex and to the ER. These findings indicate that retrograde transport may serve as a common rote of transport for a number of different cationic low molecular weight compounds (Sandoval and Molitoris, 2003).

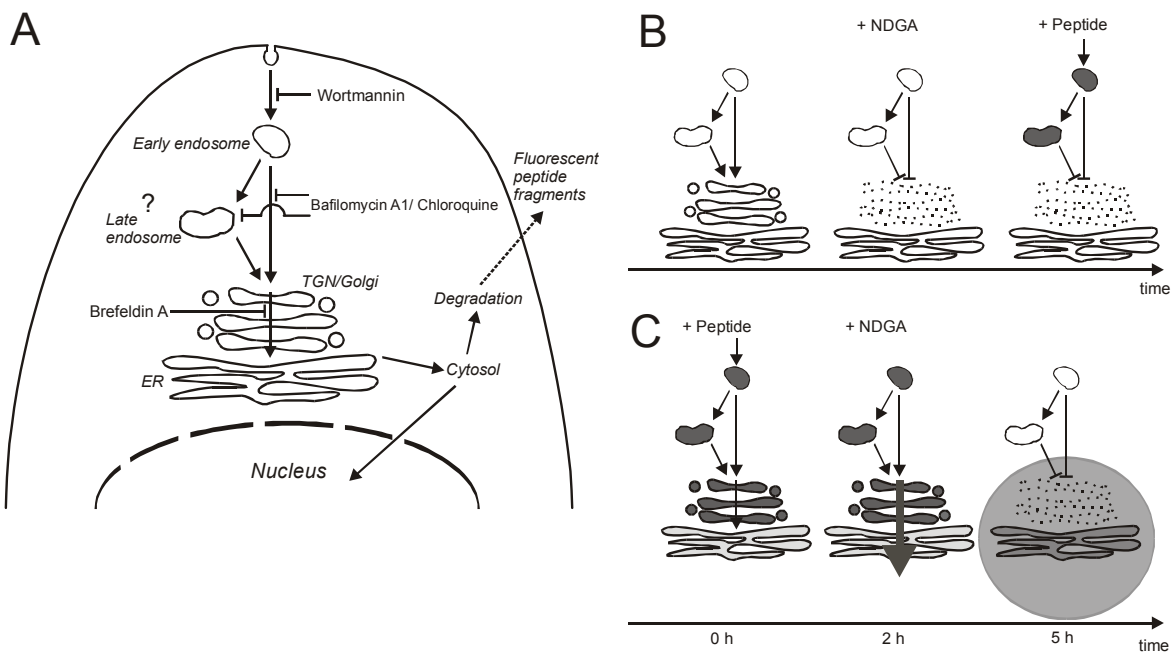

Figure 5.9 Dissection of intracellular trafficking of cationic CPPs by small molecule drugs. (A) Summary of the results of CPP-trafficking along the endosomal and retrograde pathway obtained using small molecule inhibitors. (B, C) Effect of NDGA on the localization and trafficking of cationic CPPs upon (B) incubation of cells with the compound before addition of peptide and (C) addition after a 2 h pulse with peptide that allowed the peptide to enter the Golgi and trans-Golgi network. Dark shades indicate an accumulation of peptide in the respective compartment.

5.5 Materials and Methods

5.5.1 Materials

Standard chemicals for peptide chemistry were obtained from Fluka (Deisenhofen, Germany) and Merck (Darmstadt, Germany); solvents were p. a. grade. Fmoc-amino acids were purchased from Novabiochem (Heidelberg, Germany), Senn Chemicals (Dielsdorf, Switzerland), and Orpegen Pharma (Heidelberg, Germany). The isomeric mixture of (5)6-carboxyfluorescein was from Fluka, AlexaFluor 647-dextran (anionic; MW 10,000 Da) and Bodipy TR ceramide were obtained from Mobitech (Göttingen, Germany). Bafilomycin A1 was from Tocris Biotrend (Bristol, UK), chloroquine diphosphate from Fluka, nordihydroguaiaretic acid (NDGA) from Alexis Biochemicals (Grünberg, Germany), wortmannin from Calbiochem (Bad Soden, Germany) and brefeldin A from Sigma (Taufkirchen, Germany).

5.5.2 Peptide synthesis

Automated peptide synthesis was performed by solid-phase Fmoc/tBu-chemistry using an automated peptide synthesizer for multiple peptide synthesis (RSP5032, Tecan, Hombrechtlikon, Switzerland) in 2 ml syringes according to the following protocol: Fmoc-amino acids (twelve-fold excess) were coupled by *in situ* activation using DIC/HOBt for 90 min followed by removal of the Fmoc-protecting group by treatment with piperidine/DMF (1:4, v/v) twice for 8 min. The resin was washed with DMF (6x) after each coupling and deprotection step. The side chain of Tyr was tBu-protected, the side chain of Arg was Pbf-protected, the side chains of Gln and Asn were Trt-protected and the side chains of Lys and Trp were Boc-protected. Peptide amides were synthesized on Rink amide resin (Rapp Polymere, Tübingen, Germany).

Peptides were cleaved off the resin by treatment with TFA/TIS/EDT/H_2O (92.5:2.5:2.5:2.5, v/v/v/v) for 4 h. Crude peptides were precipitated by adding cold diethyl ether (-20°C). The precipitated peptides were collected by centrifugation and resuspended in cold diethyl ether. This procedure was repeated twice. Finally peptides were dissolved in tBuOH/H_2O (4:1, v/v) and lyophilized.

5.5.3 Labeling of peptides with carboxyfluorescein

N-terminal labeling of peptides with 5(6)-carboxyfluorescein was essentially performed as described (Fischer et al., 2003): Fmoc-deprotected, resin bound peptides were reacted with 5 equiv of 5(6)-carboxyfluorescein, DIC, HOBt, each in DMF for 16 h in 2 ml syringes on a shaker at RT. Reactions were stopped by washing the resins 3 times each with DMF, MeOH, DCM and diethyl ether. Subsequently, peptides were treated with piperidine/DMF (1:4, v/v) in order to remove ester bound carboxyfluorescein (Fischer *et al.*, 2003). Completeness of amine acylation was confirmed using the Kaiser-Test (Sarin et al., 1981).

5.5.4 HPLC

Peptides and conjugates were analyzed by analytical RP-HPLC using a water (0.1% TFA) (solvent A)/ACN (0.1% TFA) (solvent B) gradient on a Waters 600 System (Eschborn, Germany) with detection at 214 nm. The samples were analyzed on an analytical column (Nucleosil 100, 250 x 2 mm, C18 column, 5 μm particle diameter; Grom, Herrenberg, Germany), using a linear gradient from 10% B to 100% B within 30 min (flow rate: 0.3 ml/min). Peptides were purified by preparative RP-HPLC (Nucleosil 300, 250 x 20 mm, C18 column, 10 μm particle diameter; Grom, Herrenberg, Germany) on a Waters 600 Multisolvent Delivery System (flow rate: 10 ml/min). Gradients were adjusted according to the elution profiles and peak profiles obtained from the analytical HPLC chromatograms.

5.5.5 MALDI-TOF-MS of synthetic peptides.

1 µl of DHAP matrix (20 mg of DHAP, 5 mg of ammonium citrate in 1 ml of isopropyl alcohol/H_2O (4:1, v/v)) was mixed with 1 µl of each sample (dissolved in ACN/water (1:1) at a concentration of 1 mg/ml) on a gold target. Measurements were performed using a MALDI-TOF system (G2025A, Hewlett-Packard, Waldbronn, Germany). For signal generation 20-50 laser shots were added up in the single shot mode.

5.5.6 Peptide stock solutions

Carboxyfluorescein-labeled peptides were dissolved in DMSO at concentrations of 10 mM. These stock solutions were further diluted 1:20 in ddH_2O. Peptide concentrations were determined by UV/VIS-spectroscopy of a further 1:100 dilution in 0.1 M Tris/HCl buffer (pH 8.8) with absorptions measured at 492 nm and assuming a molar extinction coefficient of 75,000 L/(mol·cm).

5.5.7 Cell culture

The adherent MC57 fibrosarcoma cell line (Hosaka et al., 1986) and HeLa cells were grown in a 5% CO_2 humidified atmosphere at 37°C in RPMI 1640 medium with stabilized glutamine and 2.0 g/L $NaHCO_3$ (PAN Biotech, Aidenbach, Germany) supplemented with 10% fetal calf serum (PAN Biotech), 100 U/ml penicillin, and 100 μg/ml streptomycin (Biochrom, Berlin, Germany). Both cell lines were passaged by trypsinization with trypsin/EDTA (0.05/0.02% (w/v)) (Biochrom) in PBS every third to fourth day.

5.5.8 Flow cytometry

MC57 or HeLa cells were seeded at a density of 50,000 per well in 24 well plates (Sarstedt, Nümbrecht, Germany) in serum-containing RPMI 1640. One day later, the cells were washed with serum-free RPMI 1640 and incubated in 200 µl serum-free RPMI 1640 containing the appropriate inhibitors. After the indicated periods of time, peptides were added as described in the results section. Each condition was tested in duplicate. After a 2 h incubation, cells were washed with PBS, detached by trypsinization for 10 min, suspended in ice cold PBS containing 0.1% (w/v) BSA, and measured immediately by flow cytometry. The fluorescence of 5000 vital cells was acquired. Vital cells were gated based on sideward scatter and forward scatter.

For pulse/chase experiments, MC57 cells were washed three times with PBS after 2 h peptide incubation and then incubated with 500 µl serum-free RPMI 1640 for additional 3 h. Cells were then washed with PBS, detached by trypsinization for

10 min, suspended in ice cold PBS containing 0.1% (w/v) BSA, and measured by flow cytometry as described above. In order to compare the pulse and the pulse/chase values, fluorescence intensities of fluorescent calibration beads (Mobitech) were also acquired for each series of measurements.

5.5.9 Confocal laser scanning microscopy

Confocal laser scanning microscopy was performed on an inverted LSM510 laser scanning microscope (Carl Zeiss, Göttingen, Germany) fitted with a Plan-Apochromat 63x 1.4 N.A. lens. All measurements were performed with living, non-fixed cells.

MC57 cells were seeded at a density of 10,000/well in eight-well chambered cover glasses (Nunc, Wiesbaden, Germany). Two days later, before addition of inhibitors or peptides, cells were washed once with serum-free RPMI 1640. Bafilomycin A1 was added at a concentration of 300 nM in 200 µl serum-free RPMI 1640 30 min before addition of peptides. After 2 h incubation with peptides, images were acquired immediately at RT with excess peptide in the medium.

For double detection of fluorescein-labeled peptides and AlexaFluor 647-dextran the 488 nm line of an Argon Ion laser and the light of a 633 nm Helium/Neon laser were directed over an HFT UV/488/633 beam splitter and fluorescence was detected using an NFT 545 beam splitter in combination with a BP 505-530 band pass filter for fluorescein detection and an LP 650 long pass filter for AlexaFluor 647-detection. Peptides and AlexaFluor 647-dextran were added as indicated in the results section. After 2 h cells were washed three times with serum-free RPMI 1640 followed immediately by confocal microscopy at RT. For the induction of retrograde transport, after 2 h incubation with peptide and dextran, cells were washed three times with serum-free RPMI 1640 followed by incubation with 25 µM NDGA for 3 h in RPMI.

For double detection of fluorescein-labeled peptides and Bodipy TR ceramide the 488 nm line of an Argon-ion laser and the light of a 543 nm Helium/Neon laser were directed over an HFT UV/488/543 beam splitter and fluorescence was detected using an NFT 545 beam splitter in combination with a BP 505-530 band pass filter for fluorescein detection and an LP 560 long pass filter for Bodipy-detection.

Staining of the Golgi complex in living cells with fluorescent ceramide was essentially performed as described by the supplier. Briefly MC57 and HeLa cells were seeded at a density of 10,000/well in eight-well chambered cover glasses. Two days later, cells were washed once with ice-cold HBSS + 10 mM HEPES (pH 7.4) (HBSS/HEPES), and then incubated with HBSS/HEPES (containing 5 μM sphingolipid and 5 μM BSA, prepared as described by the supplier) for 30 min on ice and in the dark. Cells were rinsed three times with ice-cold HBSS/HEPES and incubated with the indicated peptide in serum-free medium for 1 h at 37°C in the incubator. Confocal microscope images were then acquired immediately at RT with excess peptide in the medium.

5.5.10 MALDI-TOF-MS of peptide-containing cell culture supernatant

A confluent cell layer of MC57 cells in a 25 cm^2 tissue culture flask was washed once with serum-free RPMI 1640 and incubated with 1 ml serum-free RPMI 1640 containing 30 μM Fluo-Tat. After 2 h the cells were detached using 5 mM EDTA/PBS, transferred into a fresh tube and washed twice with 10 ml PBS. EDTA/PBS was used instead of trypsin/EDTA/PBS in order to exclude that peptide fragments were generated by residual amounts of trypsin during the chase period. Cells were then suspended in 500 μl serum-free RPMI 1640 and incubated for 3 h at 37°C in the incubator. The cells were spun down and the cell-free supernatant was acidified using 100 μl 0.1% HCl. The yellow sample (the yellow colour originated from phenol red) was immediately desalted on a G1001A Sample Prep Station (Hewlett Packard) and concentrated to a volume of about 10 μl in a Speed-Vac concentrator. MS-analysis was performed using a “Future” MALDI-TOF-MS (GSG, Mess-und Analysengeräte GmbH, Bruchsal). 1 μl of DHAP matrix was mixed with 1 μl of the sample on a gold target. For signal generation 35-50 laser shots were added up in the single shot mode (positive ion mode). Instrument calibration was performed using two synthetic peptides (calculated $[M + H]^+$: 1156.7 and 2859.4 Da).

5.5.11 Co-incubation of MC57 and HeLa cells

Intracellular peptide stability was investigated essentially as described elsewhere (Elmquist *et al.*, 2003). A confluent cell layer of MC57 cells in a 25 cm^2 tissue culture flask was washed once with serum-free RPMI 1640 and incubated with 1 ml serum-free RPMI 1640 containing 15 μM Fluo-Antp. After 2 h the cells were washed twice with PBS, detached by trypsinization for 10 min at 37°C, transferred into a fresh tube and washed three times with 10 ml PBS (to remove trypsin and extracellular trypsinized peptide). Cells were then lysed in 200 μl 0.1% HCl for 10 min at RT. The cell lysate was then centrifuged for 10 min at 4°C and 14,000 rpm. The peptide-containing supernatant was immediately desalted and concentrated to a volume of about 10 μl, as described above. MS-analysis of the sample was performed using a “Future” MALDI-TOF-MS, as described above.

5.5.12 Co-incubation of MC57 and HeLa cells

For co-incubation experiments 5,000 of each MC57 and HeLa cells per well were seeded in an eight-well chambered cover glass. Two days later, cells were washed once with serum-free RPMI 1640 and 200 μl serum-free RPMI 1640 was added. Peptides were added as indicated in the results section. After 2 h peptide incubation, pictures were immediately acquired at RT, leaving excess peptide in the medium.

5.5.13 Quantification of cellular internalization of fluorescein-labeled CPPs by fluorescence emission spectroscopy in whole cell lysates

MC57 and HeLa cells were seeded in 6 well plates (Sarstedt) in serum-containing RPMI 1640. Two days later, the confluent cell layer was washed with serum-free RPMI 1640 and incubated with 500 μl serum-free RPMI 1640 +/- bafilomycin A1 for 30 min. Then Fluo-Antp was added and after 2 h incubation, cells were washed twice with PBS, detached by trypsinization for 15 min, transferred into a fresh tube and washed twice with 10 ml PBS (to remove trypsin

and trypsinized peptide). Cells were then lysed in 200 μl NP-40 lysis buffer (0.5% (v/v) NP-40, 150 mM NaCl, 5 mM EDTA, 50 mM TRIS, pH 7.0, containing protease inhibitor cocktail, Roche Diagnostics, Mannheim, Germany). The lysates were then sonicated and centrifuged for 30 min at 4°C and 14.000 rpm. Fluorescein concentrations were determined in the supernatant using an LS50B spectrofluorometer (Perkin-Elmer, Norwalk, CT, USA), with excitation at 492 nm and detection of emission at 520 nm. The protein content of the lysates was determined using a commercially available Bradford protein assay kit (Bio-Rad Laboratories, München, Germany). Each condition was tested in duplicate.

6. A doubly-labeled Penetratin analogue as a ratiometric sensor for intracellular proteolytic stability

This chapter will be submitted in 2005. The author of this thesis contributed all figures presented.

6.1 Summary

The cellular delivery of bioactive molecules by cell-penetrating peptides (CPPs) is rapidly gaining significance in biomedical research. Given endocytosis as an import mechanism for cationic CPPs it is required to assess in detail the consequences of this import mechanism on intracellular integrity of the vector and cargo. In this work a Penetratin analogue terminally labeled with two different fluorophores was synthesized and used as a sensor to quantitatively dissect the contribution of intracellular proteolytic activities on break-down. Using a panel of protease inhibitors, the endocytic compartment was identified as the major site of degradation. In contrast, inhibition of the proteasome had little effect on intracellular peptide integrity. The ability to monitor break-down of CPPs once inside the cell will enable a rational optimization of the peptide-based delivery of vaccines and therapeutic oligonucleotides.

6.2 Introduction

The lipid bilayer of the plasma protects the cellular content from entry of pathogens and molecules that interfere with cellular function and replication. Only molecules within a narrow range of molecular size, net charge and polarity are able to directly cross the plasma membrane by passive diffusion along a concentration gradient (Lipinski *et al.*, 2001). However, the introduction of membrane-impermeable molecules into mammalian cells has important implications in biomedical research as well as in basic science (Stephens *et al.*, 2001). Applications include the import of siRNAs interfering with gene expression (Chiu *et al.*, 2004) or peptides that disrupt molecular interactions in cellular signal transduction (Prochiantz, 1996).

Peptide-mediated import has been attracting growing attention as a delivery technology during the last decade (for reviews see (Fischer et al., 2001;Langel, 2002)). Cell-penetrating peptides (CPPs) represent a group of functional peptides with little cell-type specificity. These peptides mediate the non-invasive import of cargo molecules into cells *ex vivo* as well as in whole animals (Schutze-Redelmeier et al., 1996;Schwarze et al., 1999). Cargos have been peptides (Prochiantz, 1996;Hawiger, 1999), proteins as large as 120 kDa (Rojas et al., 1998;Schwarze *et al.*, 1999), oligonucleotides (Astriab-Fisher et al., 2002), plasmids (Singh et al., 1999), siRNA (Muratovska *et al.*, 2004), peptide nucleic acids (PNAs) (Pooga *et al.*, 1998b) and even nanoparticles (Lewin et al., 2000). The majority of these cargos exert their biological activity inside the cytoplasm or the nucleus of the treated cells. It is therefore generally assumed that CPPs mediate the transfer of these cargos into these two compartments

The amphipathic and basic Penetratin peptide, derived from the third helix of the homeodomain of the *Drosophila* Antennapedia transcription factor, has been used widely as a CPP (Derossi et al., 1994). Despite its broad acceptance as a molecular carrier, the mechanism of internalization of the Penetratin peptide is still not fully understood. Originally, the internalization of the Penetratin peptide into the cytoplasm had been described to occur by a direct translocation across the plasma membrane independently of endocytosis (Derossi et al., 1994). Consistent with this early cellular data, the transfer of Penetratin across a pure lipid bilayer

without forming pores (Thoren *et al.*, 2000;Persson et al., 2003) was demonstrated.

However recent data demonstrated that endocytosis is clearly involved in the internalization of the Penetratin peptide (Drin *et al.*, 2003;Fischer *et al.*, 2004). Functionally, the endocytic uptake was supported by the observation that the Penetratin peptide promotes the endocytosis of high molecular weight cargo upon binding to cell surface glycosaminoglycans (Console et al., 2003). However, for cationic CPPs taken up by endocytosis the mechanism by which these molecules are actually released into the cytoplasm still needs to be resolved. Evidence was presented that endosomal acidification is involved in this process (Potocky et al., 2003;Fischer *et al.*, 2004;Vendeville et al., 2004). In addition, independently of the actual membrane translocation step, a strong propensity to bind to the plasma membrane had been shown to be crucial for cellular uptake (Drin et al., 2001).

In order to gain insight into the molecular details of membrane permeation, the secondary structure of CPPs and especially the one of the Penetratin peptide has been a matter of great interest. Circular dichroism measurements showed that Penetratin peptides are randomly structured in aqueous buffers (Magzoub et al., 2001). Binding to model membranes induces distinct secondary structure, the nature of which depends strongly on the experimental conditions and model system. Both β-sheet and α-helical structures have been reported (Berlose et al., 1996;Bellet-Amalric et al., 2000;Lindberg and Graeslund, 2001;Persson et al., 2001;Magzoub et al., 2002;Salamon et al., 2003). Membrane charge and the peptide/lipid ratio have impact on the conformation of the peptide (Christiaens et al., 2002;Magzoub *et al.*, 2002;Magzoub et al., 2003).

Given the endocytic uptake of Penetratin and other cationic CPPs two key questions arise. First, the role of peptide-membrane interactions for trafficking and cytoplasmic release inside the cell has not been clarified. Secondly, the break-down by endolysosomal proteases has not been investigated. In order to answer these questions, specific biosensors that report on the state of the peptide inside the cell are required.

The analysis of cellular trafficking and peptide membrane interactions has benefited greatly from the incorporation of fluorophores as reporter moieties. In cellular applications, the trafficking and distribution of fluorescently labeled CPPs may be followed in living cells (Waizenegger et al., 2002;Richard et al., 2003). Live

cell experiments avoid the problems associated with the fixation of CPP-loaded cells (Richard et al., 2003). In addition, loading efficiencies may be compared quantitatively by flow cytometry (Richard *et al.*, 2003;Fischer *et al.*, 2004). In biophysical analyses, the dependence of the spectral characteristics of a fluorophore on the environment has been employed for the generation of sensors to probe for membrane interactions and transfer across lipid bilayers (Christiaens *et al.*, 2002).

A major difference between biophysical and cellular experiments is the exposure to proteolytic activities in the latter case. In order to exploit the potential of fluorescence-based biosensors for the analysis of the trafficking and interactions of CPPs inside the cell, a biosensor has to report on both, the chemical environment and the integrity of the peptide. This combination of read-outs may be achieved via incorporation of two different fluorophores. Peptides incorporating two different fluorescent dyes have served as sensors for conformational changes (Wei et al., 1994;Geoghegan et al., 2000) and proteolytic breakdown (Cummings et al., 2002). Förster (Fluorescence) resonance energy transfer (FRET) (Clegg, 1995) provides a sensitive read-out for molecular events affecting the proximity of the reporter groups.

To our knowledge all investigations using fluorescently labeled CPPs so far were limited to the attachment of only one single fluorophore. The majority of these studies have been performed with fluorescein-labeled analogues. Applications of 7-nitrobenz-2-oxo-1,3-diazol-4-yl (NBD) (Drin et al., 2001), rhodamine-based dyes (Penco et al., 2001;Fischer et al., 2002) and indocyanine-based fluorophores (Fischer *et al.*, 2002) have been reported, however. Combinations of dyes suitable for FRET-based sensors can readily be selected from this panel of fluorophores.

In order to address the molecular details of intracellular trafficking and break-down, we synthesized a Penetratin analogue terminally labeled with fluorescein and tetramethylrhodamine. *In vitro* analyses of the spectral characteristics confirmed that this peptide constitutes a sensitive biosensor for membrane interactions and proteolytic break-down. By incubation of cells with this peptide in the presence of a variety of protease inhibitors we could quantitatively account for

the contribution of distinct proteolytic activities. Protocols were developed for detecting the fraction of intact peptide in cell lysates as well as in intact cells.

6.3. Results

6.3.1 Straight-forward synthesis of doubly-labeled Penetratin

The synthesis of the doubly-labeled Penetratin analogue benefited from a previously presented Rink amide-based resin for the synthesis of peptide collections labeled with carboxyfluorescein (Fluo) at the C-terminus (Fischer et al., 2003, Chapter 3). This resin is preloaded with a lysine carrying a tritylated carboxyfluorescein at its α-amino group. Following automated solid-phase peptide synthesis (SPPS) of the Penetratin peptide (termed Antp, sequence RQIKIWFQNRRMKWKK (Derossi et al., 1994)), the N-terminus was derivatized manually with carboxytetramethylrhodamine (Tamra) using the succinimidylester (Figure 6.1. A). The resulting peptide was cleaved off the resin and analyzed. The purity of the doubly-labeled Penetratin analogue (Tamra-Antp-Fluo, sequence: Tamra-RQIKIWFQNRRMKWKK-εLys(Fluo)-NH_2) after reduction of the methionine sulfoxide (Beck and Jung, 1994) was 80% (HPLC, 214 nm; Fig. 6.1 B and C), a purity comparable with the one of unlabeled Penetratin synthesized according to the same protocol on Rink amide resin. Standard RP-HPLC purification was sufficient to obtain the peptide in high purity for further applications. The synthesis strategy eliminates the need for orthogonal side chain protecting groups for the introduction of two different labels (Hoogerhout et al., 1999) and is therefore applicable to the straightforward synthesis of collections of different CPPs.

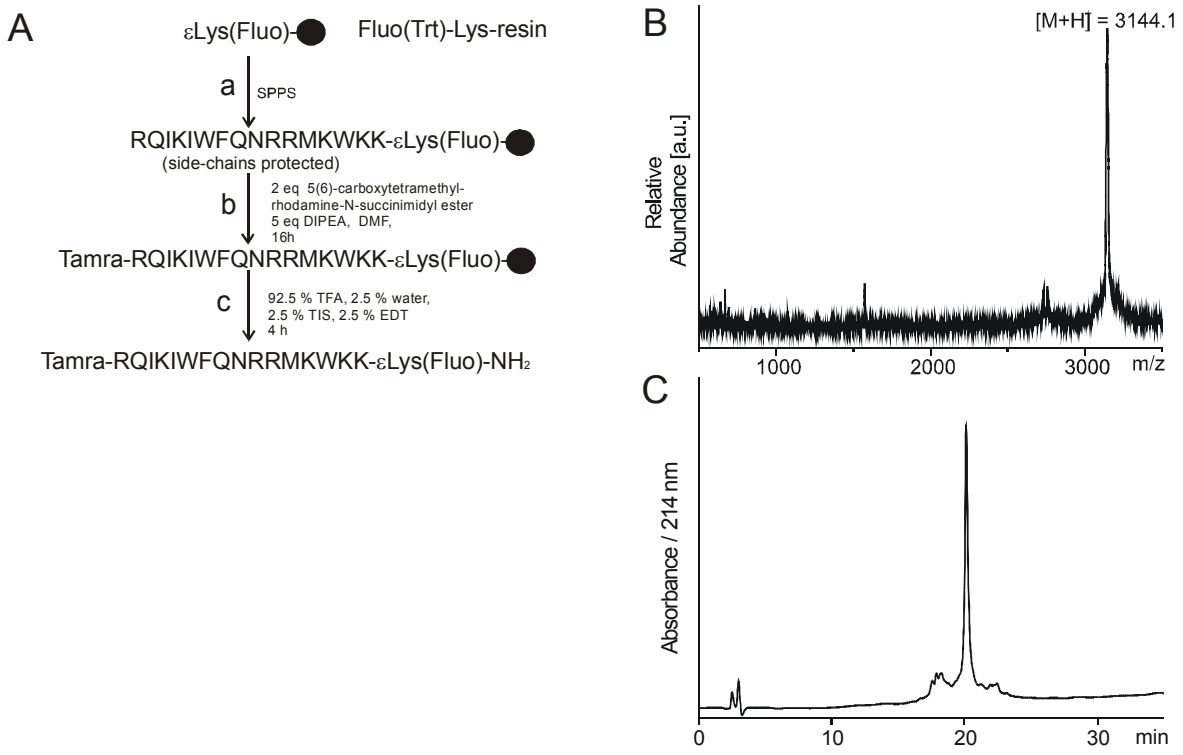

Figure 6.1 (A) Scheme for the synthesis of the doubly-labeled Penetratin peptide amide Tamra-RQIKIWFQNRRMKWKK-εLys(Fluo)-NH_2 (Tamra-Antp-Fluo). The Penetratin peptide is assembled by automated solid-phase peptide synthesis (a) on the free ε-amino group of the N_α-carboxyfluorescein-labeled lysyl-Rink amide resin (Fischer et al., 2003), followed by (b) introduction of the second fluorophore at the N-terminus of the solid-phase bound peptide, and (c) cleavage of the peptide amide off the resin and side-chain deprotection. In order to further increase the purity of the raw product, the methionine sulfoxide was subsequently reduced as described previously (Beck *et al.*, 1994). (B) MALDI-TOF mass spectrum (theor. $[M+H]^+$ = 3145.7 Da) and (C) HPLC elution profile of the crude Tamra-RQIKIWFQNRRMKWKK-εLys(Fluo)-NH_2 peptide.

6.3.2 In vitro proteolytic digestion of Tamra-Antp-Fluo

Fluo and Tamra were selected as a pair of fluorophores for Förster resonance energy transfer (FRET) (i) because of their large spectral overlap, (ii) the availability of optimized synthesis procedures, and (iii) the compatibility of these dyes with the import of CPPs (Fischer et al., 2002). The emission spectrum of fluorescein overlaps extensively with the absorption spectrum of Tamra, making this pair very suitable for energy transfer experiments to determine distances within and between labeled macromolecules (Murchie et al., 1989;Sjöback et al., 1995). Nevertheless fluorescence emission spectra showed that the fluorescence of both dyes in the Tamra-Antp-Fluo peptide was almost completely quenched (Fig. 6.2 A, B), a result

which is consistent with previous reports (Wei *et al.*, 1994;Packard et al., 1997). This loss of fluorescence in both channels was attributed to a mechanism involving intramolecular dimer formation of the two fluorophors (Wei et al., 1994). As expected, upon digestion with trypsin the fluorescence emission of both fluorophores was enhanced significantly (Fig. 6.2 A, B).

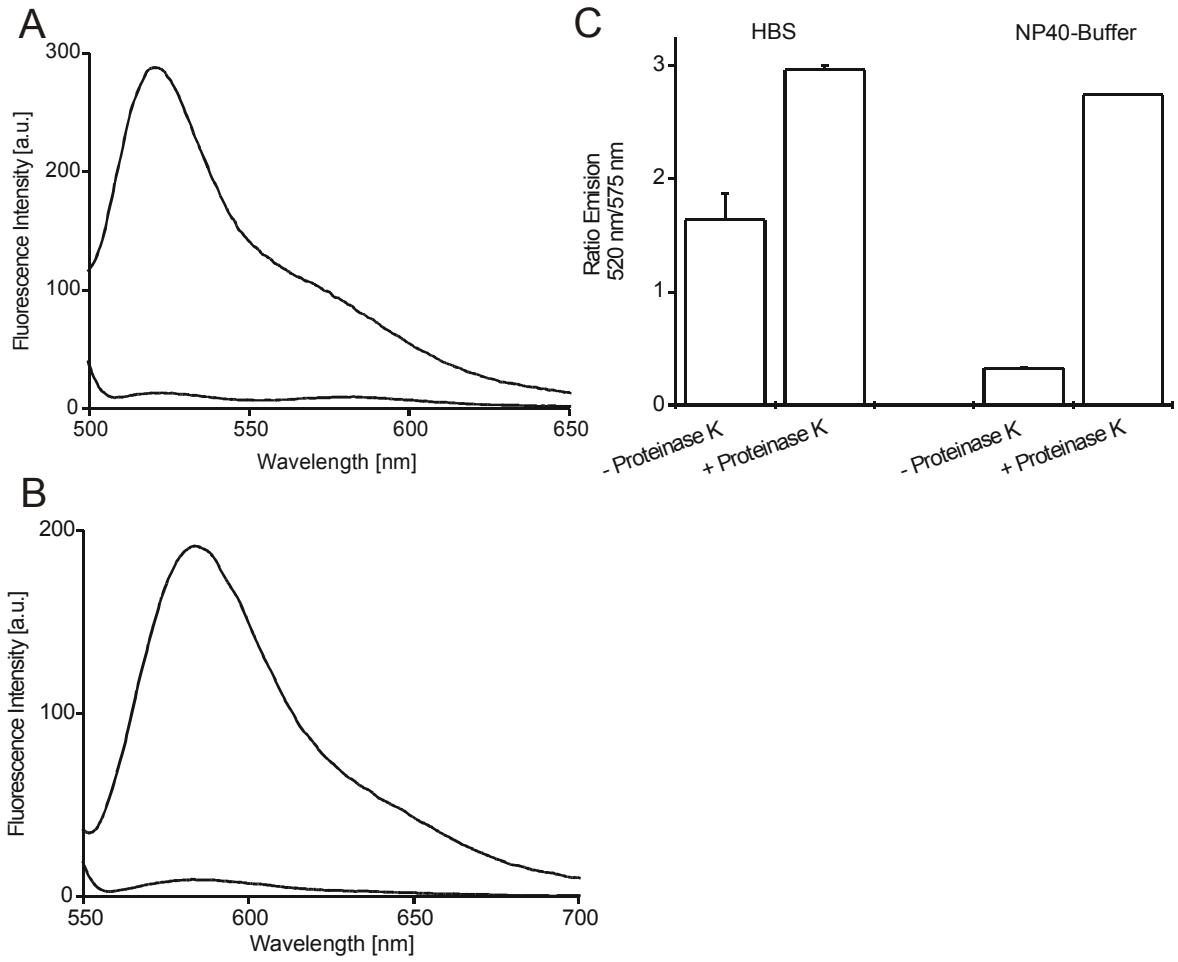

Figure 6.2 Tamra-Antp-Fluo as proteolytic sensor. Fluorescence emission spectra of Tamra-Antp-Fluo (100 nM) in HBS with excitation at (A) 492 nm and (B) 541 nm with (upper curves) and without (lower curves) digestion with proteinase K (100 μg/ml, 1 h, 37°C). (C) Fluorescence ratios were calculated for the data shown in A (digest in HBS, first two columns) and for an identical digest in NP40 lysis buffer. Each condition was tested in duplicate; error bars represent the absolute deviations from the mean value.

In order to rule out that the differences in fluorescence emission were caused by the adhesion of the intact peptide to plastic and glass (Chico et al., 2003), the ratio of the fluorescein versus rhodamine emission upon excitation at 492 nm was calculated (Fig.

6.2 C). This strategy renders the detection of changes in the fluorescence spectra robust towards changes in concentration (Miyawaki et al., 1997). The ratio was almost doubled upon proteinase K-digestion in HBS buffer from about 1.7 to 3.0. In detergent-containing NP40-lysis buffer the ratiometric difference between intact and digested peptide was far more pronounced, the ratio was about 0.3 for the intact peptide and 2.8 for the digested peptide.

6.3.3 Monitoring peptide/membrane interactions with Tamra-Antp-Fluo

It was shown previously, that the binding of a 13 amino acid peptide terminally labeled with fluorescein and rhodamine to an antibody specific for the peptide, diminished the dimer quenching (Wei et al., 1994). Instead, FRET was detected. Dimer quenching and FRET therefore provide the basis for a robust read-out for molecular interactions that spatially separate the termini of a peptide. We therefore investigated whether the induction of secondary structure upon binding of Penetratin to lipid bilayers resulted in a similar change in the spectral characteristics. Emission spectra were recorded for the Penetratin analogue in the presence of small unilamellar phospholipid vesicles (SUVs). A strong increase of Tamra emission and the ratio of Tamra over fluorescein emission upon excitation at 492 nm (fluorescein excitation) were observed in the presence of SUVs, consistent with the presence of FRET (Fig. 6.3 A, B). The disruption of the fluorophore dimer upon binding to SUVs was further substantiated by the increase in Tamra emission upon excitation at 541 nm (Fig. 6.3 C). In order to exclude that the increase in Tamra fluorescence was due solely to an increase in quantum yield of this fluorophore upon interaction with the lipid bilayer, the mono Tamra-labeled control peptide (Tamra-RQIKIWFQNRRMKWKK-NH_2) was tested as well. Significantly less Tamra emission was observed in the presence of SUVs upon excitation at 492 nm (Fig. 6.3 D). For the Tamra-Antp-Fluo analogue, FRET is therefore a read-out for the interaction of the peptide with phospholipid membranes. In summary, the Tamra-Antp-Fluo peptide is a sensitive ratiometric sensor for membrane-induced conformational changes and proteolytic break-down. The ratiometric determination of the spectral characteristics renders the use of this peptide robust to changes in concentration.

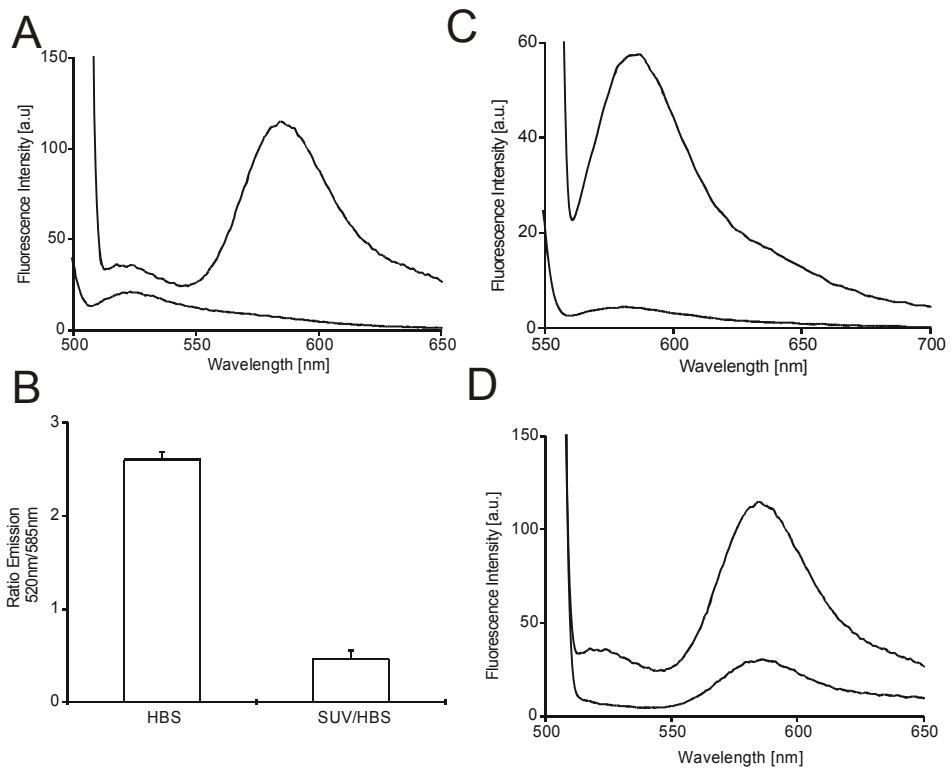

Figure 6.3 Tamra-Antp-Fluo as a sensor for peptide/membrane interactions. (A) Fluorescence emission spectra of Tamra-Antp-Fluo, with excitation at 492 nm in the absence (lower curve) or presence (upper curve) of small unilamellar vesicles (SUV). (B) Fluorescence ratios calculated from the data shown in A (Each condition was tested in duplicate; error bars represent the absolute deviations from the mean value.) (C) Fluorescence emission spectra of Tamra-Antp-Fluo (upper curve) and Tamra-Antp (lower curve) with excitation at 492 nm in the presence of SUV. (D) Fluorescence emission spectra of Tamra-Antp-Fluo (upper curve) and Tamra-Antp (lower curve) with excitation at 540 nm in the presence of SUV.

6.3.4 Confocal fluorescence microscopy of Tamra-Antp-Fluo-incubated cells

The *in vitro* spectral characteristics should render Tamra-Antp-Fluo a sensitive sensor for probing the state of this peptide inside mammalian cells. As a first step we performed live cell confocal fluorescence microscopy of murine MC57 cells incubated with Tamra-Antp-Fluo. In these cells, the Penetratin peptide was demonstrated to access the cytoplasm in an endocytosis and acidification-dependent manner (Fischer *et al.*, 2004). The Tamra-Antp-Fluo peptide was taken up efficiently (Fig. 6.4). A high degree of co-localization for the fluorescence of both fluorophores could be observed in vesicular structures. However, little Tamra fluorescence was detectable within the

cytoplasm or the nucleus. In contrast, pronounced fluorescein fluorescence was present in these compartments. Furthermore, some vesicular structures contained either fluorescein or Tamra. This differential localization is indicative of proteolytic breakdown within the endocytic compartment and preferential release of fluorescein labeled fragments into the cytoplasm. We have observed previously, that Tamra-labeled peptides have a higher propensity for being retained in vesicular structures (Fischer et al., 2002).

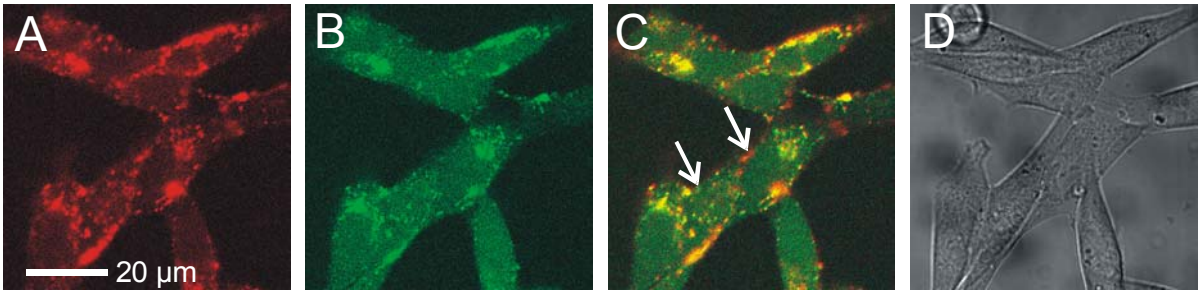

Figure 6.4 Cellular co-localization studies using Tamra-Antp-Fluo. MC57 cells were incubated with 1 µM Tamra-Antp-Fluo for 2 h. Living cells were then analyzed by confocal laser scanning microscopy in the presence of peptide in the medium. Panel A shows the Tamra fluorescence, panel B the fluorescein, panel C the superposition of both fluorescence channels and panel D shows the transmission picture. Arrows indicate spots where only one single fluorophore is present.

6.3.5 Ratiometric fluorescence emission measurements in cell lysates

Next, we intended to identify in more detail the degree of break-down and the proteases involved in the intracellular degradation of the peptide. The incubation of cells with different inhibitors that affect the activity of cellular proteases should lead to different fluorescence properties within subcellular compartments, as it was presented for doubly-labeled dextrans (Zen et al., 1992) or transferrins (Zen *et al.*, 1992;van Weert et al., 1995). Inside intact cells, the reduction of fluorescein fluorescence by the acidic conditions in the endosomes (Sjöback *et al.*, 1995) and concentration quenching sets a limit to a quantitative assessment of the proteolytic break-down using a microscopic approach (Chen *et al.*, 1988).

For this reason, we complemented the cellular analyses by spectral analyses in cell lysates. MC57 cells were pulsed with the Tamra-Antp-Fluo peptide in the absence and presence of inhibitors that affect the activity of proteases inside the cell. After the peptide incubation the cell suspensions were first split into two aliquots (Fig. 6.5 A).

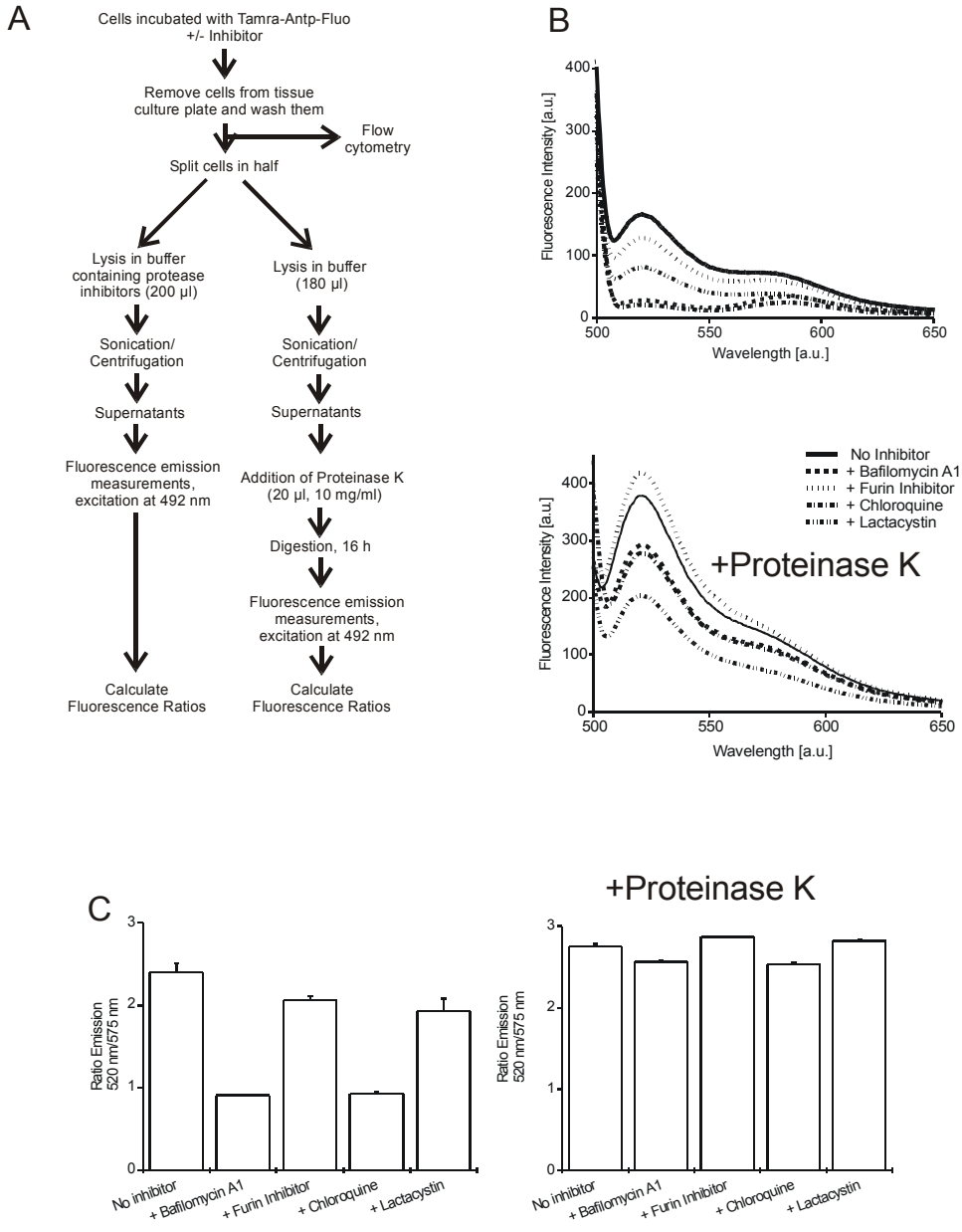

Figure 6.5 Ratiometric fluorescence emission spectroscopy in cell lysates. (A) Protocol for the measurement of fluorescence emission ratios in cell lysates. (B) MC57 cells were incubated with 3 µM Tamra-Antp-Fluo for 2 h in serum-free medium in the absence or presence of different inhibitors (100 µM chloroquine, 300 nM bafilomycin A1, 50 µM furin inhibitor, 50 µM lactacystin). The inhibitors were added 30 min prior to the peptide. Cells were then washed, removed from the tissue culture plate using EDTA/PBS. Cell lysates were then prepared as described in the experimental section. In brief one half was lysed in NP40-lysis buffer containing protease inhibitors. After sonication and centrifugation, fluorescence emission spectra were recorded immediately with excitation at 492 nm (upper panel). The other half of the peptide pulsed cells was lysed in NP40-lysis buffer. After sonication and centrifugation, proteinase K was added. Lysates were then digested for 16 h at 37°C. Fluorescence emission spectra were then recorded with excitation at 492 nm (lower panel). (C) Fluorescence ratios were calculated from the data shown in B. Each condition was tested in duplicate; error bars represent the absolute deviations from the mean value.

One half of the cell population was lysed in the presence of protease inhibitors to prevent post-lysis proteolysis. Fluorescence emission spectra upon fluorescein excitation were recorded immediately (Fig. 6.5 B, upper panel). The second half of the cell suspensions were lysed in lysis buffer. These aliquots of the lysates were then digested with proteinase K in order to cleave all peptides present in the lysates before recording of emission spectra (Fig. 6.5 B, lower panel). The higher the contribution of a proteolytic activity to the degradation, the higher the difference in the fluorescence ratios should be for both aliquots of one sample.

A set of four different inhibitors was selected. Bafilomycin A1 (Bowman et al., 1988;Clague et al., 1994) and chloroquine (de Duve *et al.*, 1974;Kozak *et al.*, 1999) represent widely used inhibitors of endosomal acidification (for review see, (Mellman et al., 1986)) and therefore also inhibitors of endolysosomal proteolysis. For cationic CPPs both drugs abolished the release of theses peptides into the cytoplasm (Fischer *et al.*, 2004), indicating that for cationic CPPs endosomal acidification and maturation are required for accessing the cytoplasm. The role of endosomal acidification has been validated for proteolytically stable (Frackenpohl et al., 2001) cell-penetrating β-peptides (Potocky et al., 2003) and in an functional assay for the HIV-1-Tat protein (Vendeville *et al.*, 2004;Rayne et al., 2004). As a proteolytic inhibitor that blocks a major protease activity in the cytoplasm lactacystin was selected, a bacterial metabolite that selectively inhibits the 20S proteasome (Fenteany et al., 1995;Dick et al., 1996). Finally, a furin synthetic inhibitor was included. The protease furin is ubiquitously expressed and localized mainly in the trans-Golgi network, although some portion of the furin molecules cycle between this compartment and the cell surface. Furin cleaves proteins and peptides within stretches containing cationic amino acid residues (Nakayama, 1997) and more importantly furin was recently demonstrated to cleave the HIV-1 Tat protein in monocytoid cells (Tikhonov et al., 2004).

Digestion with proteinase K led to fluorescence emission ratios very similar to the value of 2.8 for all samples observed for digested Tamra-Antp-Fluo in NP-40 lysis buffer (Fig. 6.2 C). For cells pulsed with peptide in the absence of inhibitor, the ratio was 2.3 indicative of significant degradation of peptides inside the cells. Bafilomycin A1 and chloroquine had the strongest effects. The emission ratios decreased in both cases to about 0.9. Lactacystin and the furin inhibitor had a little, albeit significant effect on the emission ratios (Fig. 6.5 C). These results suggest that the endosomal

passage has a major impact on the integrity of the peptide inside the cell. The proteasome seems to cleave only a rather small amount of the intracellular peptide.

6.3.6 Cysteine proteases mediate the intracellular degradation of Penetratin

Endolysosomal proteases require an acidic pH for activity. For this reason, the inhibitory effect on endolysosomal proteolysis exerted by both bafilomycin A1 and chloroquine is rather indirect, through inhibition of acidification. Therefore at this stage it could not be concluded whether the increased integrity of the peptides caused by both drugs was due to the inhibition of endolysosomal proteases or due to the inhibition of an acidification-dependent entry into the cytoplasm (Potocky *et al.*, 2003;Fischer *et al.*, 2004). In the latter case, lactacystin-insensitive cytoplasmic proteases would contribute significantly to the break-down. In order to resolve this issue peptide-pulsed cells were incubated with the broadband cysteine protease inhibitors leupeptin (Vidard et al., 1991) and E-64d (Tamai et al., 1986). Members of the aspartic acid and cysteine proteases make up most of the proteases that are present in the endolysosomal compartment. Most mammalian lysosomal cysteine proteases are known as cathepsins, although not all cathepsins are cysteine proteases (Honey and Rudensky, 2003). Both leupeptin and E-64d reduced the proteolytic degradation of Tamra-Antp-Fluo significantly, albeit not as drastically as bafilomycin A1 (Fig. 6.6 A).

The investigation of intracellular proteolysis of proteins and peptides is of high general relevance for the cellular import of bioactive molecules. In immunology, in particular, the endolysosomal pathway is the major route of entry and processing for foreign antigens to be presented by antigen-presenting cells. Analysis of the processing of peptides and proteins in the endolysosomal compartment is therefore of major significance, both, for understanding the basis of antigen-presentation and for the development of immunotherapeutics (Honey *et al.*, 2003). Cellular analyses by flow cytometry are well established within immunological research. For this reason, we next tested whether the ratiometric approach was also applicable to this technique. In this case, different concentrations were tested for E-64d and leupeptin. For both inhibitors, the ratiometric values within the cell lysates correlated with the concentration of the inhibitor (Fig. 6.6 B). The same finding was observed for the

analysis of cellular fluorescence by flow cytometry (Fig. 6.6 C). The differences in the absolute ratiometric values determined with both techniques may be due, first, to the different size of the spectral windows, and second, due to concentration- and pH-dependent quenching effects of the fluorophores inside the cells. Still, both sets of values exhibited a strong linear correlation (Fig. 6.6 D).

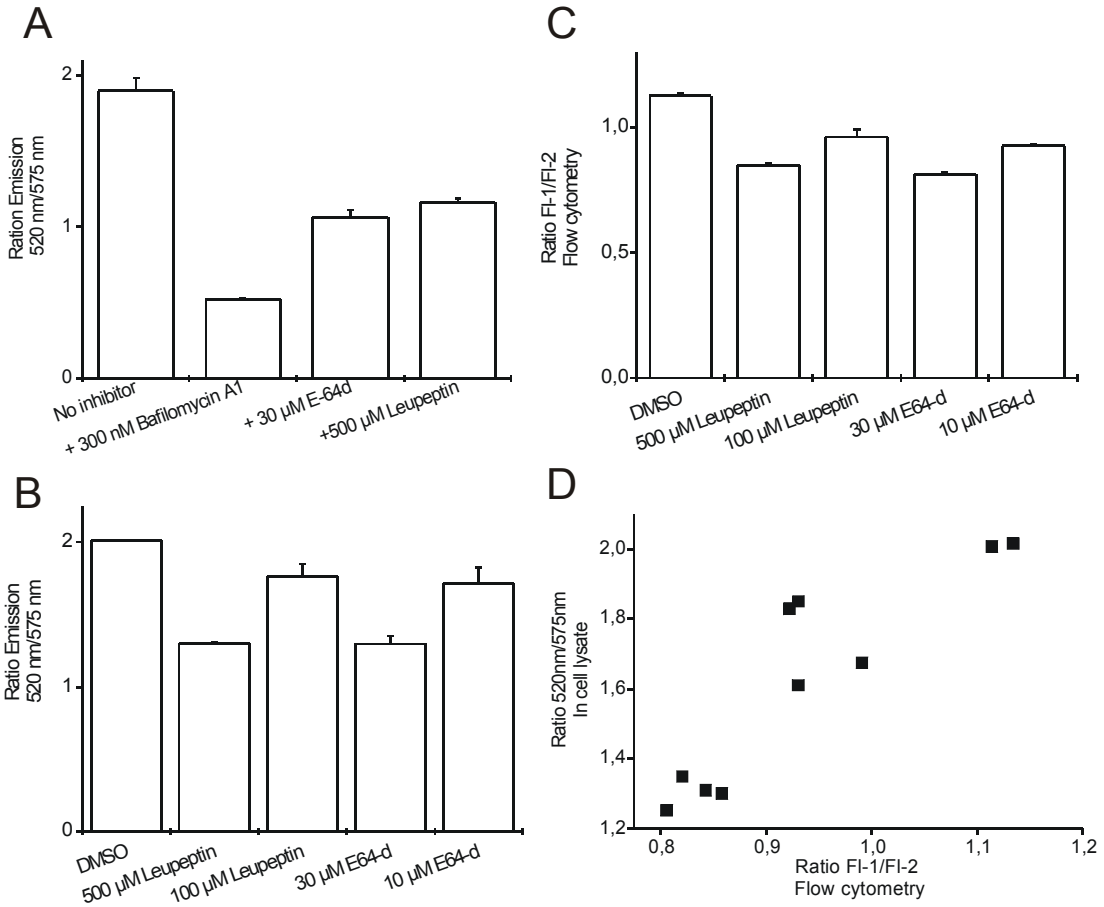

Figure 6.6 Involvement of cysteine proteases in the cellular degradation of Tamra-Antp-Fluo. (A) MC57 cells were incubated with Tamra-Antp-Fluo (4 µM) for 2 h in serum-free medium in the absence or presence of different inhibitors, as indicated. The inhibitors were added 30 min prior to the peptide. Cells were then washed, detached from the tissue culture plate using EDTA/PBS. Cells were then washed once more lysed in NP40-lysis buffer containing protease inhibitors. After sonication and centrifugation, fluorescence emission spectra were recorded immediately with excitation at 492 nm and fluorescence ratios were calculated from the data. (B) The same procedure as under (A) was performed applying different concentrations of cysteine protease inhibitors (ratios in cell lysates are shown, each condition was tested in duplicate; error bars represent the absolute deviations from the mean value) (C) A small fraction of the cells from (B) was subjected to flow cytometry analysis before lysis and ratios of FL-1 (fluorescein) versus FL-2 (Tamra) were calculated. Each condition was tested in duplicate; error bars represent the absolute deviations from the mean value. (D) For each condition the different ratios obtained in B (measurements in cell lysates) and C (flow cytometric data) were plotted.

6.3.7 The endolysomal compartment is the major site of degradation of Penetratin

Since both E-64d and leupeptin are not selective towards endolysosomal cysteine proteases it could not be ruled out that the inhibition of cytoplasmic cysteine proteases, such as calpains, also accounted for the enhanced peptide stability. This could especially be the case as (i) endosomal acidification was shown also to play a role for the release of proteolytically stable peptides into the cytoplasm and (ii) the proteasome contributed little to the degradation of the peptides. Live cell confocal microscopy was performed in the absence or presence of different inhibitors in order to resolve this ambiguity.

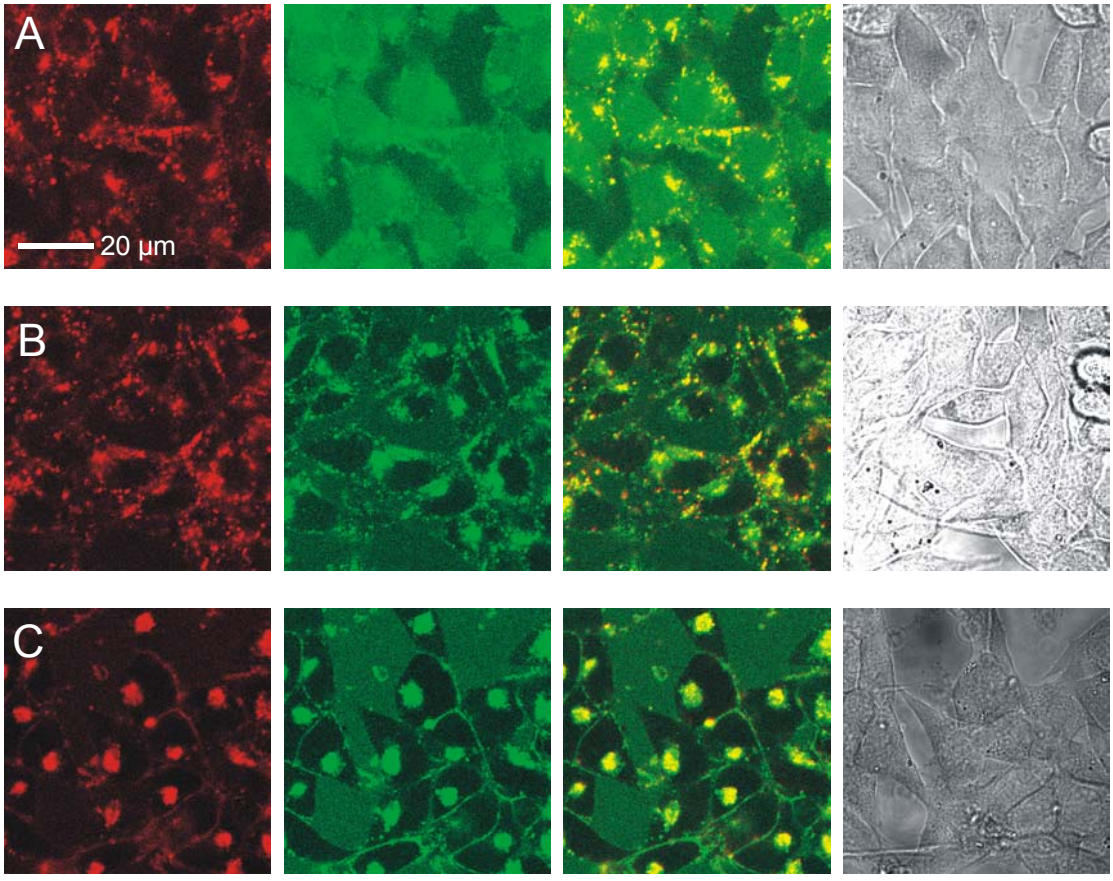

Figure 6.7 Impact of cysteine protease inhibitors on subcellular distribution of Tamra-Antp-Fluo. MC57 cells were incubated with Tamra-Antp-Fluo (4 µM) for 2 h in serum-free medium in the absence or presence of different inhibitors (panels A, no inhibitor; panels B, 300 nM bafilomycin A1; panels C, 30 µM E-64d). The inhibitors were added 30 min prior to the peptide. Left panels show the Tamra fluorescence, the fluorescein channel, the superposition of both fluorescence channels. Right panels show the transmission pictures.

If the degradation was mediated primarily by endolysosomal cysteine proteases, the co-localization of both fluorophores should increase. Incubation of cells with E-64d increased the degree of co-localization and reduced the cytoplasmic fluorescein fluorescence (Fig. 6.7 B). Still the E-64d induced phenotype was different from the one induced by bafilomycin A1 (Fig. 6.7 C). Instead of being concentrated at a region next to the nucleus for bafilomycin A1, peptide-loaded vesicles were strongly present also in the periphery of the cells

6.4 Discussion

The results presented in this paper provide a first semi-quantitative account of the intracellular fate of the cell-penetrating peptide Penetratin. The analyses were based on an analogue of the Penetratin peptide, terminally labeled with two different fluorescent dyes. The synthetic route originated from our previously developed Fluo(Trt)-Lys-resin (Fischer et al., 2003), demonstrating that this reagent provides a straight-forward and rapid access to highly pure doubly-labeled peptides, when compared to other previously published protocols for this dye combination (Wei *et al.*, 1994;Hoogerhout *et al.*, 1999;Li *et al.*, 1999;Kruger *et al.*, 2002). The fluorescence characteristics of Tamra-Antp-Fluo provided a sensitive read-out for the interaction with lipid bilayers and proteolytic break-down. Detection of the conformational changes induced upon membrane interaction in fact greatly benefited from the dimer quenching observed for conformationally disordered peptides, labeled with these two fluorophores. The fluorescence characteristics were fully compatible with analyses by fluorescence spectroscopy, confocal laser scanning microscopy and flow cytometry.

Our data underline that a large fraction of the peptide entering the cell within 2 h incubation had been degraded in the endolysosomal compartment. Our analyses therefore confirm that the endocytic uptake has a major impact on peptide integrity. The small but significant effect of lactacystin demonstrates, however, that intact peptide reaches the cytosol. By a combination of results obtained for the effects of bafilomycin A1 and chloroquine on the one hand, and leupeptin and E-64d on the other hand, the amount of peptide reaching the cytosol in an intact form can be estimated to be around 10-20% of the total peptide entering the cell.

In the original contribution on Penetratin it was found that this peptide is mainly found in its intact form inside the cell (Derossi et al., 1994). The assay was based on the detection of biotinylated peptides using Western Blot analysis. Another more recent contribution has investigated the intracellular stability of the CPP pVEC as a CPP using matrix-assisted laser desorption ionization mass spectrometry. One might argue that the preparation of cell lysates introduces novel artefacts similar to those introduced by fixation (Richard et al., 2003). However, one major advantage of the doubly-labeled peptide is that the same molecule can

be applied to different fluorescence-based techniques. The results can then be cross-validated. We demonstrate that the measurements in the cell lysates strongly correlated with live cell techniques i.e. flow cytometry and live cell fluorescence microscopy. The results obtained for the doubly-labeled Penetratin analogue also demonstrate that one needs to be cautious about the results obtained for peptides carrying only one label. Elimination of cytoplasmic fluorescein fluorescence upon incubation with leupeptin and E-64d indicates that this fluorescence may originate from fluorescein-labeled peptide fragments released into the cytoplasm.

Interestingly, our results suggest that the proteasome contributes little to the degradation of the cytosolic population of peptides. The contribution of the proteasome is in line with observations obtained from processing studies dealing with penetrating-MHC I epitope constructs (Pietersz et al., 2001). This result is highly relevant or the development of CPP-based peptide vaccines, since CPPs offer the advantage of a rational vaccine design. In a recent study, Tat-epitope constructs were joined via furin-sensitive linkers, which led to enhanced generation of peptide/MHC complexes (Lu *et al.*, 2004).

6.5 Materials and Methods

6.5.1 Materials

Standard chemicals for peptide chemistry were obtained from Fluka (Deisenhofen, Germany) and Merck (Darmstadt, Germany); solvents were p. a. grade. Fmoc-amino acids were purchased from Novabiochem (Heidelberg, Germany), Senn Chemicals (Dielsdorf, Switzerland), and Orpegen Pharma (Heidelberg, Germany). Fmoc-Lys(Dde)-OH was purchased from Novabiochem (Läufelfingen, Schweiz). Rink amide resin was from Rapp Polymere (Tübingen, Germany). The isomeric mixtures of 5(6)-carboxyfluorescein (Fluo) and 5(6)-carboxytetramethylrhodamine (Tamra)-N-succinimidylester were from Fluka (Deisenhofen, Germany). Bafilomycin A1 was from Tocris Biotrend (Bristol, UK), chloroquine diphosphate from Fluka, the furin inhibitor (Dec-RVKR-CMK) from Calbiochem (Bad Soden, Germany), lactacystin from Prof. Corey (Harvard University, USA), E-64d from Serva (Heidelberg, Germany) and leupeptin from Bachem (Bubendorf, Switzerland). 1-palmitoyl-2-oleoyl-phosphatidylcholine (POPC) and 1-palmitoyl-2-2-oleoyl-phosphatidylglycerol (POPG) were purchased from Avanti Polar Lipids (Alabaster, Alabama, USA).

6.5.2 Peptide synthesis and analysis

Automated peptide synthesis was performed by solid-phase Fmoc/tBu-chemistry using an automated peptide synthesizer for multiple peptide synthesis (RSP5032, Tecan, Hombrechtlikon, Switzerland) in 2 ml syringes according to the following protocol: Fmoc-amino acids (twelve-fold excess) were coupled by *in situ* activation using DIC/HOBt for 90 min followed by removal of the Fmoc-protecting group by treatment with piperidine/DMF (1:4, v/v) twice for 8 min. The resin was washed with DMF (6x) after each coupling and deprotection step. Side chains of Asn and Gln were Trt-protected and the side chains of Lys and Trp were Boc-protected, the side chain of Arg was Pbf-protected. Peptides were cleaved off the resin by treatment with TFA/TIS/EDT/H_2O (92.5:2.5:2.5:2.5, v/v/v/v) for 4 h. Crude peptides were precipitated by adding cold diethyl ether (-20°C). The precipitated peptides

were collected by centrifugation and resuspended in cold diethyl ether. This procedure was repeated twice. Finally, peptides were dissolved in tBuOH/H_2O (4:1, v/v) and lyophilized.

Peptides and conjugates were analyzed by analytical RP-HPLC using a water (0.1% TFA) (solvent A)/ACN (0.1% TFA) (solvent B) gradient on a Waters 600 System (Eschborn, Germany) with detection at 214 nm. The samples were analyzed on an analytical column (Nucleosil 100, 250 x 2 mm, C18 column, 5 μm particle diameter; Grom, Herrenberg, Germany), using a linear gradient from 10% B to 100% B within 30 min (flow rate: 0.3 ml/min). Both peptides were purified by preparative RP-HPLC (Nucleosil 300, 250 x 20 mm, C18 column, 10 μm particle diameter; Grom, Herrenberg, Germany) on a Gilson preparative system (Bad Camberg, Germany, equipped with a 321 Pump and a 156 UV/Vis Detector, flow rate 10 ml/min). Gradients were adjusted according to the elution profiles and peak profiles obtained from the analytical HPLC chromatograms. Peptide purities of both peptides used in this study were > 98% (214 nm, HPLC).

MALDI-TOF-MS. 1 μl of 2,5-dihydroxyacetophenone (DHAP) matrix (20 mg of DHAP, 5 mg of ammonium citrate in 1 ml of isopropyl alcohol/H_2O (4:1, v/v)) was mixed with 1 μl of each sample (dissolved in ACN/water (1:1) at a concentration of 1 mg/ml) on a gold target. Measurements were performed using a MALDI-TOF system (G2025A, Hewlett-Packard, Waldbronn, Germany). For signal generation 20-50 laser shots were added up in the single shot mode.

6.5.3 Solid-phase synthesis of Tamra-Antp-Fluo and Tamra-Antp

The doubly-labeled peptide Tamra-Antp-Fluo was synthesized using our previously developed Fluo(Trt)-Lys-Rink amide resin (Fischer et al., 2003). The peptide RQIKIWFQNRRMKWKK-$CONH_2$ was assembled on this resin in a 15 μmol scale as described above. A small fraction of this peptide was cleaved off and analyzed (RQIKIWFQNRRMKWKK-εLys(Fluo)-$CONH_2$, (purity 80% (HPLC, 214 nm), calc. $[M+H]^+$ = 2733.3 Da, exp. $[M+H]^+$ = 2733.3 Da, determined by MALDI-MS)). 5 μmol of the resin bound and side-chain protected peptide was then reacted with 5(6)-carboxytetramethylrhodamine-N-succinimidyl ester (10 μmol,

5.3 mg) in DMF (200 μl) containing DIPEA (25 μmol, 4.3 μl). After 16 h, the resin was thoroughly washed. Cleavage and deprotection of the doubly-labeled peptide amide was performed as described above. The peptide was dissolved in ACN/water, lyophilized and analyzed by HPLC and MALDI-MS. Methionine sulfoxide reduction was performed as described elsewhere (Beck *et al.*, 1994). The peptide was then purified as described by preparative HPLC for spectroscopic characterization.

The mono labeled peptide Tamra-Antp (Tamra-RQIKIWFQNRRMKWKK-$CONH_2$) was synthesized on Rink amide resin in a 15 μmol scale. N-terminal labeling with Tamra and all other steps were performed as described above for Tamra-Antp-Fluo.

Both peptides were dissolved in DMSO at concentrations of 10 mM. These stock solutions were further diluted 1:20 in ddH_2O. Peptide concentrations were determined by UV/VIS-spectroscopy of a further 1:100 dilution in methanol. Absorptions of these solutions were measured at 540 nm (ε = 95.000 l/(mol·cm)).

6.5.4 Fluorescence emission spectra

Fluorescence emission spectra were recorded at RT using an LS50B spectrofluorometer (Perkin-Elmer, Norwalk, CT, USA). The spectra were corrected for the sensitivity of the detection system. The excitation and emission bandwidths were set to 10 nm.

6.5.5 Preparation of small unilamellar vesicles (SUVs)

Vesicles were prepared by initially dissolving the phospholipids (1-palmitoyl-2-2-oleoyl-phosphocholine (=POPC) and 1-palmitoyl-2-2-oleoyl-phosphoglycerol (=POPG)) at a concentration of 25 mg/ml in chloroform. Then the appropriate volumes of both solutions were mixed to obtain a ratio of 70/30 (w/w, POPC/POPG)). The solvent was removed by placing the sample under high vacuum. The dried lipids were then dispersed in the appropriate volume of HBS buffer (final concentration 1 mM). The solution was vigorously mixed and incubated for 1 h at RT. The sample was then mixed again and sonicated untill the

solution turned clear. All steps for SUV-containing solutions were performed using glass tubes and glass syringes, in order to prevent adsorption of the lipids to plastic surfaces.

6.5.6. Cell culture

The adherent MC57 fibrosarcoma cell line (Hosaka et al., 1986) was grown in a 5% CO_2 humidified atmosphere at 37°C in RPMI 1640 medium with stabilized glutamine and 2.0 g/l $NaHCO_3$ (PAN Biotech, Aidenbach, Germany) supplemented with 10% fetal calf serum (PAN Biotech), 100 U/ml penicillin, and 100 µg/ml streptomycin (Biochrom, Berlin, Germany). Both cell lines were passaged by trypsinization with trypsin/EDTA (0.05/0.02% (w/v)) (Biochrom) in PBS every third to fourth day.

6.5.7 Confocal laser scanning microscopy

Confocal laser scanning microscopy was performed on an inverted LSM510 laser scanning microscope (Carl Zeiss, Göttingen, Germany) fitted with a Plan-Apochromat 63x 1.4 N.A. lens. All measurements were performed with living, non-fixed cells. MC57 cells were seeded at a density of 10,000/well in eight-well chambered cover glasses (Nunc, Wiesbaden, Germany). Two days later, before addition of inhibitors or peptides, cells were washed once with serum-free RPMI 1640. The indicated inhibitor was added in 200 µl serum-free RPMI 1640 30 min before addition of peptides. After 2 h incubation with peptides, images were acquired immediately at RT with excess peptide in the medium. For double detection of fluorescein and Tamra the 488 nm line of an Argon-Ion laser and the light of a 543 nm Helium-Neon laser were directed over an HFT 488/543 beam splitter and fluorescence was detected using an NFT 545 beam splitter in combination with a BP 505-530 band pass filter for fluorescein detection and an LP 560 long pass filter for Tamra-detection.

6.5.8 Fluorescence emission measurements in cell lysates

MC57 were seeded in 6 well plates (Sarstedt, Nümbrecht, Germany) in serum-containing RPMI 1640. Two days later, the confluent cell layer was washed with

serum-free RPMI 1640 and incubated with 500 µl serum-free RPMI 1640 (+/- the indicated inhibitor) for 30 min. Then Tamra-Antp-Fluo was added and after 2 h incubation, cells were washed twice with PBS, detached using EDTA (5 mM)/PBS (10 min at 37°C), transferred into a fresh tube and washed twice with 1 ml PBS. A small fraction of the cells was used for flow cytometric analysis. Cell suspensions were then resuspended in 1 ml PBS and split into half. Both suspensions were then transferred into a fresh tube and spun down. Following removal of the supernatants, one half was lysed in 200 µl NP-40 lysis buffer (0.5% (v/v) NP-40, 150 mM NaCl, 5 mM EDTA, 50 mM TRIS, pH 7.0, containing protease inhibitor cocktail (Roche Diagnostics, Mannheim, Germany). Theses lysates were then sonicated and centrifuged for 30 min at 4°C and 14,000 rpm. Fluorescence emission spectra of the supernatants were recorded immediately (excitation 492 nm). These lysates were always stored on ice. The second half of the cells was lysed in 180 µl NP-40 lysis buffer. Theses lysates were then also sonicated and centrifuged for 30 min at 4°C and 14.000 rpm. 20 µl of proteinase K-solution (10 mg/ml, Sigma, Taufkirchen) was then added to the supernatants. After 16 h fluorescence emission spectra of the supernatants were recorded (excitation 492 nm).

6.5.8 Flow cytometry

Flow cytometry was performed on a FACS-Calibur (Becton Dickinson). The fluorescence of 5000 vital cells was acquired. Vital cells were gated based on sideward and forward scatter. For calculating the fluorescence emission ratios the median fluorescence intensities of 5000 vital cells were taken. Under the experimental conditions, about 35% of the fluorescein emission intensity was detectable in the FL-2 channel (= Tamra-channel), whereas no fluorescence emission from Tamra was detectable in the FL-1 channel (fluorescein-channel). The data obtained were not compensated for this cross-talk.

7 References

1. Adamczyk,M., Fishpaugh,J.R., and Heuser,K.J. (1997). Preparation of succinimidyl and pentafluorophenyl active esters of 5- and 6- carboxyfluorescein. *Bioconjug. Chem.,* **8,** 253-255.

2. Aletras,A., Barlos,K., Gatos,D., Koutsogianni,S., and Mamos,P. (1995). Preparation of the very acid-sensitive Fmoc-Lys(Mtt)-OH. *Int. J. Pept. Protein Res.,* **45,** 488-496.

3. Aliprantis,A.O., Yang,R.B., Mark,M.R., Suggett,S., Devaux,B., Radolf,J.D., Klimpel,G.R., Godowski,P., and Zychlinsky,A. (1999). Cell activation and apoptosis by bacterial lipoproteins through toll-like receptor-2. *Science,* **285,** 736-739.

4. Andrieu,M., Loing,E., Desoutter,J.F., Connan,F., Choppin,J., Gras-Masse,H., Hanau,D., Dautry-Varsat,A., Guillet,J.G., and Hosmalin,A. (2000). Endocytosis of an HIV-derived lipopeptide into human dendritic cells followed by class I-restricted CD8(+) T lymphocyte activation. *Eur. J. Immunol.,* **30,** 3256-3265.

5. Anthoni,U., Christophersen,C., Nielsen,P.H., Püschl,A., and Schaumburg,K. (1995). Structure of red and orange fluorescein. *Struct. Chem.,* **6,** 161-165.

6. Astriab-Fisher,A., Sergueev,D., Fisher,M., Shaw,B.R., and Juliano,R.I. (2002). Conjugates of antisense oligonucleotides with the Tat and antennapedia cell-penetrating peptides: Effects on cellular uptake, binding to target sequences, and biologic actions. *Pharm. Res.,* **19,** 744-754.

7. Aubin,J.E. (1979). Autofluorescence of viable cultured mammalian cells. *J. Histochem. Cytochem.,* **27,** 36-43.

8. Augustyns,K., Kraas,W., and Jung,G. (1998). Investigation of the stability of the Dde-protecting group used in peptide synthesis - migration to an unprotected lysine. *J. Pept. Res.,* **51,** 127-133.

9. Bark,S.J. and Hahn,K.M. (2000). Fluorescent indicators of peptide cleavage in the trafficking compartments of living cells: Peptides site-specifically labeled with two dyes. *Methods,* **20,** 429-435.

10. Barlos,K., Gatos,D., Koutsogianni,S., Schäfer,W., Stavropoulos,G., and Wenqing,Y. (1991). Darstellung und Einsatz von N-Fmoc-O-Trt-Hydroxyaminosäuren zur "Solid Phase" Synthese von Peptiden. *Tetrahedron Lett.,* **21,** 471-474.

11. Barth,H., Blöcker,D., Behlke,J., Bergsma-Schutter,W., Brisson,A., Benz,R., and Aktories,K. (2000). Cellular uptake of *Clostridium botulinum* C2 toxin requires oligomerization and acidification. *J. Biol. Chem.,* **275,** 18704-18711.

12. Barth,M., Fischer,R., Brock,R., and Rademann,J. (2005). Reversible cross-linking of hyperbranched polymers: A strategy for the combinatorial decoration of multivalent scaffolds. *Angew. Chem. Int. Ed.,* **44,** 1560-1563.

13. Beck,W. and Jung,G. (1994). Convenient reduction of S-oxides in synthetic peptides, lipopeptides and peptide libraries. *Lett. Pept. Sci.,* **1,** 31-37.

14. Bellet-Amalric,E., Blaudez,D., Desbat,B., Graner,F., Gauthier,F., and Renault,A. (2000). Interaction of the third helix of Antennapedia homeodomain and a phospholipid monolayer,

studied by ellipsometry and PM-IRRAS at the air-water interface. *Biochim. Biophys. Acta,* **1467,** 131-143.

15. Berlose,J.P., Convert,O., Derossi,D., Brunissen,A., and Chassaing,G. (1996). Conformational and associative behaviours of the third helix of antennapedia homeodomain in membrane-mimetic environments. *Eur. J. Biochem.,* **242,** 372-386.

16. Bourel,L., Carion,O., Gras-Masse,H., and Melnyk,O. (2000). The deprotection of Lys(Mtt) revisited. *J. Pept. Sci.,* **6,** 264-270.

17. Bowman,E.J., Siebers,A., and Altendorf,K. (1988). Bafilomycins: a class of inhibitors of membrane ATPases from microorganisms, animal cells, and plant cells. *Proc. Natl. Acad. Sci. U. S. A.,* **85,** 7972-7976.

18. Brand,L. and Johnson,M.L. (1997). Fluorescence spectroscopy. *Methods Enzymol.,* **278**.

19. Braun,V. (1975). Covalent lipoprotein from the outer membrane of Escherichia coli. *Biochim. Biophys. Acta,* **415,** 335-377.

20. Brinkley,M. (1992). A brief survey of methods for preparing protein conjugates dyes, haptens, and cross-linking reagents. *Bioconjug. Chem.,* **3,** 2-13.

21. Brock,R., Vamosi,G., Vereb,G., and Jovin,T.M. (1999). Rapid characterization of green fluorescent protein fusion proteins on the molecular and cellular level by fluorescence correlation microscopy. *Proc. Natl. Acad. Sci. U. S. A.,* **96,** 10123-10128.

22. Bycroft,B.W., Chan,W.C., Chhabra,S.R., and Hone,N.D. (1993). A novel lysine-protecting procedure for continous flow solid phase synthesis of branched peptides. *J. Chem. Soc. , Chem. Commun.,* 778-779.

23. Chen,L., Wright,L.R., Chen,C.-H., Oliver,S.F., Wender,P.A., and Mochly-Rosen,D. (2001). Molecular transporters for peptides: delivery of a cardioprotective epsilon PKC agonist peptide into cells and intact ischemic heart using a transport system, R-7. *Chem. Biol.,* **8,** 1123-1129.

24. Chen,R.F. and Knutson,J.R. (1988). Mechanism of fluorescence concentration quenching of carboxyfluorescein in liposomes: energy transfer to nonfluorescent dimers. *Anal. Biochem.,* **172,** 61-77.

25. Chico,D.E., Given,R.L., and Miller,B.T. (2003). Binding of cationic cell-permeable peptides to plastic and glass. *Peptides,* **24,** 3-9.

26. Chiu,Y.L., Ali,A., Chu,C.Y., Cao,H., and Rana,T.M. (2004). Visualizing a Correlation between siRNA Localization, Cellular Uptake, and RNAi in Living Cells. *Chem. Biol.,* **11,** 1165-1175.

27. Christiaens,B., Symoens,S., Verheyden,S., Engelborghs,Y., Joliot,A., Prochiantz,A., Vandekerckhove,J., Rosseneu,M., Vanloo,B., and Vanderheyden,S. (2002). Tryptophan fluorescence study of the interaction of penetratin peptides with model membranes. *Eur. J. Biochem.,* **269,** 2918-2926.

28. Clague,M.J., Urbe,S., Aniento,F., and Gruenberg,J. (1994). Vacuolar ATPase activity is required for endosomal carrier vesicle formation. *J. Biol. Chem.,* **269,** 21-24.

29. Clegg,R.M. (1995). Fluorescence resonance energy transfer. *Curr. Opin. Biotechnol.,* **6,** 429-435.

30. Console,S., Marty,C., Garcia-Echeverria,C., Schwendener,R., and Ballmer-Hofer,K. (2003). Antennapedia and HIV TAT "protein transduction domains" promote endocytosis of high Mr cargo upon binding to cell surface glycosaminoglycans. *J. Biol. Chem.,* **278,** 35109-35114.

31. Cummings,R.T., Salowe,S.P., Cunningham,B.R., Wiltsie,J., Park,Y.W., Sonatore,L.M., Wisniewski,D., Douglas,C.D., Hermes,J.D., and Scolnick,E.M. (2002). A peptide-based fluorescence resonance energy transfer assay for Bacillus anthracis lethal factor protease. *Proc. Natl. Acad. Sci. U. S. A.,* **99,** 6603-6606.

32. de Duve,C., DeBarsy,T., Poole,A., Trouet,A., Tulkens,P., and Van Hoof,F. (1974). Lysosomotropic Agents. *Biochem. Pharmacol.,* **23,** 2495-2531.

33. Dedier,S., Reinelt,S., Rion,S., Folkers,G., and Rognan,D. (2001). Use of fluorescence polarization to monitor MHC-peptide interactions in solution. *J. Immunol. Methods,* **255,** 57-66.

34. Dengjel,J., Schoor,O., Fischer,R., Reich,M., Kraus,M., Kreymborg,K., Altenberend,F., Kalbacher,H., Brock,R., Driesen,C., Rammensee,H.-G., and Stevanovic,S. (2005). Autophagy promotes MHC-II presentation of peptides from intracellular source proteins. *Proc. Natl. Acad. Sci. U. S. A.,* **in print 2005**.

35. Deres,K., Schild,H., Wiesmuller,K.H., Jung,G., and Rammensee,H.G. (1989). In vivo priming of virus-specific cytotoxic T lymphocytes with synthetic lipopeptide vaccine. *Nature,* **342,** 561-564.

36. Derossi,D., Calvet,S., Trembleau,A., Brunissen,A., Chassaing,G., and Prochiantz,A. (1996). Cell internalization of the third helix of the antennapedia homeodomain is receptor-independent. *J. Biol. Chem.,* **271,** 18188-18193.

37. Derossi,D., Joliot,A.H., Chassaing,G., and Prochiantz,A. (1994). The third helix of the Antennapedia Homeodomain translocates through biological membranes. *J. Biol. Chem.,* **269,** 10444-10450.

38. Dettin,M., Scarinci,C., Zanotto,C., Cabrelle,A., de Rossi,A., and di Bello,C. (1998). Design, synthesis and CD4 binding studies of a fluorescent analogue of a peptide that enhances HIV-1 infectivity. *J. Pept. Res.,* **51,** 110-115.

39. Dick,L.R., Cruikshank,A.A., Gernier,L., Melandri,F.D., Nunes,S.L., and Stein,R.L. (1996). Mechanistic studies on the inactivation of the proteasome by lactacystin. *J. Biol. Chem.,* **271,** 7273-7276.

40. Dokka,S., Toledovelasquez,X., Shi,X.L., Wang,L.Y., and Rojanasakul,Y. (1997). Cellular delivery of oligonucleotides by synthetic import peptide carrier. *Pharm. Res.,* **14,** 1759-1764.

41. Drecktrah,D., de Figueiredo,P., Mason,R.M., and Brown,W.J. (1998). Retrograde trafficking of both Golgi complex and TGN markers to the ER induced by nordihydroguaiaretic acid and cyclofenil diphenol. *J. Cell. Sci.,* **111,** 951-965.

42. Drin,G., Cottin,S., Blanc,E., Rees,A.R., and Temsamani,J. (2003). Studies on the internalization mechanism of cell-penetrating peptides. *J. Biol. Chem.,* **278,** 31192-31201.

43. Drin,G., Mazel,M., Clair,P., Mathieu,D., Kaczorek,M., and Temsamani,J. (2001). Physico-chemical requirements for cellular uptake of pAntp peptide. *Eur. J. Biochem.,* **268,** 1304-1314.

44. Du,C., Yao,SY., Rojas,M., and Lin,Y.-Z. (1998). Conformational and topological requirements of cell-permeable peptide function. *J. Pept. Res.,* **15,** 235-243.

45. Eichholtz,T., de Bont,D.B., de Widt,J., Liskamp,R.M., and Ploegh,H.L. (1993). A myristoylated pseudosubstrate peptide, a novel protein kinase C inhibitor. *J. Biol. Chem.,* **268,** 1982-1986.

46. Elmquist,A. and Langel,Ü. (2003). In vitro uptake and stability study of pVEC and its All-D analog. *Biol. Chem.,* **384,** 387-393.

47. Elmquist,A., Lindgren,M., Bartfai,T., and Langel,Ü. (2001). VE-cadherin-derived cell-penetrating, pVEC, with carrier functions. *Exp. Cell Res.,* **269,** 237-244.

48. Falnes,P.O., Wesche,J., and Olsnes,S. (2001). Ability of the Tat basic Domain and VP22 to mediate cell binding, but not membrane translocation of the Diphteria Toxin A-Fragment. *Biochemistry,* **40,** 4349-4358.

49. Fenteany,G., Standaert,R.F., Lane,W.S., Choi,S., Corey,E.J., and Schreiber,S.L. (1995). Inhibition of proteasome activities and subunit-specific amino-terminal threonine modification by lactacystin. *Science,* **268,** 726-731.

50. Fischer,P.M., Krausz,E., and Lane,D.P. (2001). Cellular delivery of impermeable effector molecules in the form of conjugates with peptides capable of mediating membrane translocation. *Bioconjug. Chem.,* **12,** 825-841.

51. Fischer,P.M., Zhelev,N.Z., Wang,S., Melville,J.E., Fahraeus,R., and Lane,D.P. (2000). Structure-activity relationship of truncated and substituted analogues of the intracellular delivery vector Penetratin. *J. Pept. Res.,* **55,** 163-172.

52. Fischer,R., Fotin-Mleczek,M., and Brock,R. (2005a). Break on through to the other side - Biophysics and cell biology shed light on cell-penetrating peptides. *ChemBioChem,* **in print 2005**.

53. Fischer,R., Hufnagel,H.-J., Baechle,D., Stoevesandt,O., Jung,G., and Brock,R. (2005b). *In vitro* and *in vivo* applications of doubly-labelled fluorescent cell-penetrating peptides. *To be submitted 2005*.

54. Fischer,R., Köhler,K., Fotin-Mleczek,M., and Brock,R. (2004). A stepwise dissection of the intracellular fate of cationic cell-penetrating peptides. *J. Biol. Chem.,* **279,** 12625-12635.

55. Fischer,R., Mader,O., Jung,G., and Brock,R. (2003). Extending the applicability of carboxyfluorescein in solid-phase synthesis. *Bioconjug. Chem,* **14,** 653-660.

56. Fischer,R., Waizenegger,T., Köhler,K., and Brock,R. (2002). A quantitative validation of fluorophore-labelled cell-permeable peptide conjugates: fluorophore and cargo dependence. *Biochim. Biophys. Acta,* **1564,** 365-374.

57. Fittipaldi,A., Ferrari,A., Zoppe,M., Arcangeli,C., Pellegrini,V., Beltram,F., and Giacca,M. (2003). Cell membrane lipid rafts mediate caveolar endocytosis of HIV-1 tat fusion proteins. *J. Biol. Chem.,* **278,** 34141-34149.

58. Flechsler,I., Surovoy,A., Charisse,K., Bayer,E., and Jung,G. (1998). Comparison of antisense vectors and antisense oligonucleotides delivered by means of the new cationic lipids unifectin and maxifectin. *Adv. Exp. Med. Biol,* **451,** 469-472.

59. Fleckenstein,B., Jung,G., and Wiesmuller,K.H. (1999). Quantitative analysis of peptide-MHC class II interaction. *Semin. Immunol.,* **11,** 405-416.

60. Fompeydie,D. and Levillain,P. (1980). Equilibre entre formes structurales de l'eosine et de la fluorescein moleculaires.Influence des solvants. *Bulletin de la societe chimique de France,* I-459-I-465.

61. Ford,K.G., Souberbielle,B.E., Darling,D., Farzaneh,F., and . (2001). Protein transduction: an alternative to genetic intervention? *Gene Ther.,* **8,** 1-4.

62. Frackenpohl,J., Arvidsson,P.I., Schreiber,J.V., and Seebach,D. (2001). The outstanding biological stability of beta- and gamma-peptides toward proteolytic enzymes: an in vitro investigation with fifteen peptidases. *ChemBioChem,* **2,** 445-455.

63. Frankel,A.D. and Pabo,C.O. (1988). Cellular uptake of the tat protein from human immunodefiency virus. *Cell,* **55,** 1189-1193.

64. Fringeli,U.P. and Fringeli,M. (1979). Pore formation in lipid membranes by alamethicin. *Proc. Natl. Acad. Sci. U. S. A.,* **76,** 3852-3856.

65. Fujihara,S.M., Cleaveland,J.S., Grosmaire,L.S., Berry,K.K., Kennedy,K.A., Blake,J.J., Loy,J., Rankin,B.M., Ledbetter,J.A., and Nadler,S.G. (2000). A D-amino acid peptide inhibitor of NF-κB nuclear localization is efficacious in models of inflammatory disease. *J. Immunol.,* **165,** 1004-1012.

66. Fulop,L., Penke,B., and Zarandi,M. (2001). Synthesis and fluorescent labeling of beta-amyloid peptides. *J. Peptide Sci.,* **7,** 397-401.

67. Futaki,S. (2002). Arginine-rich peptides: potential for intracellular delivery of macromolecules and the mystery of the translocation mechanisms. *Int. J. Pharm.,* **245,** 1-7.

68. Futaki,S., Suzuki,T., Ohashi,W., Yagami,T., Tanaka,S., Ueda,K., and Sugiura,Y. (2001). Arginine-rich peptides. *J. Biol. Chem.,* **276,** 5836-5840.

69. Garred,O., van Deurs,B., and Sandvig,K. (1995). Furin-induced cleavage and activation of Shiga toxin. *J. Biol. Chem.,* **270,** 10817-10821.

70. Geoghegan,K.F., Rosner,P.J., and Hoth,L.R. (2000). Dye-pair reporter systems for protein-peptide molecular interactions. *Bioconjug. Chem.,* **11,** 71-77.

71. Giriat,I. and Muir,T.W. (2003). Protein semi-synthesis in living cells. *J. Am. Chem. Soc.,* **125,** 7180-7181.

72. Gras-Masse,H. (2003). Lipid vector for the delivery of peptides towards intracellular pharmacological targets. *J. Mol. Recognit.,* **16,** 234-239.

73. Gruenberg,J. (2001). The endocytic pathway: A mosaic of domains. *Nat. Rev. Mol. Cell Biol.,* **2,** 721-730.

74. Habermann,E. (1972). Bee and wasp venoms. *Science,* **177,** 314-322.

75. Hanke,W., Methfessel,C., Wilmsen,H.U., Katz,E., Jung,G., and Boheim,G. (1983). Melittin and a chemically modified trichotoxin form alamethicin-type multi-state pores. *Biochim. Biophys. Acta,* **727,** 108-114.

76. Hawiger,J. (1999). Noninvasive intracellular delivery of funtional peptides and proteins. *Curr. Opin. Chem. Biol.,* **3,** 89-94.

77. Hoff,A., André,T., Fischer,R., Voss,S., Hulko,M., Marquardt,U., Wiesmüller,K.-H., and Brock,R. (2004). Chemolabile cellular microarrays for the screening of small compounds and peptides. *Mol. Divers.,* **8,** 311-320.

78. Hoffmann,P., Heinle,S., Schade,U.F., Loppnow,H., Ulmer,A.J., Flad,H.D., Jung,G., and Bessler,W.G. (1988). Stimulation of human and murine adherent cells by bacterial lipoprotein and synthetic lipopeptide analogues. *Immunobiology,* **177,** 158-170.

79. Honey,K. and Rudensky,A.Y. (2003). Lysosomal cysteine proteases regulate antigen presentation. *Nat. Rev. Immunol.,* **3,** 472-482.

80. Hoogerhout,P., Stittelaar,K.J., Brugghe,H.F., Timmermans,J.A.M., ten Hove,G.J., Jiskoot,W., Hoekman,J.H.G., and Roholl,P.J.M. (1999). Solid-phase synthesis and application of double-fluorescent-labeled lipopeptides, containing a CTL-epitope from the measles fusion protein. *J. Pept. Res.,* **54,** 436-443.

81. Horng,T., Barton,G.M., and Medzhitov,R. (2001). TIRAP: an adapter molecule in the Toll signaling pathway. *Nat. Immunol.,* **2,** 835-841.

82. Hosaka,Y., Yasuda,Y., Seriburi,O., Moran,M.G., and Fukai,K. (1986). *In vitro* secondary generation of cytotoxic T lymphocytes in mice with mumps virus and their mumps-specific cytotoxicity among paramyxoviruses. *J. Virol.,* **57,** 1113-1118.

83. Irmscher,G. and Jung,G. (1977). [The hemolytic properties of the membrane modifying peptide antibiotics alamethicin, suzukacillin and trichotoxin (author's transl)]. *Eur. J. Biochem.,* **80,** 165-174.

84. Jack,R.W. and Jung,G. (1998). Natural peptides with antimicrobial activity. *Chimia,* **52,** 48-55.

85. Jans,D.A., Xiao,C.-Y., and Lam,M.H.C. (2000). Nuclear targeting signal recognition: a key control point in nuclear transport. *Bioessays,* **22,** 532-544.

86. Joliot,A., Pernelle,C., Deagostini-Bazin,H., and Prochiantz,A. (1991). Antennapedia homeobox peptide regulates neural morphogenesis. *Proc. Natl. Acad. Sci. U. S. A.,* **88,** 1864-1868.

87. Jones,J., Heim,R., Hare,E., Stack,J., and Pollok,B.A. (2000). Development and application of a GFP-FRET intracellular caspase assay for drug screening. *J. Biomol. Screen.,* **5,** 307-318.

88. Jung,G. and Beck-Sickinger,A.G. (1992). Multiple peptide synthesis methods and their applications. *Angew. Chem. Int. Ed.,* **31,** 367-383.

89. Jung,G.E. (1996). *Combinatorial Peptide and Nonpeptide Libraries: A Handbook.* Wiley-VCH, Weinheim.

90. Jung,G.E. (1999). *Combinatorial Chemistry: Synthesis, Analysis, Screening.* Wiley-VCH, Weinheim.

91. Kim,D.T., Mitchell,D.J., Brockstedt,D.G., Fong,L., Nolan,G.P., Fathman,C.G., Engleman,E.G., and Rothbard,J.B. (1997). Introduction of soluble proteins into the MHC Class I pathway by conjugation to an HIV tat peptide. *J. Immunol.,* **159,** 1666-1668.

92. Kozak,S.L., Kuhmann,S.E., Platt,E.J., and Kabat,D. (1999). Roles of CD4 and coreceptors in binding, endocytosis, and proteolysis of gp120 envelope glycoproteins derived from human immunodeficiency virus type 1. *J. Biol. Chem.,* **274,** 23499-23507.

93. Kruger,R.G., Dostal,P., and McCafferty,D.G. (2002). An economical and preparative orthogonal solid phase synthesis of fluorescein and rhodamine derivatized peptides: FRET substrates for the Staphylococcus aureus sortase SrtA transpeptidase reaction. *Chem. Comm.,* **18,** 2092-2093.

94. Langel,Ü. (2002). *Cell Penetrating Peptides: Processes and Applications.* CRC Press, Boca Raton, FL.

95. Lewin,M., Carlesso,N., Tung,C.-H., Tang,X.-W., Cory,D., Scadden,D.T., and Weissleder,R. (2000). Tat peptide-derivatized magnetic nanoparticles allow in vivo tracking and recovery of progenitor cells. *Nat. Biotechnol.,* **18,** 410-414.

96. Li,Y. and Glazer,A.N. (1999). Design, synthesis, and spectroscopic properties of peptide-bridged fluorescence energy-transfer cassettes. *Bioconjug. Chem.,* **10,** 241-245.

97. Lien,E., Sellati,T.J., Yoshimura,A., Flo,T.H., Rawadi,G., Finberg,R.W., Carroll,J.D., Espevik,T., Ingalls,R.R., Radolf,J.D., and Golenbock,D.T. (1999). Toll-like receptor 2 functions as a pattern recognition receptor for diverse bacterial products. *J. Biol. Chem.,* **274,** 33419-33425.

98. Lin,Y.-Z., Yao,SY., Veach,R.A., Torgerson,T.R., and Hawiger,J. (1995). Inhibition of nuclear translocation of transcription factor NF-κB by a synthetic peptide containing a cell membrane-permeable motif and nuclear localization sequence. *J. Biol. Chem.,* **270,** 14255-14258.

99. Lindberg,M. and Graeslund,A. (2001). The position of the cell penetrating peptide penetratin in SDS micelles determined by NMR. *FEBS Lett.,* **497,** 39-44.

100. Lipinski,C.A., Lombardo,F., Dominy,B.W., and Feeney,P.J. (2001). Experimental and computational approaches to estimate solubility and permeability in drug discovery and development settings. *Adv. Drug Deliv. Rev.,* **46,** 3-26.

101. Liu,X.-Y., Timmons,S., Lin,Y.-Z., and Hawiger,J. (1996). Identification of a functionally important sequence in the cytoplasmic tail of integrin β3 by using cell-permeable peptide analogs. *Proc. Natl. Acad. Sci. U. S. A.,* **93,** 11819-11824.

102. Loffet,A. and Zhang,H.X. (1993). Allyl-based groups for side-chain protection of amino acids. *Int. J. Pept. Protein Res.,* **42,** 346-351.

103. Loing,E., Andrieu,M., Thiam,K., Schorner,D., Wiesmuller,K.H., Hosmalin,A., Jung,G., and Gras-Masse,H. (2000). Extension of HLA-A*0201-restricted minimal epitope by N epsilon-palmitoyl-lysine increases the life span of functional presentation to cytotoxic T cells. *J. Immunol.,* **164,** 900-907.

104. Lord,J.M. and Roberts,L.M. (1998). Toxin entry: retrograde transport through the secretory pathway. *J. Cell. Biol.,* **140,** 733-736.

105. Lu,J., Higashimoto,Y., Appella,E., and Celis,E. (2004). Multiepitope trojan antigen peptide vaccines for the induction of antitumor CTL and Th immune responses. *J Immunol.,* **172,** 4575-4582.

106. Lu,J., Wettstein,P.J., Higashimoto,Y., Appella,E., and Celis,E. (2001). TAP-independent presentation of CTL epitopes by trojan antigens. *J. Immunol.,* **166,** 7063-7071.

107. Mader,O., Reiner,K., Egelhaaf,H.-J., Fischer,R., and Brock,R. (2004). Structure property analysis of pentamethine indocyanine dyes: Identification of a new dye for life science applications. *Bioconjug. Chem.,* **15,** 70-78.

108. Magzoub,M., Eriksson,L.E.G., and Graslund,A. (2002). Conformational states of the cell-penetrating peptide penetratin when interacting with phospholipid vesicles: effects of surface charge and peptide concentration. *Biochim. Biophys. Acta,* **1563,** 53-63.

109. Magzoub,M., Eriksson,L.E.G., and Gräslund,A. (2003). Comparison of the interaction, positioning, structure induction and membrane pertubation of cell-penetrating peptides and non-translocating variants with phospholipid vesicles. *Biophys. Chem.,* **103,** 271-288.

110. Magzoub,M., Kilk,K., Eriksson,L.E.G., Langel,Ü., and Gräslund,A. (2001). Interaction and structure induction of cell-penetrating peptides in the presence of phospholipid vesicles. *Biochim. Biophys. Acta,* **1512,** 77-89.

111. Mai,J.C., Shen,H., Watkins,S.C., Cheng,T., and Robbins,P.D. (2002). Efficiency of protein transduction is cell type-dependent and is enhanced by dextran sulfate. *J. Biol. Chem.,* **277,** 30208-30218.

112. Mann,D.A. and Frankel,A.D. (1991). Endocytosis and targeting of exogenous HIV-1 Tat protein. *EMBO J.,* **10,** 1733-1739.

113. Matsuzaki,K., Yoneyama,S., and Miyajima,K. (1997). Pore formation and translocation of melittin. *Biophys. J.,* **73,** 831-838.

114. Mattingly,P.G. (1992). Preparation of 5- and 6-(aminomethyl)fluorescein. *Bioconjug. Chem.,* **3,** 430-431.

115. Mellman,I., Fuchs,R., and Helenius,A. (1986). Acidification of the endocytic and exocytic pathways. *Annu. Rev. Biochem.,* **55,** 663-700.

116. Merdan,T., Kunath,K., Fischer,D., Kopecek,J., and Kissel,T. (2002). Intracellular processing of poly(ethylene imine)/ribozyme complexes can be observed in living cells by using confocal laser scanning microscopy and inhibitor experiments. *Pharm. Res.,* **19,** 140-147.

117. Metzger,J.W., Sawyer,W.H., Wille,B., Biesert,L., Bessler,W.G., and Jung,G. (1993). Interaction of immunologically-active lipopeptides with membranes. *Biochim. Biophys. Acta,* **1149,** 29-39.

118. Mitchell,D.J., Kim,D.T., Steinman,L., Fathman,C.G., and Rothbard,J.B. (2000). Polyarginine enters cells more efficiently than other polycationic homopolymers. *J. Pept. Res.,* **56,** 318-325.

119. Miyawaki,A., Llopis,J., Heim,R., McCaffery,J.M., Adams,J.A., Ikura,M., and Tsien,R.Y. (1997). Fluorescent indicators for Ca2+ based on green fluorescent proteins and calmodulin. *Nature,* **388,** 882-887.

120. Morris,M.C., Depollier,J., Mery,J., Heitz,F., and Divita,G. (2001). A new peptide carrier for the delivery of biologically active proteins into mammalian cells. *Nat. Biotechnol.,* **19,** 1173-1176.

121. Mueller,P. and Rudin,D.O. (1968). Action potentials induced in biomolecular lipid membranes. *Nature,* **217,** 713-719.

122. Muratovska,A. and Eccles,M.R. (2004). Conjugate for efficient delivery of short interfering RNA (siRNA) into mammalian cells. *FEBS Lett.,* **558,** 63-68.

123. Murchie,A.I., Clegg,R.M., von Kitzing,E., Duckett,D.R., Diekmann,S., and Lilley,D.M. (1989). Fluorescence energy transfer shows that the four-way DNA junction is a right-handed cross of antiparallel molecules. *Nature,* **341,** 763-766.

124. Myou,S., Leff,A.R., Myo,S., Boetticher,E., Tong,J., Meliton,A.Y., Liu,J., Munoz,N.M., and Zhu,X. (2003). Blockade of inflammation and airway hyperresponsiveness in immune-sensitized mice by dominant-negative phosphoinositide 3-kinase-TAT. *J. Exp. Med.,* **198,** 1573-1582.

125. Nagai,Y., Miyazaki,M., Aoki,R., Zama,T., Inouye,S., Hirose,K., Iino,M., and Hagiwara,M. (2000). A fluorescent indicator for visualizing cAMP-induced phosphorylation in vivo. *Nat. Biotechnol.,* **18,** 313-316.

126. Nakayama,K. (1997). Furin: a mammalian subtilisin/Kex2p-like endoprotease involved in processing of a wide variety of precursor proteins. *Biochem. J.,* **327,** 635.

127. Nekhotiaeva,N., Elmquist,A., Rajarao,G.K., Hällbrink,M., Langel,Ü., and Good,L. (2004). Cell entry and antimicrobial properties of eukarytic cell-penetrating peptides. *FASEB J.,* **18,** 394-396.

128. Nishikawa,K., Sawasdikosol,S., Fruman,D.A., Lai,J., Songyang,Z., Burakoff,S.J., Yaffe,M.B., and Cantley,L.C. (2000). A peptide library approach identifies a specific inhibitor for the ZAP-70 protein tyrosine kinase. *Mol. Cell,* **6,** 969-974.

129. Noguchi,H., Matsushita,M., Okitsu,T., Moriwaki,A., Tomizawa,K., Kang,S., Li,S.T., Kobayashi,N., Matsumoto,S., Tanaka,K., Tanaka,N., and Matsui,H. (2004). A new cell-permeable peptide allows successful allogeneic islet transplantation in mice. *Nat. Med.,* **10,** 305-309.

130. Oess,S. and Hildt,E. (2000). Novel cell permeable motif derived from the PreS2-domain of hepatitis-B virus surface antigens. *Gene Ther.,* **7,** 750-758.

131. Olsen,M.J., Stephens,D., Griffiths,D., Daugherty,P., Georgiou,G., and Iverson,B.L. (2000). Function-based isolation of novel enzymes from a large library. *Nat. Biotechnol.,* **18,** 1071-1074.

132. Olsnes,S., Klingenberg,O., and Wiedlocha,A. (2003). Transport of exogenous growth factors and cytokines to the cytosol and to the nucleus. *Physiol. Rev.,* **83,** 163-182.

133. Owens,M.A. and Loken,M.T. (1995). *Flow cytometry: Principles for clinical laboratory practice*, . Wiley-Liss, New York, pp. 28-29.

134. Packard,B.Z., Komoriya,A., Toptygin,D.D., and Brand,L. (1997). Structural characteristics in fluorophores that form intramolecular H-type dimers in a protease substrate. *J. Phys. Chem. B,* **101,** 5070-5074.

135. Papini,A.M., Mazzanti,B., Nardi,E., Traggiai,E., Ballerini,C., Biagioli,T., Kalbacher,H., Beck,H., Deeg,M., Chelli,M., Ginanneschi,M., Massacesi,L., and Vergelli,M. (2001). Palmitoyl derivatives of GpMBP epitopes: T-cell response and peptidases susceptibility. *J Med. Chem,* **44,** 3504-3510.

136. Pearce,D.A., Walkup,G.K., and Imperiali,B. (1998). Peptidyl chemosensors incorporating a FRET mechanism for detection of Ni(II). *Bioorg. Med. Chem. Lett.,* **8,** 1963-1968.

137. Penco,S., Scarfi,S., Giovine,M., Damonte,G., Millo,E., Villaggio,B., Passalacqua,M., Pozzolini,M., Garre,C., and Benatti,U. (2001). Identification of an import signal for, and the nuclear localization of, human lactoferrin. *Biotechnol. Appl. Biochem.,* **34,** 151-159.

138. Perez,F., Liedo,P.-M., Karagoeos,D., Vincent,J.-D., Prochiantz,A., and Ayala,J. (1994). Rab3A and Rab3B carboxy-terminal peptides are both potent and specific inhibitors of prolactin release by rat cultured anterior pituitary cells. *Mol. Endocrinol.,* **8,** 1278-1287.

139. Persson,D., Thoren,P.E.G., Herner,M., Lincoln,P., and Norden,B. (2003). Application of a novel analysis to measure the binding of the membrane-translocating peptide penetratin to negatively charged liposomes. *Biochemistry,* **42,** 421-429.

140. Persson,D., Thoren,P.E.G., and Norden,B. (2001). Penetratin-induced aggregation and subsequent dissociation of negatively charged phospholipid vesicles. *FEBS Lett.,* **505,** 307-311.

141. Pietersz,G.A., Li,W., and Apostolopoulos,V. (2001). A 16-mer peptide (RQIKIWFQNRRMKWKK) from antennapedia preferentially targets the class I pathway. *Vaccine,* **19,** 1397-1405.

142. Pillay,C.S., Elliott,E., and Dennison,C. (2002). Endolysosomal proteolysis and its regulation. *Biochem. J.,* **363,** 417-429.

143. Plank,C., Oberhauser,B., Mechtler,K., Koch,C., and Wagner,E. (1994). The influence of endosome-disruptive peptides on gene transfer using synthetic virus-like transfer systems. *J. Biol. Chem.,* **269,** 12918-12924.

144. Pooga,M., Hällbrink,M., Zorko,M., and Langel,Ü. (1998a). Cell penetration by transportan. *FASEB J.,* **12,** 67-77.

145. Pooga,M., Kut,C., Kihlmark,M., Hallbrink,M., Fernaeus,S., Raid,R., Land,T., Hallberg,E., Bartfai,T., and Langel,U. (2001). Cellular translocation of proteins by transportan. *FASEB J.,* **15,** 1451-1453.

146. Pooga,M., Soomets,U., Hällbrink,M., Valkna,A., Saar,K., Rezaei,K., Kahl,U., Hao,J.-X., Xu,X.-J., Wiesenfeld-Hallin,Z., Hökfelt,T., Bartfei,T., and Langel,Ü. (1998b). Cell penetrating PNA constructs regulate galanin receptor levels and modify transmission in vivo. *Nat. Biotechnol.,* **16,** 857-861.

147. Potocky,T.B., Menon,A.K., and Gellman,S.H. (2003). Cytoplasmic and nuclear delivery of a TAT-derived peptide and a beta-peptide after endocytic uptake into HeLa cells. *J. Biol. Chem.,* **278,** 50188-50194.

148. Prochiantz,A. (1996). Getting hydrophilic compounds into cells: lessons from homeoproteins. *Curr. Opin. Neurobiol.,* **6,** 629-634.

149. Rayne,F., Vendeville,A., Bonhoure,A., and Beaumelle,B. (2004). The Ability of Chloroquine To Prevent Tat-Induced Cytokine Secretion by Monocytes Is Implicated in Its In Vivo Anti-Human Immunodeficiency Virus Type 1 Activity. *J. Virol.,* **78,** 12054-12057.

150. Rejman,J., Oberle,V., Zuhorn,I.S., and Hoekstra,D. (2004). Size-dependent internalization of particles via the pathways of clathrin- and caveolae-mediated endocytosis. *Biochem. J.,* **377,** 159-169.

151. Richard,J.P., Melikov,K., Vives,E., Ramos,C., Verbeure,B., Gait,M.J., Chernomordik,L.V., and Lebleu,B. (2003). Cell-penetrating peptides-A reevaluation of the mechanism of cellular uptake. *J. Biol. Chem.,* **278,** 585-590.

152. Rojas,M., Donahue,J.P., Tan,Z., and Lin,Y.Z. (1998). Genetic engineering of proteins with cell membrane permeability. *Nat. Biotechnol.,* **16,** 370-375.

153. Rojas,M., Yao,S.Y., and Lin,Y.-Z. (1996). Controlling epidermal growth factor (EGF)-stimulated Ras activation in intact cells by a cell-permeable peptide mimicking phosphorylated EGF receptor. *J. Biol. Chem.,* **271,** 27456-27461.

154. Rossi,F.M. and Kao,J.P.Y. (1997). Practical method for the multigram separation of the 5- and 6 isomers of carboxyfluorescein. *Bioconjug. Chem.,* **8,** 495-497.

155. Rötzschke,O., Falk,K., Stevanovic,S., Jung,G., Walden,P., and Rammensee,H.-G. (1991). Exact prediction of a natural T cell epitope. *Eur. J. Immunol.,* **21,** 2891-2894.

156. Rudolph,C., Plank,C., Lausier,J., Schillinger,U., Müller,R.H., and Rosenecker,J. (2003). Oligomers of the arginine-rich motif of the HIV-1 tat protein are capable of transferring plasmid DNA into cells. *J. Biol. Chem.,* **278,** 11411-11418.

157. Ryser,H.J. and Hancock,R. (1965). Histones and basic polyamino acids stimulate the uptake of albumin by tumor cells in culture. *Science,* **150,** 501-503.

158. Ryser,H.J. and Shen,W.C. (1978). Conjugation of methotrexate to poly(L-lysine) increases drug transport and overcomes drug resistance in cultured cells. *Proc. Natl. Acad. Sci. U. S. A.,* **75,** 3867-3870.

159. Salamon,Z., Lindblom,G., and Tollin,G. (2003). Plasmon-waveguide resonance and impedance spectroscopy studies of the interaction between penetratin and supported lipid bilayer membranes. *Biophys. J.,* **84,** 1796-1807.

160. Sandoval,R.M. and Molitoris,B.A. (2003). Gentamicin traffics retrograde through the secretory pathway and is released into the cytosol via the endoplasmic reticulum. *Am. J. Physiol. Renal Physiol.,* **286,** F617-F624.

161. Sandvig,K. and van Deurs,B. (2000). Entry of ricin and shiga toxin into cells: moelcular mechanisms and medical perspectives. *EMBO J.,* **19,** 5943-5950.

162. Sandvig,K. and van Deurs,B. (2002). Transport of protein toxins into cells: pathways used by ricin, cholera toxin and shiga toxin. *FEBS Lett.,* **529,** 49-53.

163. Sarin,V.K., Kent,S.B.H., Tam,J.P., and Merrifield,R.B. (1981). Quantitative monitoring of solid phase peptide synthesis by the ninhydrin reaction. *Anal. Biochem.,* **117,** 147-157.

164. Scheller,A., Oehlke,J., Wiesner,B., Dathe,M., Krause,E., Beyermann,M., Melzig,M., and Bienert,M. (1999). Structural requirements for cellular uptake of alpha-helical amphipathic peptides. *J. Pept. Sci.,* **5,** 185-194.

165. Scheller,A., Wiesner,B., Melzig,M., Bienert,M., and Oehlke,J. (2000). Evidence for an amphipathicity independent cellular uptake of amphipathic cell-penetrating peptides. *Eur. J. Biochem.,* **267,** 6043-6049.

166. Scherer,L.J. and Rossi,J.J. (2003). Approaches for the sequence-specific knockdown of mRNA. *Nat. Biotechnol.,* **21,** 1457-1465.

167. Schmidt,M.C., Rothen-Rutishauser,B., Rist,B., Beck-Sickinger,A.G., Wunderli-Allenspach,H., Rubas,W., Sadee,W., and Merkle,H.P. (1998). Translocation of human calcitonin in respiratory nasal epithelium is associated with self-assembly in lipid membrane. *Biochemistry,* **37,** 16582-16590.

168. Schneekloth,J.S., Jr., Fonseca,F.N., Koldobskiy,M., Mandal,A., Deshaies,R., Sakamoto,K., and Crews,C.M. (2004). Chemical genetic control of protein levels: selective in vivo targeted degradation. *J. Am. Chem. Soc.,* **126,** 3748-3754.

169. Schörner,D. (1999). Lokalisation und Funktionalität von MHC-I-restringierten Lipopeptiden bei T-Lymphom Zellinien., . Dissertation, Universität Tübingen.

170. Schulz,A., Adermann,K., Eulitz,M., Feller,S.M., and Kardinal,C. (2000). Preparation of disulfide-bonded polypeptide heterodimers by titration of thio-activated peptides with thiol-containing peptides. *Tetrahedron,* **56,** 3889-3891.

171. Schutze-Redelmeier,M.-P., Gournier,H., Garcia-Pons,F., Moussa,M., Joliot,A.H., Volovitch,M., Prochiantz,A., and Lemonnier,F.A. (1996). Introduction of exogenous antigens into the MHC class I processing and presentation pathway by Drosophila antennapedia homeodomain primes cytotoxic T cells in vivo. *J. Immunol.,* **157,** 655.

172. Schwarze,S.R., Ho,A., Vocero-Akbani,A., and Dowdy,S.F. (1999). In vivo protein transduction: Delivery of a biologically active protein into the mouse. *Science,* **285,** 1569-1572.

173. Sheldon,K., Liu,D., Ferguson,J., and Gariepy,J. (1995). Loligomers: Design of de novo peptide-based intracellular vehicles. *Proc. Natl. Acad. Sci. U. S. A.,* **92,** 2056-2060.

174. Shen,W.C. and Ryser,H.J. (1978). Conjugation of poly-L-lysine to albumin and horseradish peroxidase: a novel method of enhancing the cellular uptake of proteins. *Proc. Natl. Acad. Sci. U. S. A.,* **75,** 1872-1876.

175. Simeoni,F., Morris,M.C., Heitz,F., and Divita,G. (2003). Insight into the mechanism of the peptide-based gene delivery system MPG: implcations for delivery of siRNA into mammalian cells. *Nucleic Acids Res.,* **31,** 2717-2724.

176. Simonsen,A., Lippe,R., Christoforidis,S., Gaullier,J.-M., Brech,A., Callaghan,J., Toh,B.-H., Murphy,C., Zerial,M., and Stenmark,H. (1998). EAA1 links PI(3)K function to Rab5 regulation of endosome fusion. *Nature,* **394,** 494-498.

177. Singh,D., Bisland,S.K., Kawamura,K., and Gariepy,J. (1999). Peptide-based intracellular shuttle able to facilitate gene transfer in mammalian cells. *Bioconjug. Chem.,* **10,** 745-754.

178. Sjöback,R., Nygren,J., and Kubista,M. (1995). Absorption and fluorescence properties of fluorescein. *Spectrochim. Acta A,* **51,** L7-L21.

179. Smith,A.E. and Helenius,A. (2004). How viruses enter animal cells. *Science,* **304,** 237-242.

180. Southwick,P.L., Ernst,L.A., Tauriello,E.W., Parker,S.R., Mujumdar,R.B., Mujumdar,S.R., Clever,H.A., and Waggoner,A.S. (1990). Cyanine dye labeling reagents--carboxymethylindocyanine succinimidyl esters. *Cytometry,* **11,** 418-430.

181. Stephens,D.J. and Pepperkok,R. (2001). The many ways to cross the plasma membrane. *Proc. Natl. Acad. Sci. U. S. A.,* **98,** 4295-4298.

182. Stoevesandt,O., Elbs,M., Köhler,K., Lellouch,A.C., Fischer,R., André,T., and Brock,R. (2005). Peptide Microarrays for the Detection of Molecular Interactions in Cellular Signal Transduction. *Proteomics,* **in print 2005**.

183. Surovoy,A., Flechsler,I., and Jung,G. (1998). A novel series of serum-resistant lipoaminoacid compounds for cellular delivery of plasmid DNA. *Adv. Exp Med. Biol,* **451,** 461-467.

184. Suzuki,T., Futaki,S., Niwa,M., Tanaka,S., Ueda,K., and Sugiura,Y. (2002). Possible existence of common internalization mechanisms among arginine-rich peptides. *J. Biol. Chem.,* **277,** 2437-2443.

185. Takeshima,K., Chikushi,A., Lee,K.-K., Yonehara,S., and Matsuzaki,K. (2003). Translocation of analogues of the antimicrobial peptides Magainin and Buforin across human cell membranes. *J. Biol. Chem.,* **278,** 1310-1315.

186. Tamai,M., Matsumoto,K., Omura,S., Koyama,I., Ozawa,Y., and Hanada,K. (1986). In vitro and in vivo inhibition of cysteine proteinases by EST, a new analog of E-64. *J. Pharmacobiodyn.,* **9,** 672-677.

187. Theisen,P., McCollum,C., Upadhya,K., Jacobson,K., Vu,H., and Andrus,A. (1992). Fluorescent dye phosphoramidite labelling of oligonucleotides. *Tetrahedron Lett.,* **33,** 5033-5036.

188. Theodore,L., Derossi,D., Chassaing,G., Llirbat,B., Kubes,M., Jordan,P., Chneiweiss,H., Godement,P., and Prochiantz,A. (1995). Intraneuronal delivery of protein kinase C pseudosubstrate leads to growth cone collapse. *J. Neurosci.,* **15,** 7158-7167.

189. Thoren,P.E.G., Persson,D., Isakson,P., Goksor,M., Onfeldt,A., and Norden,B. (2003). Uptake of analogs of penetratin, Tat(48-60) and oligoargine in live cells. *Biochem. Biophys. Res. Commun.,* **307,** 100-107.

190. Thoren,P.E.G., Persson,D., Karlsson,M., and Norden,B. (2000). The antennapedia peptide penetratin translocates across lipid bilayers-the first direct observation. *FEBS Lett.,* **482,** 265-268.

191. Tikhonov,I., Ruckwardt,T.J., Berg,S., Hatfield,G.S., and David,P.C. (2004). Furin cleavage of the HIV-1 Tat protein. *FEBS Lett,* **565,** 89-92.

192. Trehin,R., Krauss,U., Muff,R., Meinecke,M., Beck-Sickinger,A.G., and Merkle,H.P. (2004). Cellular internalization of human calcitonin derived peptides in MDCK monolayers: a comparative study with Tat(47-57) and penetratin(43-58). *Pharm. Res.,* **21,** 33-42.

193. van Deurs,B., Sandvig,K., Petersen,O.W., Olsnes,S., Simons,K., and Griffiths,G. (1988). Estimation of the amount of internalized ricin that reaches the *trans*-Golgi network. *J. Cell. Biol.,* **106,** 253-267.

194. van Weert,A.W.M., Dunn,K.W., Geuze,H.J., Maxfield,F.R., and Stoorvogel,W. (1995). Transport from late endosomes to lysosomes, but not sorting of integral membrane proteins in endosomes, depends on the vacuolar proton pump. *J. Cell. Biol.,* **130,** 821-834.

195. Vendeville,A., Rayne,F., Bonhoure,A., Bettache,N., Montcourrier,P., and Beaumelle,B. (2004). HIV-1 Tat enters T-cells using coated pits before translocating from acidified endosomes and eliciting biological responses. *Mol. Biol. Cell,* **15,** 2347-2360.

196. Verhoeven,A.J., Leusen,J.H., Kessels,G.C., Hilarius,P.M., de Bont,D.B., and Liskamp,R.M. (1993). Inhibition of neutrophil NADPH oxidase assembly by a myristoylated pseudosubstrate of protein kinase C. *J. Biol. Chem.,* **268,** 18593-18598.

197. Vidard,L., Rock,K.L., and Benacerraf,B. (1991). The generation of immunogenic peptides can be selectively increased or decreased by proteolytic enzyme inhibitors. *J. Immunol.,* **147,** 1786-1791.

198. Violini,S., Sharma,V., Prior,J.L., Dyszlewski,M., and Piwnica-Worms,D. (2002). Evidence for a plasma membrane-mediated permeability barrier to Tat basic domain in well-differentiated epithelial cells: lack of correlation with heparan sulfate. *Biochemistry,* **41,** 12652-12661.

199. Vives,E., Brodin,P., and Lebleu,B. (1997). A truncated HIV-1 Tat protein basic domain rapidly translocates through the plasma membrane and accumulates in the cell nucleus. *J. Biol. Chem.,* **272,** 16010-16017.

200. Voss,S*., Fischer,R*., Ulmer,A.J., Jung,G., Wiesmuller,K.H., and Brock,R. (2005). A ratiometric fluorescence-based LPS-sensor*,* **to be submitted 2005**.

201. Wadia,J.S., Stan,R.V., and Dowdy,S.F. (2004). Transducible TAT-HA fusogenic peptide enhances escape of TAT-fusion proteins after lipid raft macropinocytosis. *Nat. Med.,* **10,** 310-315.

202. Waizenegger,T., Fischer,R., and Brock,R. (2002). Intracellular concentration measurements in adherent cells: A comparison of import efficiencies of cell-permeable peptides. *Biol. Chem.,* **383,** 291-299.

203. Wallace,R.W. (1997). Emerging molecular targets. *Drug Disc. Today,* **2,** 124-125.

204. Wang,R.-F. and Wang,H.Y. (2002). Enhancement of antitumor immunity by prolonging antigen presentation on dendritic cells. *Nat. Biotechnol.,* **20,** 149-154.

205. Weber,P.J.A., Bader,J.E., Folkers,G., and Beck-Sickinger,A.G. (1998). A fast and inexpensive method for N-terminal fluorescein-labeling of peptides. *Bioorg. Med. Chem. Lett.,* **8,** 597-600.

206. Wei,A.-P., Blumenthal,D.K., and Herron,J.N. (1994). Antibody-mediated fluorescence enhancement based on shifting the intramolecular dimer<->monomer equilibrium of fluorescent dyes. *Anal. Chem.,* **66,** 1500-1506.

207. Wiesmüller,K.-H., Brich,M., Jung,G., Sparbier,K., and Walden,P. (1955). Peptide binding to MHC class I molecules analyzed by confocal microscopy. *Eur. J. Cell Biology,* **66,** 389-393.

208. Wolf,B., Hauschildt,S., Uhl,B., Metzger,J., Jung,G., and Bessler,W.G. (1989). Localization of the cell activator lipopeptide in bone marrow-derived macrophages by electron energy loss spectroscopy (EELS). *Immunol. Lett,* **20,** 121-126.

209. Zaro,J.L. and Shen,W.C. (2003). Quantative comparsion of membrane transduction and endocytosis of oligopeptides. *Biochem. Biophys. Res. Commun.,* **307,** 241-247.

210. Zasloff,M. (1987). Magainins, a class of antimicrobial peptides from Xenopus skin: isolation, characterization of two active forms, and partial cDNA sequence of a precursor. *Proc. Natl. Acad. Sci. U. S,* **84,** 5449-5453.

211. Zasloff,M. (2002). Antimicrobial peptides of multicellular organisms. *Nature,* **415,** 389-395.

212. Zen,K., Biwersi,J., Periasamy,N., and Verkman,A.S. (1992). Second messengers regulate endosomal acidification in Swiss 3T3 fibroblasts. *J. Cell. Biol.,* **119,** 99-110.

213. Zhang,L., Torgerson,T.R., Liu,X.Y., Timmons,S., Colosia,A.D., Hawiger,J., and Tam,J.P. (1998). Preparation of functionally active cell-permeable peptides by single-step ligation of two peptide modules. *Proc. Natl. Acad. Sci U. S A,* **95,** 9184-9189.

214. Zuhorn,I.S., Kalicharan,R., and Hoekstra,D. (2002). Lipoplex-mediated transfection of mammalian cells occurs through the cholesterol-dependent clathrin-mediated pathway of endocytosis. *J. Biol. Chem.,* **277,** 18021-18028.

8 Publications and presentations

8.1 Original Publications

2002

Waizenegger T, **Fischer R**, Brock R
„Intracellular concentration measurements in adherent cells: a comparison of import efficiencies of cell-permeable peptides"
Biological Chemistry, 383, 291-299, 2002

Fischer R, Waizenegger T, Köhler K, Brock R
„A quantitative validation of fluorophore-labelled cell-permeable peptide conjugates: fluorophore and cargo dependence of import"
Biochimica et Biophysica Acta, 1564, 365-374, 2002

2003

Fischer R, Mader O, Jung G, Brock R
„Extending the applicability of carboxyfluorescein in solid-phase synthesis"
Bioconjugate Chemistry, 14, 653-660, 2003

2004

Mader O, Reiner K, Egelhaaf HJ, **Fischer R**, Brock R
„Structure property analysis of pentamethine indocyanine dyes: Identification of a new dye for life science applications"
Bioconjugate Chemistry, 15, 70-78, 2004

Fischer R, Köhler K, Fotin-Mleczek M, Brock R
„A stepwise dissection of the intracellular fate of cationic cell-penetrating peptides"
Journal of Biological Chemistry, 279, 12625-12635, 2004

Hoff A, André T, **Fischer R**, Hulko M, Marquardt U, Wiesmüller KH, Brock R
„Chemolabile cellular microarrays for screening of small compounds and peptides"
Molecular Diversity, 8, 311 - 320, 2004

2005

Bächle D, Cansier A, **Fischer R**, Brandenburg J, Burster T, Driessen C, Kalbacher H
„Biotinylated fluorescent substrates for the sensitive and specific determination of Cathepsin D activity"
Journal of Peptide Science, 11, 166-174, 2005

Barth M, **Fischer R**, Brock R, Rademann J
„Reversible cross-linking of hyperbranched polymers: A strategy for the combinatorial decoration of multivalent scaffolds"
Angewandte Chemie, International Edition, 44, 1560, 2005

Stoevesandt O, Elbs M, Köhler K, Lellouch AC, **Fischer R**, Andre T, Brock R
„Peptide microarrays for the detection of molecular interactions in cellular signal transduction"
Proteomics, accepted for publication, 2005

Dengjel J, Schorr O, **Fischer R**, Reich M, Kraus M, Kreymborg K, Altenberend F, Kalbacher H, Brock R, Driessen C, Rammensee HG, Stevanovic S
„Autophagy promotes MHC-II presentation of peptides from intracellular sources"
Proceedings of the National Academy of Sciences of the USA, accepted for publication, 2005

8.2 Submitted manuscripts

Voss S, **Fischer R**, Ulmer AJ, Jung G, Wiesmüller KH, Brock R
„CD-14-derived peptides with LPS-binding and - neutralizing capacity"
Submitted, 2005

Fotin-Mleczek M, Mader O, **Fischer R**, Duchardt F, Scheurich P, Brock R
„Cationic cell-penetrating peptides interfere with TNF signalling by induction of TNF receptor internalisation"
Submitted, 2005

8.3 Review articles

Fischer R, Fotin-Mleczek M, Brock R
„Break on through to the other side – Facts and speculations about cell-penetrating peptides"
Invited review for ChemBioChem, Accepted for publication 2005

Fotin-Mleczek M, **Fischer R**, Brock R
„Endocytosis and cationic cell-penetrating peptides – A merger of concepts and methods"
Invited review for Current Pharmaceutical Design, Accepted for publication 2005

8.4 Posters

2000

Hoff A, Wiendl H, Voss S, **Fischer R**, Melms A, Wiesmüller KH, Jung G, Brock R
"A model for the quantitative analysis of cellular immunity in multiple sclerosis by fluorescence microscopy and fluorescence correlation microscopy"
World Congress on Cellular and Molecular Biology, 2000, October 8 to15, Jena, Germany.

2001

Fischer R, Waizenegger T, Jung G, Brock R
"Intracellular concentration measurements with nanomolar sensitivity – cell-permeable peptides as tools for the analysis of T cell signal transduction"
ENII Conference 2001, The Immune System in Health and Disease: Immunology and Cancer, May 16 – 20, Ile des Embiez, France

2002

Fischer R, Mader O, Jung G, Brock R
"Extending the applicability of carboxyfluorescein in solid-phase synthesis"
27th European Peptide Symposium, 2002, August 31 – September 6, Sorrent, Italy

Köhler K, **Fischer R**, Waizenegger T, Brock R
"Cell-permeable peptides as inhibitors of T cell signal transduction: correlation of activity with intracellular processing"
27th European Peptide Symposium, 2002, August 31 – September 6, Sorrent, Italy

Köhler K, **Fischer R**, Waizenegger T, Wiendl H, Brock R.
"Adding content to cell-permeable peptide-inhibitor constructs in intracellular target validation: Descriptors of pharmacokinetics and intracellular proteolytic break-down"
8th Annual Conference and Exhibition of "The Society for Biomolecular Screening", "High Information Content Screening", 2002, September 22 –26, The Hague, Netherlands

Werth D, Mader O, **Fischer R**, Brock R, Nordheim A, Heidenreich O
"Inhibition of ternary complex formation at the c-fos SRE by peptides"
ELSO-conference, 2002, June 29 – July 3, Nice, France

2003

Fischer R, Köhler K, Waizenegger T, Brock R
"A quantitative validation of fluorophore-labeled cell-permeable peptide conjugates: fluorophore and cargo dependence of import"
Cellular Transport Strategies for Targeting of Epitopes, Drugs and Receptor Molecules (CellTarget), 2003, March 6 – 9, Budapest, Hungary

Köhler K, **Fischer R**, Waizenegger T, Wiendl H, Brock R
"Pharmacokinetics and intracellular proteolytic breakdown as parameters for the biological activity of cell-permeable inhibitor peptides"
Cellular Transport Strategies for Targeting of Epitopes, Drugs and Receptor Molecules (CellTarget), 2003, March 6 – 9, Budapest, Hungary

Fischer R, Mader O, Jung G, Brock R
"Parallel solid-phase synthesis of FRET-peptides"
6th German Peptide Symposium, 2003, March 23 – 26, Berlin, Germany

Mader O, Reiner K, Egelhaaf HJ, **Fischer R**, Brock R
"A new pentamethine indocyanine dye for life science applications"
6th German Peptide Symposium, 2003, March 23 – 26, Berlin, Germany

Mader O, Reiner K, Egelhaaf HJ, **Fischer R**, Brock R
"A new pentamethine indocyanine dye of life science applications"
8th Conference on Methods and Applications of Fluorescence, 2003, August 24 – 27, Prague, Czech Republic

Fischer R, Köhler K, Fotin-Mleczek M, Brock R
"Cationic cell-penetrating peptides: Cytosolic delivery of MHC epitopes via the endosomal pathway"
34th Annual Meeting of the German Society of Immunology, 2003, September 24 – 27, Berlin, Germany

Hoff A, André T **Fischer R**, Voss S, Wiesmüller KH, Brock R
"A cell-chip for the analysis of antigen uptake in cellular immunity"
34th Annual Meeting of the German Society of Immunology, 2003, September 24 – 27, Berlin, Germany

2004

Elbs M, Hoff A , André T, Stoevesandt O, Lellouch AC, **Fischer R**, Malissen B, Wiesmüller KH, Brock R
„Peptide microarrays for functional proteomics in vitro and in cells"
Statusseminar: Chiptechnologien, Mikroarrays, Hygiene und Gesundheit, 2004, January 26 – 27, Frankfurt, Germany

Voss S, **Fischer R**, Ulmer AJ, Jung G, Wiesmüller KH, Brock R
"CD-14-derived peptides with LPS-binding and neutralising capacity"
Toll 2004, May 8 – 11, Taormina, Italy

Elbs M, Stoevesandt O, André T, Lellouch AC, **Fischer R**, Brock R
„Peptide microarrays as sensors for the formation of molecular complexes in cellular signal transduction“
The 8th World Congress on Biosensors, Granada, Spain

Fischer R, Fotin-Mleczek M, Brock R
“The import mechanism of cationic cell-penetrating peptides and its implications for the delivery of peptide inhibitors of signal transduction”
Chemistry meets Biology, 2nd Symposium of the EMBO Young Investigator Programme, 2004, June 5 – 6, Heidelberg, Germany

Fischer R, Fotin-Mleczek M, Brock R
“The import mechanism of cationic cell-penetrating peptides and its implications for the delivery of peptide inhibitors of signal transduction”
3rd International and 28th European Peptide Symposium, 2004, September 5 – 10, Prague, Czech Republic

Fischer R, Hufnagel HJ, Jung G, Brock R
“In vitro and in vivo applications of doubly-labeled fluorescent cell-penetrating peptides”
3rd International and 28th European Peptide Symposium, 2004, September 5 – 10, Prague, Czech Republic

Voss S, **Fischer R**, Ulmer AJ, Jung G, Wiesmüller KH, Brock R
“Identification of a CD-14-derived peptide with LPS-neutralizing capacity”
3rd International and 28th European Peptide Symposium, 2004, September 5 – 10, Prague, Czech Republic

Hoff A, André T **Fischer R**, Wiesmüller KH, Brock R
“Cell-penetrating peptides in cellular microarrays”
3rd International and 28th European Peptide Symposium, 2004, September 5 – 10, Prague, Czech Republic

Fotin-Mleczek M, Mader O, **Fischer R**, Brock R
“Cationic cell-penetrating peptides modulate cellular signal transduction by promoting receptor internalization”
3rd International and 28th European Peptide Symposium, 2004, September 5 – 10, Prague, Czech Republic

Bächle D**, Fischer R**, Brandenburg J, Brock R, Kalbacher H
“Synthesis and application of a new cell-penetrating cathepsin D substrate”
3rd International and 28th European Peptide Symposium, 2004, September 5 – 10, Prague, Czech Republic

Barth M**, Fischer R**, Brock R, Rademann J
“Reversibly cross-linked dendrimers – A strategy for the facile synthesis and combinatorial variation of complex, multivalent protein-mimics”
3rd International and 28th European Peptide Symposium, 2004, September 5 – 10, Prague, Czech Republic

9 Academic Teachers

Academic teachers at the Eberhard-Karls-Universität, Tübingen

Prof. Albert, Prof. Bisswanger, Prof. Bock, Prof. Bohley, Prof. Breyer-Pfaff, Dr. Buchmann, Prof. Eckstein, Prof. Eisele, Prof. Fröhlich, Prof. Gauglitz, Prof. Götz, Prof. Häfelinger, Prof. Hagenmaier, Prof. Hamprecht, Prof. M. Hanack, Dr. Hartmann, Prof. Hoffmann, Prof. Jung, Dr. Günzl, Prof. Lindner, Dr. Kalbacher, Prof. Maier, Prof. Mecke, Prof. Nakel, Prof. Ninnemann, Prof. Oberhammer, Prof. Oelkrug, Prof. Pfaff, Prof. Pfeiffer, PD Dr. Pommer, Prof. Poralla, Prof. Probst, Prof. Rammensee, Prof. Reutter, Prof. Schurig, Prof. Staudt, Prof. Stegmann, Prof. Dr. Stevanovic, PD Dr. Stoeva, Prof. Strähle, Prof. Voelter, Prof. Weber, Prof. Wegmann, Prof. Werringloer, Prof. Weser, Prof. Wiesinger, Prof. Wiesmüller, Prof. Wohlleben

Academic teachers at the University of Michigan, Ann Arbor

Prof. Chen, Prof. Engelke, Prof. Fuller, Prof. Guan, Prof. Kerpolla, Dr. Mann, Prof. Marletta, Prof. Saper, Prof. Thiele

LEBENSLAUF (DEUTSCH)

DOKTORARBEIT

März 2001 – September 2004 Anfertigung der Doktorarbeit

„Parallel Synthesis, Characterization and Cellular Pharmacokinetics of Fluorescent Cell-Penetrating Peptides"

- betreut von Prof. Dr. Günther Jung, Institut für Organische Chemie, Eberhard-Karls-Universität Tübingen
- durchgeführt am Institut für Organische Chemie und am Interfakultären Institut für Zellbiologie, Eberhard-Karls-Universität Tübingen, Arbeitsgruppe „Zelluläre Signaltransduktion", Laborleiter Dr. Roland Brock

STUDIUM - BIOCHEMIE

Dezember 2000	Diplom Biochemie
April 2000 – Dezember 2000	Anfertigung der Diplomarbeit „*Struktur-Funktions-Analyse fluoreszenzmarkierter zellpermeabler und MHC-Klasse I-bindender Peptide mit Fluoreszenzspektroskopie und Fluoreszenzmikroskopie"* - am Institut für Organische Chemie, Arbeitsgruppe Prof. Dr. Günther Jung, Eberhard-Karls-Universität Tübingen
März 2000	Mündliche Diplomprüfung (Biochemie, Organische Chemie, Pharmakologie/Toxikologie)
August 1998 – Mai 1999	Studium an der University of Michigan, Ann Arbor, USA
Oktober 1997	Vordiplomprüfung
April 1995 – Dezember 2000	Studium der Biochemie an der Eberhard-Karls-Universität Tübingen

STIPENDIUM

April 1995 – Dezember 2000 Stipendiat der „Bayerischen Begabtenförderung"

AUSLANDSERFAHRUNG

August 1998 – Mai 1999 Studium an der University of Michigan, Ann Arbor, USA